Thesis presented to the Instituto Tecnológico de Aeronáutica, in partial fulfillment of the requirements for the degree of Doctor of Science in the Graduate Program of Physics, Field of Nuclear Physics.

Flavia Pereira da Rocha

BEYOND-GRAVITOMAGNETISM APPROXIMATION OF GENERAL RELATIVITY APPLIED TO SOLAR SYSTEM AND STUDY OF CHARGED COMPACT OBJECTS IN $F(R, \mathcal{T})$ THEORY OF GRAVITY

Thesis approved in its final version by signatories below:

Manuel Malheiro

Prof. Dr. Manuel M. B. Malheiro de Oliveira

Advisor

Gerson Otto Ludwig

Prof. Dr. Gerson Ludwig

Co-advisor

Prof. Dra. Emília Villani

Pro-Rector of Graduate Courses

Campo Montenegro
São José dos Campos, SP - Brazil
2021

Cataloging-in Publication Data
Documentation and Information Division

Rocha, Flavia Pereira da
Beyond-Gravitomagnetism approximation of General Relativity applied to Solar system and Study of Charged Compact Objects in $f(R, \mathcal{T})$ Theory of Gravity / Flavia Pereira da Rocha. São José dos Campos, 2021.
93f.

Thesis of Doctor of Science – Course of Physics. Area of Nuclear Physics – Instituto Tecnológico de Aeronáutica, 2021. Advisor: Prof. Dr. Manuel M. B. Malheiro de Oliveira. Co-advisor: Prof. Dr. Gerson Ludwig.

1. Campos Gravitacionais. 2. Eletromagnetismo. 3. Gravidade. 4. Teoria da relatividade. 5. Astrofísica. 6. Física. I. Instituto Tecnológico de Aeronáutica. II. Title.

BIBLIOGRAPHIC REFERENCE

ROCHA, Flavia Pereira da. **Beyond-Gravitomagnetism approximation of General Relativity applied to Solar system and Study of Charged Compact Objects in $f(R, \mathcal{T})$ Theory of Gravity**. 2021. 93f. Thesis of Doctor of Science – Instituto Tecnológico de Aeronáutica, São José dos Campos.

CESSION OF RIGHTS

Flavia Pereira da Rocha
Av. Cidade Jardim, 679
12.233-066 – São José dos Campos–SP

BEYOND-GRAVITOMAGNETISM APPROXIMATION OF GENERAL RELATIVITY APPLIED TO SOLAR SYSTEM AND STUDY OF CHARGED COMPACT OBJECTS IN $F(R, \mathcal{T})$ THEORY OF GRAVITY

Flavia Pereira da Rocha

Thesis Committee Composition:

Prof. Dr.	César Henrique Lenzi	Presidente	-	ITA
Prof. Dr.	Manuel M. B. Malheiro de Oliveira	Advisor	-	ITA
Prof. Dr.	Gerson Ludwig	Co-advisor	-	INPE
Prof. Dra.	Nadja Simão Magalhães	Membro Interno	-	UNIFESP
Prof. Dr.	Marcio Eduardo da Silva Alves	Membro Externo	-	UNESP
Prof. Dr.	Jaziel Goulart Coelho	Membro Externo	-	UTFPR

ITA

To my family.

Acknowledgments

First and foremost, I would like to thank God for guiding me and making me trust that everything is possible.

I also would like to express my sincere gratitude to my advisor Prof. Dr. Manuel Malheiro for all the support of my Ph.D study and research, for his enthusiasm, motivation and immense knowledge. His guidance helped me in all my academic life in to now. Thank you very much prof. Manuel.

Besides my advisor I would like to thank the rest of my thesis committee: my co-advisor Prof. Dr. Gerson Ludwig and Prof. Dr. Rubens Marinho Jr. It was a great privilege and honor to work and study under their guidance. Thank you very much for all the knowledge shared.

My sincere thanks also goes to Profs. Dr. Carlos Bomfim, Dr. Tobias Frederico, Dr. Wayne de Paula, Dr. Brett Carlson, Dr. Pedro Pompéia, Dra. Nádia Simões and Dra. Marisa Roberto for their classes that were fundamental in my formation, encouragement, insightful comments and hard questions.

I thank my fellows: Sílvia Nunes, Carla Cursino, Larissa Nascimento, Vanderli Laurindo Jr., Ronaldo Lobato, Emanuel Chimanski, Armando Pinto and, Geanderson Carvalho for all the fun and friendship we have had in the last six years. I'm also extremely grateful to my friends Sérgio Pilling, Carla Osmarin, Khashayar Kianfar and to my beloved Kamyar Mohseni for all the support.

Last but not the least, I would like to thank my family, my parents Antonio and Vera for their love, prayers, caring and sacrifices for educating and preparing me for my future. I am thankful to my sisters: Glaucia and Jessica for all the companionship, love and for being the best sisters in the world.

To CAPES for financial support.

"One, remember to look up at the stars and not down at your feet.
Two, never give up work. Work gives you meaning and purpose and life is empty without it.
Three, if you are lucky enough to find love, remember it is there and don't throw it away."
— Stephen Hawking

Resumo

Neste trabalho, derivamos, pela primeira vez, a expansão de ambos os lados da equação de campo de Einstein no regime de campo fraco até a ordem $1/c^4$. Essa abordagem leva a uma forma espandida do gravitomagnetismo, a qual chamamos *Beyond Gravitomagnetism* (BGEM). A métrica obtida a partir dessa abordagem inclui um termo quadrático no potencial, que não aparece na forma convencial do gravitomagnetismo e que é essencial para obter o valor correto para o problema do avanço do periélio de Mercúrio. A métrica obtida também é aplicada ao problema clássico da deflexão da luz pelo Sol levando também ao valor correto, mostrando assim a viabilidade dessa abordagem. Além disso, também investigamos a configuração de equilíbrio de anãs brancas carregadas no contexto de teoria de gravidade $f(R, \mathcal{T})$, onde R e $\mathcal{T}$ são o escalar de Ricci e o traço do tensor energia momento, respectivamente. Mostramos, a partir da nova equação de equilíbrio hidrostático para o funcional específico $f(R, \mathcal{T}) = R + 2\chi\mathcal{T}$, onde χ é uma constante de acoplamento da matéria-geometria e para um ansatz Gaussiano para a carga elétrica, conseguimos obter algumas propriedades para anãs brancas carregadas, a saber: massa, raio, carga, campo elétrico, pressão efetiva e densidade de energia. Mostramos que estrelas anãs brancas carregadas no contexto da teoria $f(R, \mathcal{T}) = R + 2\chi\mathcal{T}$ possuem carga elétrica superficial abaixo do limite de Schwinger de 1.3×10^{18}V/m. Além disso, uma característica marcante do acoplamento entre os efeitos da carga e a teoria de gravidade $f(R, \mathcal{T}) = R+2\chi\mathcal{T}$ é que as modificações na gravidade de fundo aumentam o raio estelar, que por sua vez diminui o campo elétrico da superfície, aumentando assim a estabilidade estelar de estrelas carregadas em comparação com a teoria GR. Por fim, nosso estudo revela que o atual modelo de gravidade $f(R, \mathcal{T})$ pode explicar adequadamente a massa das anãs brancas acima do limite de Chandrasekhar, que supostamente são a razão por trás das SN Ia superluminosas que permanecem praticamente inexplicadas pela Relatividade Geral.

Abstract

In this work, the expansion of both sides of Einstein's field equations in the weak-field approximation, up to terms of order $1/c^4$, is derived. This approach leads to an extended form of gravitomagnetism properly named Beyond Gravitomagnetism (BGEM). The metric of BGEM includes a quadratic term in the gravitoelectric potential. This term does not appear in conventional gravitomagnetism, but is essential in achieving the exact value of Mercury's perihelion advance. The new metric is also applied to the classical problem of light deflection by the Sun, giving the correct result and showing the feasibility of this approach. Another subject approached in this work concerns to the equilibrium configuration of white dwarfs composed of a charged perfect fluid are investigated in the context of the $f(R, \mathcal{T})$ gravity, for which R and $\mathcal{T}$ stand for the Ricci scalar and the trace of the energy-momentum tensor, respectively. By considering the functional form $f(R, \mathcal{T}) = R + 2\chi\mathcal{T}$, where χ is the matter-geometry coupling constant, and for a Gaussian ansatz for the electric distribution, some physical properties of charged white dwarfs were derived, namely: mass, radius, charge, electric field, effective pressure and energy density; their dependence on the parameter χ was also derived. We have showed that charged white dwarf stars in the context of the $f(R, \mathcal{T})$ have surface electric fields below the Schwinger limit of 1.3×10^{18}V/m. In particular, a striking feature of the coupling between the effects of charge and $f(R, \mathcal{T})$ gravity theory is that the modifications in the background gravity increase the stellar radius, which in turn diminishes the surface electric field, thus enhancing stellar stability of charged stars in comparison with General Relativity (GR). Most importantly, our study reveals that the present $f(R, \mathcal{T})$ gravity model can suitably explain the super-Chandrasekhar limiting mass white dwarfs, which are suppose to be the reason behind the over-luminous SNeIa and remain mostly unexplained in the background of GR theory.

List of Figures

List of Tables

List of Abbreviations and Acronyms

EGEM	Extended Gravitomagnetism
GEM	Gravitomagnetism
GPA	Gravity Probe A
GPB	Gravity Probe B
GRT	General Relativity Theory
GR	General Relativity
LT	Lense-Thirring
SR	Special Relativity

List of Symbols

r	Distance
$\vec{r}$	Distance vector
$g^{\mu\nu}$	Metric tensor
$\eta^{\mu\nu}$	Minkowski metric
$G_{\mu\nu}$	Einstein tensor
$T^{\mu\nu}$	Energy-momentum tensor
R_s	Schwarzchild Radius

Contents

1 Introduction

In 1905, Albert Einstein published the so-called Special Relativity Theory (SR) which made a great revolution in physics by presenting a new concept of space and time, i.e., the notions of absolute space and absolute time from the Newtonian mechanics were changed to a new notion of space-time, as pointed in (MISNER *et al.*, 1973). However, SR is a kinematic and dynamic modification of Newtonian mechanics derived from two principles:

- The physical laws must be the same for any inertial observers;
- The velocity of light in the vacuum is a universal constant for inertial observers.

Ten years later, Einstein published the theory of general relativity (GR) which determines that massive objects cause a distortion in space-time, which is felt as gravity, i.e., gravitation is a manifestation of space-time curvature (D'INVERNO, 1992). This theory describes how space-time is affected by the mass distribution present in the Universe. In other words, GR is a geometric theory of gravitation that extends the restricted relativity to accelerated referential, introducing the principle that gravitational and inertial forces are equivalent.

The dynamics of General Relativity are described by a set of equations known as Einstein's field equations (MOORE, 2015). These equations relate to the geometric properties of space-time, described by a metric and its derivatives of first and second order with the energy-momentum tensor of matter. The energy-momentum tensor is the generalization of the energy and momentum concepts of a particle for the description of fields, and it is through this tensor that the distribution of matter is described. This means that geometry tells matter how to move, and matter tells geometry how to curve.

The field equations govern the motion of the planets in the solar system; it governs the deflection of light by the Sun, Earth, and Universe as well; it governs the collapse of a star to form a black hole; it governs the evolution of space-time singularities at the endpoint of collapse, and so on. Therefore, the theory of general relativity is the standard model on which gravitation and cosmology are based (WEYL, 1922).

Furthermore, three of the most famous tests called "classical tests" were proposed to test GR, which are: perihelion precession of Mercury, the bending of light, and gravitational redshift. We will focus on two of them: the perihelion precession of Mercury and the bending of light.

The Mercury perihelion Advance was discovered by the French astronomer Le Verrier in 1846 (PARK R. S. *et al.*, 2017). It was observed that the orbit of Mercury precessed about 574.1 arcseconds per Earth-century and the Newtonian mechanics with the contribution of the perturbations caused by other planets predicts a precession of 531.6 arcseconds per Earth-century, then, the observed precession exceeds the calculated one by 43 arcseconds per Earth-century. Later, it became one of the first confirmations of GR (EINSTEIN, 1923).

Another classical effect of GR is the light bending by gravity (BELOBORODOV, 2002). As observed on Earth, light from a distant star bends when it passes near another star like the Sun. Einstein's theory predicts ($4GM/c^2R$) which is the double of the bending predicted ($2GM/c^2R$) by conventional Newtonian mechanics. The experimental confirmation organized by Eddington and Dyson with two expeditions to observe the eclipse of May 29, 1919, on Sobral (Brazil) and Principe (Gulf of Guinea) was another proof of GR (WEINBERG, 2008).

In particular, the increase of experimental and observational evidence (PEEBLES; RATRA, 2003) has brought gravitational physics itself to the status of experimental science in the sense that it is necessary to confirm that the background developed theory works well in describing observational data. Some frameworks have been constructed for gravitational physics by a number of authors, a general and unified version of the PPN formalism was developed by Will and Nordtvedt (WILL, 2014) provide a framework in which weak field tests of gravity can be interpreted, for example.

Another approach was developed in 1918 by Joseph Lense and Hans Thirring (MASHHOON *et al.*, 1984a) which used the linearized Einstein field equations, valid for a weak field scheme, along with a low-velocity approximation (KARLSSON, 2006; MASHHOON *et al.*, 1999; PFISTER, 2007). From this linearization it is possible to define four equations called gravitoelectromagnetic equations (CIUFOLINI, 2010; TAJMAR; MATOS, 2006; CLARK; TUCKER, 2000), which are analogous to Maxwell's equations, in which the mass is the perfect analogue of the electric charge. This formalism leads to a new concept in which a current of mass can generate a gravitomagnetic field similar to the magnetic field induced by a charge current in electromagnetism.

The most famous gravitomagnetic effect is the Einstein-Thirring-Lense effect (PFISTER, 2014; PFISTER, 2007), i.e., the "dragging of inertial frames" by a spinning mass. Several experiments were proposed to measure frame-dragging or Lense-Thirring precession, and the gravitomagnetic field generated by the angular momentum of a body (CIU-

FOLINI *et al.*, 1997; CIUFOLINI; PAVLIS, 2004; CIUFOLINI *et al.*, 1996; CIUFOLINI, 2010; CIUFOLINI, 1986b; IORIO; CORDA, 2011; LÄMMERZAHL; NEUGEBAUER, 2001; CHASHCHINA *et al.*, 2008; MURPHY *et al.*, 2007; SCHMID, 2009; RENZETTI, 2013b; RENZETTI, 2012; RENZETTI, 2013a; RENZETTI, 2014; RENZETTI, 2015; IORIO, 2011b; IORIO, 2009b; IORIO, 2020b; IORIO, 2019; IORIO, 2018; LUCCHESI *et al.*, 2019; LUCCHESI *et al.*, 2020): from the observations of the LAGEOS (LAser GEOdynamics Satellite) and LAGEOS II satellites, that were launched in 1976 by NASA, and jointly in 1992 by ASI (Italian Space Agency) and NASA, respectively; to the Gravity Probe B space experiment launched by NASA in 2004.

Frame-dragging was observed, by using LAGEOS and LAGEOS II, with approximately 10% accuracy, despite the actual accuracy is currently disputed, being possibly as large as 20-30% or so, as pointed out in (IORIO, 2006; IORIO, 2011b; IORIO, 2017; IORIO, 2016; IORIO *et al.*, 2013; IORIO, 2009a; IORIO, 2007b; RENZETTI, 2014). And also by the Gravity Probe B with approximately 20% accuracy (BUCHMAN *et al.*, 2015; CIUFOLINI I. *et al.*, 2016; CIUFOLINI, 1994; CIUFOLINI *et al.*, 2010; CIUFOLINI, 1996; HABIB *et al.*, 1994; IORIO, 2002; VETŐ, 2010; VESPE, 1999; CIUFOLINI *et al.*, 1990). Lastly, in 1998 the Laser Relativity Satellite (LARES) experiment, which is the improved version of LAGEOS one, was proposed. The LARES satellite has been designed to be smaller and about four times lighter than LAGEOS, with a total weight of about 100 kg and a radius of about 16 cm. Some authors (CIUFOLINI, 1986a; CIUFOLINI, 1989; CIUFOLINI I. *et al.*, 2010; LUCCHESI, 2007; IORIO, 2005; IORIO *et al.*, 2002) have shown that by combining the measured nodal precessions of LAGEOS and LARES it would be possible to get a very accurate measurement of the Lense-Thirring effect. Subsequent analyses in the literature have shown that, in fact, also the LARES mission final accuracy may be likely worst than that claimed (IORIO, 2010; IORIO, 2009d; IORIO, 2017; IORIO, 2018; IORIO, 2009c; IORIO, 2007a; RENZETTI, 2012; RENZETTI, 2013a; RENZETTI, 2015).

Moreover, several authors studied the gravitomagnetic effect in the Solar System (ROCHA *et al.*, 2015; ROCHA *et al.*, 2016; ROCHA *et al.*, 2017; IORIO, 2011a; IORIO *et al.*, 2011) because within the solar system relativistic gravity theories can be tested in the weak field limit and it was found that gravitomagnetism provides only small corrections.

Recently, Krishnan et al. (KRISHNAN *et al.*, 2020) observed the binary system PSR J1141-6545, which contains a massive white dwarf (WD) companion. The WD was formed before the gravitationally bound young radio pulsar. The authors of (KRISHNAN *et al.*, 2020) inferred that the temporal evolution of the orbital inclination of this binary is caused by the combination of a Newtonian quadrupole moment and Einstein-Thirring-Lense precession of the orbit resulting from rapid rotation of the WD. Earlier, Merloni et al. (MERLONI *et al.*, 1999) studied the frequency of Lense-Thirring precession for point masses in the Kerr metric, for an arbitrary black hole mass. They found that the preces-

sion, for point masses at or close to the innermost stable orbit and for black holes with moderate to extreme rotation, is less than but comparable to the rotation frequency. However in Ref.(IORIO, 2020a) the author criticizes this work claiming that the test presented is too optimistically.

In Ref.(ROCHA *et al.*, 2021) we propose, for the first time, an expansion of both sides of Einstein's field equations in the weak-field approximation, up to terms of order $1/c^4$. This new approach shows an extended form of gravitomagnetism (GEM) properly named Beyond Gravitomagnetism (BGEM). The metric of BGEM includes a quadratic term in the gravitoelectric potential in the time and also space metric functions in contrast with the first post-Newtonian 1PN approximation where the quadratic term appears only in the time metric function. This non-linear term does not appear in conventional GEM, but is essential in achieving the exact value of Mercury's perihelion advance. The new BGEM metric is also applied to the classical problem of light deflection by the Sun, but the contribution of the new non-linear terms produces higher-order terms in this problem and can be neglected, giving the correct result obtained already in the Lense-Thirring (GEM) approximation.

Another subject approached in this work it concerns to the modified/extended gravity theories that comes from the modified the Einstein-Hilbert action. Extended theories of gravity have aroused as an opportunity to solve problems which are still without convincing explanation within GR framework. The most famous modified theory of gravity is the $f(R)$ theory, which consists of choosing a more general action to replace the Einstein-Hilbert one, this is made by assuming that the gravitational action is given by an arbitrary function of the Ricci scalar R can be found in literature Refs. (CAPOZZIELLO, 2002; NOJIRI; ODINTSOV, 2003; CARROLL *et al.*, 2004; BERTOLAMI *et al.*, 2007).

Over the last decade, Harko et al. (HARKO *et al.*, 2011) developed a further generalization of the $f(R)$ theory of gravity by choosing a gravitational action as an arbitrary function of the Ricci scalar and also the trace of the energy-momentum tensor $\mathcal{T}$, which is called $f(R,\mathcal{T})$ theory of gravity. Within this theory, Solar System tests have been already performed (DENG; XIE, 2015; SHABANI; FARHOUDI, 2014). Studies on compact astrophysical objects have also been considered in the literature (MORAES *et al.*, 2016; CARVALHO *et al.*, 2017; DEB *et al.*, 2019a; DEB *et al.*, 2019b). In particular, modified theories of gravity have been shown to significantly elevate the maximum mass of compact objects (CAPOZZIELLO *et al.*, 2015; CARVALHO *et al.*, 2020a; CARVALHO *et al.*, 2020b; DAS; MUKHOPADHYAY, 2015; DEB *et al.*, 2019b), which means that $f(R,\mathcal{T})$ is of particular interest for the hydrostatic equilibrium configuration of compact stars.

In what concerns white dwarfs they are the final evolution state of main-sequence stars with initial masses up to $8.5 - 10.6 M_{\odot}$. However, if the WD mass grows over 1.44 $M_{\odot}$ - known as Chandrasekhar mass limit (CHANDRASEKHAR, 1931) - as in binary systems,

where the main star is receiving mass from a nearby star, a Type Ia supernova (SNIa) explosion may occur. However, with the recently observed peculiar highly over-luminous SNeIa, such as, SN 2003fg, SN 2006gz, SN 2007if, SN 2009dc (HOWELL, 2006; SCALZO, 2010) it is possible to confirm the existence of a huge Ni-mass which leads to the possibility of massive super-Chandrasekhar white dwarfs with mass $2.1-2.8\ M_{\odot}$ as their most feasible progenitors.

In addition, several authors have studied charged stars. Within them, there are investigations about the influence of the electrical charge distribution at the stellar structure of polytropic stars (RAY *et al.*, 2003; ARBAÑIL; MALHEIRO, 2015; AZAM *et al.*, 2016), anisotropic stars (DEB *et al.*, 2018) and white dwarfs (LIU *et al.*, 2014; CARVALHO *et al.*, 2018). In what concerns to charged WDs, Liu, and collaborators (LIU *et al.*, 2014) found that the charge contained in WDs can affect their structure, they have larger masses and radii than the uncharged ones. Moreover, Carvalho et al. have shown in a previous work (CARVALHO *et al.*, 2018) that the increment of the total charge from 0 to $\approx 2 \times 10^{20}$C allows to increase the total mass by approximately 55.58%, and for a large total charge, more massive stellar objects are found.

Here, we are particularly interested to study the charge effects within the framework of the $f(R, \mathcal{T})$ gravity, for the hydrostatic equilibrium configurations of white dwarfs. A few works (JING; WEN, 2016; COSTA *et al.*, 2017; PANAH; LIU, 2019; DAS; MUKHOPADHYAY, 2015; KALITA; MUKHOPADHYAY, 2018; LIU; LÜ, 2019) have achieved stable stellar models to explain super-Chandrasekhar white dwarfs in the background of the different modified theories of gravity. Although few researchers (FREIRE *et al.*, 2012; JAIN *et al.*, 2016; BANERJEE *et al.*, 2017; SALTAS *et al.*, 2018) have studied WD properties via scalar-tensor or Horndeski theories they have only derived constraints on the parameters of the theories by comparing their results with WD observational data and not discussed the issue of super-Chandrasekhar white dwarfs lie in the range 2.1 - 2.8 $M_{\odot}$.

Therefore, in Ref.(ROCHA *et al.*, 2020) the equilibrium configuration of white dwarfs composed of a charged perfect fluid are investigated in the context of the $f(R, \mathcal{T})$ gravity. By considering the functional form $f(R, \mathcal{T}) = R + 2\chi\mathcal{T}$, where χ is the matter-geometry coupling constant, and for a Gaussian ansatz for the electric distribution, some physical properties of charged white dwarfs were derived, namely: mass, radius, charge, electric field, effective pressure and energy density; their dependence on the parameter χ was also derived. In particular, the χ value important for the equilibrium configurations of charged white dwarfs has the same scale of 10^{-4} of that for non-charged stars and the order of the charge was 10^{20}C, which is scales with the value of one solar mass, i.e., $\sqrt{G}M_{\odot} \sim 10^{20}$C. We have also showed that charged white dwarf stars in the context of the $f(R, \mathcal{T})$ have surface electric fields below the Schwinger limit of 1.3×10^{18}V/m. In particular, a striking feature of the coupling between the effects of charge and $f(R, \mathcal{T})$

gravity theory is that the modifications in the background gravity increase the stellar radius, which in turn diminishes the surface electric field, thus enhancing stellar stability of charged stars in comparison with GR theory. Most importantly, our study reveals that the present $f(R, \mathcal{T})$ gravity model can suitably explain the super-Chandrasekhar limiting mass white dwarfs, which are suppose to be the reason behind the over-luminous SNeIa and remain mostly unexplained in the background of GR.

We begin chapter 2 with the General Relativity (GR) approach, starting with Einstein's field equations and solving it the first order with the weak field approximation to obtain the respective wave equation and, then, doing the slow-source approximation to get the Gravitoelectromagnetic equations. In this chapter, we will also summarize the analogy between Maxwell's equations and the gravitomagnetic equations.

In chapter 3 we will formally introduce the formalism of Beyond Gravitomagnetism starting from the linearized Einstein's field equation and expanding it to the order of $1/c^4$ to get the line element in this formalism. In this chapter, we also apply the formalism of Beyond Gravitomagnetism to Mercury's perihelion advance orbit and for the deflection of light and we find the correct value in both cases.

In chapter 4 we introduce the study of charged white dwarf in the $f(R, \mathcal{T})$ gravity. Starting from the basic formalism of $f(R, \mathcal{T})$ gravity, showing the stellar equilibrium equations, the stellar properties, and the main results.

In chapter 5 we summarize our results and provide concluding remarks.

2 General Relativity

Einstein's general relativity is one of the most elegant and rich theor known in physics. It has improved our ideas about the structure of the cosmos a step further. In this chapter we are interesting in deriving the gravitomagnetic equations from linearizing the equations of General Relativity.

2.1 Einstein's Field Equations

The general relativity (GR) describes the movement of the objects in terms of their trajectories on the space-time surface, which in turn is determined by the mass distribution of the Universe, that is, space and time are not absolute and static structures as in Newton's theory but physical entities in themselves. In GR, gravity appears as a manifestation of the curvature of space-time, i.e., the effects of curvature that we observe as a gravitational field. The interaction between space-time is such that matter curves space-time, and this in turn defines the trajectory of a particle according to its geometry. In this sense, Einstein's field equations are:

$$G_{\mu\nu} = \kappa T_{\mu\nu}, \tag{2.1}$$

where on the left side we have the Einstein tensor ($G_{\mu\nu} = R_{\mu\nu} - \frac{1}{2}g_{\mu\nu}R$), which is defined in terms of the metric tensor $g_{\mu\nu}$ which describes the space-time geometry, $R_{\mu\nu}$ is the Ricci tensor, and R is the Ricci scalar. On the right side we have the coupling constant between the field and the geometry given by $\kappa = \frac{8\pi G}{c^4}$. The energy momentum tensor $T_{\mu\nu}$ contains all the information concerning the energy and momentum of the field. In other words, if we know the energy density and the pressure of a fluid, we may build its energy momentum tensor, and then we shall know how its matter curves spacetime through the Einstein tensor, which reflects the properties of the curvature of spacetime.

Einstein's tensor and the energy momentum tensor relate the geometry of a given spacetime to its distribution of matter. It is important to remember that Einstein's tensor obeys to the contract Bianchi identities $\nabla_\mu G^{\mu\nu} = 0$. Thus, the tensor $T_{\mu\nu}$ which

is constituted to represent a given distribution of matter, must also obey a conservation law $\nabla_\mu T^{\mu\nu} = 0$.

2.1.1 Conventions

Before we proceed it is important to establish some conventions. The chosen ones here are the following: The metric tensor is defined as $g_{\mu\nu}$ and its inverse $g^{\mu\nu}$. The Minkowski metric is defined as $\eta_{\mu\nu}$, its inverse $\eta^{\mu\nu}$.

The Christoffel symbols are calculated according to the metric:

$$\Gamma^{\rho}_{\mu\nu} = \left\{ {\rho \atop \mu\nu} \right\} \equiv \frac{1}{2} g^{\rho\sigma} \left(\partial_\mu g_{\nu\sigma} + \partial_\nu g_{\mu\sigma} - \partial_\sigma g_{\mu\nu} \right). \tag{2.2}$$

The Riemann tensor/curvature can be calculated in terms of the Christofell symbols:

$$R^{\mu}{}_{\gamma\nu\beta} = \partial_\nu \Gamma^{\mu}{}_{\gamma\beta} - \partial_\beta \Gamma^{\mu}{}_{\gamma\nu} + \Gamma^{\mu}{}_{\eta\nu} \Gamma^{\eta}{}_{\gamma\beta} - \Gamma^{\mu}{}_{\eta\beta} \Gamma^{\eta}{}_{\gamma\nu}. \tag{2.3}$$

The Ricci tensor can be obtained from the Riemann tensor;

$$R_{\gamma\beta} = g^{\mu\nu} R_{\mu\gamma\nu\beta} = R^{\nu}{}_{\gamma\nu\beta}. \tag{2.4}$$

The Riemann/curvature scalar relates to the Ricci tensor as follows:

$$R = g^{\mu\nu} R_{\mu\nu} = R^{\nu}{}_{\nu}. \tag{2.5}$$

The Einstein tensor is defined in terms of the Ricci tensor, the metric and the Riemann scalar:

$$G_{\mu\nu} = R_{\mu\nu} - \frac{1}{2} g_{\mu\nu} R. \tag{2.6}$$

The energy-momentum tensor:

$$T^{\rho\sigma} \equiv \frac{2}{\sqrt{-g}} \frac{\delta \mathcal{L}_{matter}}{\delta g_{\rho\sigma}}; \tag{2.7}$$

where, $\mathcal{L}_{matter}$ is the nongravitational part of the Lagrangian density.

And the covariant derivative is defined as:

$$\nabla_\nu T^{\mu_1\cdots\mu_n}{}_{\lambda_1\ldots\lambda_m} \equiv \partial_\nu T^{\mu_1\cdots\mu_n}{}_{\lambda_1\ldots\lambda_m} + \Gamma^{\mu_1}_{\nu\sigma} T^{\sigma\mu_2\cdots\mu_n}{}_{\lambda_1\ldots\lambda_m} + \ldots + \Gamma^{\mu_1}_{\nu\sigma} T^{\mu_1\cdots\mu_{n-1}\sigma}{}_{\lambda_1\ldots\lambda_m} + - \Gamma^{\sigma}_{\nu\lambda_1} T^{\mu_1\cdots\mu_n}{}_{\sigma\lambda_2\ldots\lambda_m} - \ldots - \Gamma^{\sigma}_{\nu\lambda_m} T^{\mu_1\cdots\mu_n}{}_{\lambda_1\ldots\lambda_{m-1}\sigma}.$$

2.1.2 Weak field approximation

Einstein's field equations are non-linear and have a rather complex algebra. In weak gravitational fields, i.e, far from astrophysical sources space-time is approximately flat (D'INVERNO, 1992). In the weak field approximation the metric tensor is supposed to be a perturbation of the Minkowski metric such that $g_{\mu\nu} = \eta_{\mu\nu} + h_{\mu\nu}$. Where, the Minkowski metric is a diagonal matrix given by:

$$\eta_{\mu\nu} = \begin{bmatrix} 1 & 0 & 0 & 0 \\ 0 & -1 & 0 & 0 \\ 0 & 0 & -1 & 0 \\ 0 & 0 & 0 & -1 \end{bmatrix},$$

and $h_{\mu\nu}$ is the perturbation term such that ($|h_{\mu\nu}| \ll 1$, $|\partial_\rho h_{\mu\nu}| \ll 1$, $|\partial_\sigma \partial_\rho h_{\mu\nu}| \ll 1, \ldots$). In first order in $h_{\mu\nu}$ the inverse metric is given by $g_{\mu\nu} = \eta_{\mu\nu} + h_{\mu\nu} + O\left(h^2\right)$, and the trace of $h_{\mu\nu}$ is $h = \eta_{\rho\sigma} + h_{\rho\sigma} + O\left(h^2\right)$. From these expressions, one finds:

The Christoffel symbols:

$$\Gamma^{\rho}_{\mu\nu} = \frac{1}{2}\eta^{\rho\sigma}\left(\partial_\mu h_{\nu\sigma} + \partial_\nu h_{\mu\sigma} - \partial_\sigma h_{\mu\nu}\right) + O\left(h^2\right).$$

Ricci tensor:

$$R_{\mu\nu} = \frac{1}{2}\left(\partial_\rho\partial_\nu h^{\rho}_{\mu} - \partial_\rho\partial^\rho h_{\mu\nu} - \partial_\mu\partial_\nu h + \partial_\mu\partial_\rho h^{\rho}_{\nu}\right) + O\left(h^2\right).$$

Scalar curvature:

$$R = g^{\mu\nu}R_{\mu\nu} = \eta^{\mu\nu}R_{\mu\nu} + O\left(h^2\right) = \partial_\rho\partial_\nu h^{\nu\rho} - \partial_\rho\partial^\rho h + O\left(h^2\right). \tag{2.8}$$

And the Einstein tensor:

$$G_{\mu\nu} = \frac{1}{2}\left(\partial_\rho\partial_\nu h^{\rho}_{\mu} - \partial_\rho\partial^\rho h_{\mu\nu} - \partial_\mu\partial_\nu h + \partial_\mu\partial_\rho h^{\rho}_{\nu}\right) - \frac{1}{2}\eta_{\mu\nu}\left(\partial_\rho\partial_\sigma h^{\sigma\rho} - \partial_\rho\partial^\rho h\right). \tag{2.9}$$

Introducing the trace reverse tensor:

$$\overline{h}_{\mu\nu} = h_{\mu\nu} - \frac{1}{2}\eta_{\mu\nu}h \qquad \left(\overline{h} = -h\right), \tag{2.10}$$

$$h_{\mu\nu} = \overline{h}_{\mu\nu} - \frac{1}{2}\eta_{\mu\nu}\overline{h}. \tag{2.11}$$

With this quantity, the field equations (2.9) become,

$$G_{\mu\nu} = -\frac{1}{2}\Box\overline{h}_{\mu\nu} + \frac{1}{2}\partial_\nu\partial_\rho\overline{h}^{\rho}_{\mu} + \frac{1}{2}\partial_\mu\partial_\rho\overline{h}^{\rho}_{\nu} - \frac{1}{2}\eta_{\mu\nu}\partial_\rho\partial_\sigma\overline{h}^{\sigma\rho} = \kappa T_{\mu\nu}. \tag{2.12}$$

Where, $\kappa = \frac{8\pi G}{c^4}$ in SI units. Now, the Gauge fixing condition,

$$\partial_\sigma\overline{h}^{\sigma\rho} = 0,. \tag{2.13}$$

leads to the wave equation for gravitation in the linear approximation:

$$\Box\overline{h}_{\mu\nu} = -2\kappa T_{\mu\nu}. \tag{2.14}$$

This is the most convenient way to express the equations that result from this linear construction. In the following section we will use these equations to obtain the gravitomagnetic equations.

2.2 Gravitomagnetic equations

2.2.1 Non-relativistic Approximation for $\overline{h}_{\mu\nu}$ and $T_{\mu\nu}$

Now we are interested in making an approximation in which the source consists of a perfect non-relativistic fluid (MOORE, 2015). In this case, the pressure p_0 in the source will be negligible compared to the energy density ρ_0 and the four-velocity of the fluid u^α at each point will be such that $u^0 \approx 1$ and $u^i \approx v^i \ll 1$, where the latin indices refer to the spatial part. In this approximation, we keep only the first order terms $u^i \approx v^i$. For this case we have an approximation of low speeds. The components of the energy-momentum tensor will be:

$$T^{00} \approx \rho_0 u^0 u^0 \approx \rho_0, \tag{2.15}$$

$$T^{0i} = T^{i0} \approx \rho_0 u^0 u^i \approx \rho_0 v^i, \tag{2.16}$$

$$T^{ij} \approx \rho_0 u^i u^j \approx 0. \tag{2.17}$$

Also, an approximation for $\overline{h}$ is considered: $\overline{h}_{ij} \approx 0$, this could be the case when (MASHHOON *et al.*, 2001)

$$\overline{h}_{0\mu} \sim O\left(\frac{1}{c^2}\right),\ \overline{h}_{ij} \sim O\left(\frac{1}{c^4}\right).$$

In this approximation, we have:

$$\overline{h} = \eta^{\mu\nu}\overline{h}_{\mu\nu} = \eta^{00}\overline{h}_{00} + \eta^{ij}\overline{h}_{ij} = \eta^{00}\overline{h}_{00},$$

which, by substituting in the equation (2.11), we have:

$$h_{ij} = -\frac{1}{2}\eta_{ij}\eta^{00}\overline{h}_{00}, \tag{2.18}$$

$$h_{00} = \overline{h}_{00} - \frac{1}{2}\eta_{00}\left(\eta^{00}\overline{h}_{00}\right) = \frac{1}{2}\overline{h}_{00}, \tag{2.19}$$

$$h_{0i} = \overline{h}_{0i}, \tag{2.20}$$

$$h = -\eta^{00}\overline{h}_{00} = -2\eta^{00}h_{00}. \tag{2.21}$$

Four equations remain to be analyzed,

$$\Box\overline{h}_{0\nu} = -2\kappa T_{0\nu}, \tag{2.22}$$

as well as the gauge fixing condition (2.13), which now reads:

$$\partial_\sigma\overline{h}^{\sigma 0} = \partial_0\overline{h}^{00} + \partial_i\overline{h}^{i0} = 0, \tag{2.23}$$

$$\partial_0\overline{h}^{0i} = 0. \tag{2.24}$$

The four field equations (2.22) can be rewritten as

$$\Box\overline{h}_{00} = -2\kappa T_{00} \tag{2.25}$$

$$\Box\overline{h}_{0i} = -2\kappa T_{0i} \tag{2.26}$$

Using the following identity

$$\partial_j\left(\partial^j\overline{h}_{0i}\right) = \partial_j\left(\partial^j\overline{h}_{0i}\right) + \partial_i\left(\partial^j\overline{h}_{0j}\right) - \partial_i\left(\partial^j\overline{h}_{0j}\right) \tag{2.27}$$

and the first gauge conditions, the field equations become:

$$\partial_0\left(-\partial_i\overline{h}^{i0}\right) + \partial_i\left(\partial^i\overline{h}_{00}\right) = -2\kappa T_{00}, \tag{2.28}$$

$$\partial_0\left(\partial^0\overline{h}_{0i}\right) + \partial_i\left(\partial^j\overline{h}_{0j}\right) + \varepsilon_{nik}\partial^k\left(\varepsilon^{nmj}\partial_j\overline{h}_{0m}\right) = -2\kappa T_{0i}. \tag{2.29}$$

Again, using the gauge condition the equations became

$$\partial_i\left(\partial^i\overline{h}_{00}-\partial_0\overline{h}^i{}_0\right)=-2\kappa T_{00}, \tag{2.30}$$

$$\partial_0\left(\partial^0\overline{h}_{0i}\right)+\partial_i\left(-\partial_0\overline{h}^{00}\right)+\varepsilon_{nik}\partial^k\left(\varepsilon^{nmj}\partial_j\overline{h}_{0m}\right)=-2\kappa T_{0i}. \tag{2.31}$$

This way:

$$\partial_i\left(-\frac{1}{2}\partial^i\overline{h}_{00}+\frac{1}{2}\partial_0\overline{h}^i{}_0\right)=\kappa T_{00}, \tag{2.32}$$

$$\partial_0\frac{1}{2}\left(-\partial^i\overline{h}_{00}+\partial_0\overline{h}^i{}_0\right)-\varepsilon_{nik}\partial^k\left(\frac{1}{2}\varepsilon^{nmj}\partial_j\overline{h}_{0m}\right)=\kappa T_{0i}. \tag{2.33}$$

2.2.2 Gravitomagnetic fields

Now, we are ready to derive the gravitomagnetic equations. First of all, we need to define the gravitoelectric potential (Φ) and gravitomagnetic vector potential (A^i) and the gravitational charge density (ρ) and current (j_i) according to (MASHHOON *et al.*, 1999)

$$\Phi \equiv \frac{c^2\overline{h}_{00}}{4}, \tag{2.34}$$

$$A^i \equiv -\frac{c^2\overline{h}^i{}_0}{4}, \tag{2.35}$$

$$\rho \equiv \frac{T^{00}}{c^2}, \tag{2.36}$$

$$j^i \equiv \frac{T^{0i}}{c}, \tag{2.37}$$

by replacing in Eq.(2.32) and Eq.(2.33), we will have

$$\begin{cases}\partial_i\left(-\partial^i 2\Phi-\partial_0 2A^i\right)=c^4\kappa\rho\\ -\partial_0\left(-\partial_i 2\Phi-\partial_0 2A^i\right)+\varepsilon_{nik}\partial^k\left(2\varepsilon^{nmj}\partial_j A_m\right)=c^3\kappa j_i\end{cases}$$

Now, with the following definitions for gravitoelectric (E^i) and gravitomagnetic (B^i) fields:

$$E^i \equiv \frac{c^2}{4}\left(-\partial^i\overline{h}_{00}+\partial_0\overline{h}^i{}_0\right)=\left(-\partial^i\Phi-\partial_0 A^i\right), \tag{2.38}$$

$$B^n \equiv \frac{c^2}{4}\varepsilon^{njm}\partial_j\overline{h}_{0m}=\varepsilon^{njm}\partial_j A_m, \tag{2.39}$$

one finds

$$\begin{cases}\partial_i E^i=\frac{\kappa c^4}{2}\rho\\ -\partial_0 E_i+\varepsilon_{ink}\partial^k B^n=\frac{\kappa c^3}{2}j_i\end{cases}$$

or simply, the four gravitomagnetic equations in CGS (Gaussian) units, are:

$$\nabla \cdot \vec{E}_g = -4\pi G\rho_m \tag{2.40}$$

$$\nabla \times \vec{B}_g = -\frac{4\pi G}{c}\vec{J}_m + \frac{1}{c}\frac{\partial \vec{E}}{\partial t}, \tag{2.41}$$

$$\nabla \cdot \vec{B}_g = 0, \tag{2.42}$$

$$\nabla \times \vec{E}_g + \frac{1}{c}\frac{\partial \vec{B}_g}{\partial t} = 0. \tag{2.43}$$

The Maxwell equations in CGS units (JACKSON, 1999) are:

$$\nabla \cdot \vec{E} = 4\pi\rho_c, \tag{2.44}$$

$$\nabla \times \vec{B} = \frac{4\pi}{c}\vec{J}_c + \frac{1}{c}\frac{\partial \vec{E}}{\partial t}, \tag{2.45}$$

$$\nabla \cdot \vec{B} = 0, \tag{2.46}$$

$$\nabla \times \vec{E} + \frac{1}{c}\frac{\partial \vec{B}}{\partial t} = 0, \tag{2.47}$$

The GEM field equations contain the continuity equation $\nabla\cdot\mathbf{j}+\partial\rho/\partial t = 0$, as expected. This equations plays a role analogous to Maxwell equations in which the gravitational field generated by a given matter distribution. However, we can note that with the change from $\rho_c \to -G\rho_m$ and $\vec{J}_c \to -G\vec{J}_m$ Maxwell's equations become the gravitomagnetic equations. Where ρ_m and $\vec{J}_m$ are the density of mass-energy and $\vec{J}_m$ the mass current is given by: $\vec{J}_m = \rho_m\vec{v}$ and the negative sign denotes the attractive nature of gravitation. It's important to highlight that these equations also known as Maxwell-Mashhoon equations are only valid to weak gravitational fields, in a non-relativistic dominium what agrees with the Heaviside (HEAVISIDE, 1893) hypothesis that the Newtonian theory was incomplete. In Tab.(2.1) we compare the electromagnetism with the weak field approximation.

TABLE 2.1 – Analogy between the Electromagnetism and weak field approximation

Description	Electromagnetism	Weak field approximation
Source of field	j^ν	$T^{\mu\nu}$
Conservation law	$\partial_\nu j^\nu = 0$	$\partial_\sigma T^{\sigma\rho} = 0$
Field	A^ν	$h^{\mu\nu}$
Field equation	$\partial_\mu\partial^\mu A^\nu - \partial_\nu\partial^\mu A^\mu = 4\pi j^\nu$	$-\frac{1}{2}\Box\overline{h}_{\mu\nu}+\frac{1}{2}\partial_\nu\partial_\rho\overline{h}^{\ \rho}_{\mu}+\frac{1}{2}\partial_\mu\partial_\rho\overline{h}^{\ \rho}_{\nu}-\frac{1}{2}\eta_{\mu\nu}\partial_\rho\partial_\sigma\overline{h}^{\sigma\rho} = \kappa T_{\mu\nu}$
Gauge condition	$\partial_\mu A^\mu = 0$	$\partial_\sigma\overline{h}^{\sigma\rho} = 0$
Field equation in this gauge	$\partial_\mu\partial^\mu A^\nu = 4\pi j^\nu$	$\Box\overline{h}_{\mu\nu} = -2\kappa T_{\mu\nu}$

Furthermore, considering that all terms of $\mathcal{O}\ (c^{-4})$ are neglected in the GEM analysis,

we can write the spacetime metric as

$$ds^2 = \left(1 + 2\frac{\Phi}{c^2}\right) c^2 dt^2 - \frac{4}{c}(\vec{A} \cdot d\vec{x})dt - \left(1 - 2\frac{\Phi}{c^2}\right) \delta_{ij} dx^i dx^j, \tag{2.48}$$

where Φ is the gravitoelectric scalar potential and $\vec{A}$ is the gravitomagnetic vector potential related to the moving masses in a dynamical system. The gravitoelectric field dependence of time part of the metric is equivalent to the Newtonian potential, and the linear term in the gravitoelectric potential of the metric spacial part and the gravitomagnetic field are the new components in the gravitoelectromagnetic context.

For a complete analogy we need also the gravito-Lorentz force. It is possible to find from the Lagrangian motion of a test particle of mass m, $L = -mcds/dt$, that the gravito-Lorentz force is given by (MASHHOON, 2008):

$$\vec{F}_g = -4\frac{v}{c} \times \vec{B}_g, \tag{2.49}$$

where v is the particle velocity and B_g is the gravitomagnetic field.

In the next section the most known gravitomagnect effect which is the Lense-Thirring effect will be presented.

2.3 Lense-Thirring or "Frame-dragging" Effect

The dragging of inertial frames is a consequence of Einstein's GR (MISNER *et al.*, 1973). In particular, the Lense-Thirring (LT) or frame-dragging effect is observed when we consider a test body in the field of a rotating matter distribution, see Fig. 2.1. This effect was discovered in 1918 by the Austrian physicists Hans Thirring and Josef Lense and in homage to them, it became known as the Lense-Thirring effect. The LT effect predicts the precession of the axis of a gyroscope next to a rotating body as can be seen in (MASHHOON *et al.*, 1984a; CIUFOLINI, 2010; MURPHY, 2009). In this theory, a nonrotating, spherical mass produces the standard and well-tested Schwarzschild field.

Essentially, the frame-dragging of a gyroscope is formally similar to the change of orientation of a magnetic dipole by a magnetic field generated by an electric current in electromagnetism (CHASHCHINA *et al.*, 2008; MASHHOON *et al.*, 1984b) and it is closely related to the existence of the gravitomagnetic field described in the section 2.2.2. Thus, considering the gravitational and electromagnetic analogy, an object with spherical and rotational symmetry produces a dipole magnetic field on its exterior (MOORE, 2015):

$$\vec{B} = -\frac{G}{r^3}[3(\vec{\mu}_g \cdot \hat{r})\hat{r} - \vec{\mu}_g], \tag{2.50}$$

FIGURE 2.1 – Illustration of Lense-Thirring effect or frame-dragging effect in which space and time are dragged around a massive body. Source: (NASA, 2015)

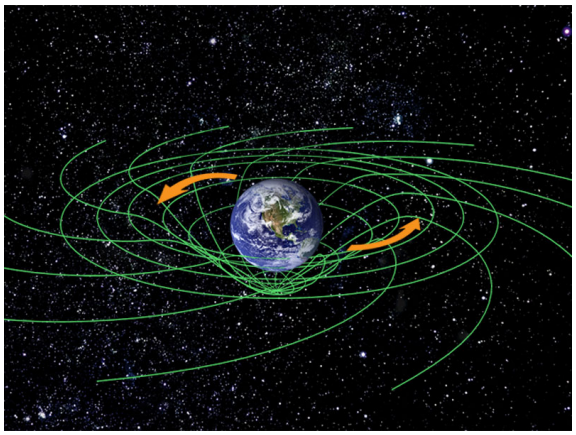

where $\vec{\mu}_g$ is the total gravitomagnetic dipole moment of the object, $\vec{r}$ is the distance from the object to the point where the field will be analyzed, and $\hat{r}$ is a unit vector pointing in the direction $\vec{r}$. By analogy, the gravitomagnetic field produced by a spherical star or planet with total spin angular momentum $\vec{S}$ is

$$\vec{B} = -\frac{G}{r^3}[3(\vec{\mu}_g \cdot \hat{r})\hat{r} - \vec{\mu}_g] = \frac{G}{2cr^3}[\vec{S} - 3(\vec{S} \cdot \hat{r})\hat{r}], \tag{2.51}$$

where factor 2 comes from $\vec{\mu}_g = \frac{1}{2c}\vec{S}$ and the minus sign comes from inversion of the gravitomagnetic field compared to the analogue magnetic field. We can use this to estimate the magnitude and direction of the Lense-Thirring effect near a rotating body of interest.

Therefore, the gravitational field surrounding a rotating mass differs from that surrounding a non-rotating one. This can be understood by analogy with the case of a rotating, uniformly charged sphere, such a sphere produces both electric and magnetic fields, whereas a non-rotating sphere produces only an electric field. Furthermore, frame-dragging has relevant astrophysical applications to the dynamics of matter falling into rotating black holes and of jets in active galactic nuclei and quasars (THORNE, 1986)

2.3.1 Gravitomagnetic fields of Magnetars like White Dwarfs

In the previous section (2.50) we introduce the Lense-Thirring effect and, we have shown that the dipole momentum is associated with the angular momentum and, in this sense, the gravitomagnetic field by a rotating body can be obtained from the GEM equations (2.40) and in MKS can be written as

$$B_g = \frac{G}{2c^2}\frac{\vec{L} - 3(\vec{L} \cdot \vec{r}/r)\vec{r}/r}{r^3} \tag{2.52}$$

at the equatorial plane, $\vec{r}$ and $\vec{L}$ are perpendicular, so their dot product vanishes, and this formula reduces to:

$$B_g = \frac{G}{2c^2}\frac{\vec{L}}{r^3}. \tag{2.53}$$

The magnitude of angular momentum of a homogeneous ball-shaped body is:

$$\vec{L} = I_{\text{ball}}\omega = \frac{2}{5}Mr^2\frac{2\pi}{P} \tag{2.54}$$

where P is the rotational period. Therefore, the gravitomagnetic field magnitude at the surface of a spherical rotating homogeneous rigid boy with mass M and rotational period P at its equator is:

$$B_g = \frac{2\pi GM}{5rc^2P}. \tag{2.55}$$

In table 2.2 we have the properties such as period, mass, radius, and inertia momentum of Magnetars like White dwarfs (LOBATO *et al.*, 2016). Following this article, mass-radius and momentum of inertia calculations for rotating white dwarfs were obtained for the corresponding rotational periods of several SGRs and AXPs this is an work in progress in our group. With this results, it is possible to find the gravitomagnetic field (B_G) and the ratio of gravitomagnetic and gravitoelectric components of Lorentz force Eq.(2.49) for these objects at their surface.

TABLE 2.2 – Properties of rotating stars considering the periods of the sources. Source: (OLAUSEN; KASPI, 2014)

Stars	P (s)	mass ($M/M_\odot$)	radius (R/km)	log (I/g cm^2)
SGR 1900+14	5.19987	1.369	1913.537	49.600
1E 1048.1-5	6.457875	1.365	1906.164	49.596
1E 2259+586	6.9790427	1.364	1903.389	49.594
SGR 1806-20	7.54773	1.363	1903.468	49.594
SGR 1833-08	7.5654084	1.363	1903.528	49.594
CXOU J01004	8.020392	1.363	1905.086	49.594
SGR 0526-66	8.0544	1.362	1905.143	49.594
SWIFT J1822	8.4377210	1.362	1901.263	49.592
4U 0142+61	8.6886924	1.362	1896.439	49.590
SGR 0418+57	9.0783882	1.362	1898.004	49.591
CXO J164710	10.610644	1.361	1902.246	49.592
1RXS J17084	11.005024	1.360	1900.912	49.592
3XMM J18524	11.558713	1.360	1895.205	49.589
1E 1841-045	11.788978	1.360	1892.255	49.588

Despite the increase in the angular momentum of the star as a white dwarf due to the increase in radius in the inertia momentum I (since the inertia momentum goes with r^2), the effect is still small, due to the formula of dipole gravitomagnetic the field B goes with $1/r^3$ also the angular momentum L goes with r^2 so B_g at the star surface goes with

TABLE 2.3 – Gravitoelectric and gravitomagnetic fields, gravito-Lorentz force and ratio of gravitomagnetic and gravitoelectric forces at the star surface.

Stars	$g = GM/r^2$	B_g (Hz)	$4vB_g$ (m/s^2)	$4vB_g/g$
SGR 1900+14	49376550	0.00026	2403.46184	4.87×10^{-5}
1E 1048.1-5	49613875	0.00021	1557.0744	3.14×10^{-5}
1E 2259+586	49722194	0.00019	1301.68164	2.62×10^{-5}
SGR 1806-20	49681616	0.00018	1140.30576	2.30×10^{-5}
SGR 1833-08	49678484	0.00018	1137.67704	2.29×10^{-5}
CXOU J01004	49597262	0.00017	1014.3492	2.05×10^{-5}
SGR 0526-66	49557908	0.00017	1010.09648	2.04×10^{-5}
SWIFT J1822	49760385	0.00016	905.6416	1.82×10^{-5}
4U 0142+61	50013860	0.00015	822.423	1.64×10^{-5}
SGR 0418+57	49931416	0.00015	787.7694	1.58×10^{-5}
CXO J164710	49672473	0.00013	585.4472	1.18×10^{-5}
1RXS J17084	49705667	0.00012	520.68096	1.05×10^{-5}
3XMM J18524	50005473	0.00012	494.25072	9.88×10^{-6}
1E 1841-045	50161510	0.00011	443.52264	8.84×10^{-6}

$1/r$. Thus, since in the surface $v = \omega r$ the term related to the gravitomagnetic force $4vB_g$ does not have a dependence on the star radius r. In table 2.3 the ratio of gravitomagnetic and gravitoelectric forces at the star surface for the magnetars seen as very massive and magnetic white dwarfs is shown and is very small of the order 10^{-5}. Outside the star this ratio depends on the particle velocity and goes with $1/r$ where r is the distance to the star center.

In the next section, we will present the experiment designed to measure this effect and others from the theory of general relativity, called classical tests.

2.4 Tests of General Relativity

2.4.1 LAGEOS and LAGEOS 2

LAGEOS (LAser GEOdynamics Satellite) was launched in 1976 by NASA and LAGEOS 2 in 1992 by ASI (Italian Space Agency) and NASA to measure - via laser ranging, "crustal movements, plate motion, polar motion, and Earth rotation". LAGEOS is a high-altitude, spherical, laser ranged satellite (see Fig. 2.2). It is made of heavy brass and aluminum (CIUFOLINI; WHEELER, 1995). They are two almost identical passive satellites covered with 426 corner cube reflectors to reflect back the laser pulses emitted by the stations of the satellite laser ranging (SLR) network (CIUFOLINI I. *et al.*, 2016). Furthermore, the GRACE (Gravity Recovery and Climate Experiment) space mission, launched in 2002 has allowed extremely accurate determinations of the Earth's gravitational field

and its temporal variations (CIUFOLINI; PAVLIS, 2004).

FIGURE 2.2 – Illustrated scheme of LAGEOS satellite structure. Adapted from: (CIUFOLINI; WHEELER, 1995)

LAGEOS and LAGEOS 2 observed the frame-dragging in 1997 - 1998 and measured with approximately 10% accuracy in 2004 - 2010 (CIUFOLINI; PAVLIS, 2004; CIUFOLINI; WHEELER, 1995; CIUFOLINI I. *et al.*, 2016). The LAGEOS, LAGEOS 2, and the Earth's gravity field determinations by the space geodesy mission GRACE (CIUFOLINI *et al.*, 2012) and their orbit can be seen in Fig. 2.3. In 2011 the dedicated space mission Gravity Probe B, reported also a test of frame-dragging with approximately 20% accuracy as we will show in the following subsection.

2.4.2 Gravity Probe B Mission

On April 20, 2004, NASA launched the Gravity Probe B mission (NASA, 2015; BIEMOND, 2004; MOORE, 2015) which took an experiment into space to test Einstein's General Theory of Relativity, more specifically the experiment sought to test two predicted effects by theory, the distortion and the space drag. The first effect is caused by the mass distribution and the second is caused by the movement of the mass.

To measure the Lense-Thirring effect and the geodetic effect the probe carried four precise gyroscopes, each consisting of an almost perfect quartz sphere electrostatically suspended camera. The gyroscope were pointed in the direction of a star guide. The star chosen was IM Pegasi, or HR8703, in the constellation of Pegasus, and about 300 light-years from us. It is a binary system (two stars orbiting a common mass center), and the reasons for this choice were, its position close to the celestial equator, to be bright enough to be observed by the telescope of the mission, and its brightness used as a reference, and, for its movement to be well known, because this system is a strong source of radio waves. The two effects predicted in relation to the star IM Pegasi are presented schematically in Fig. 2.4.

In general, the experiment consists of:

- Placing a gyroscope and a telescope in a polar-orbiting satellite, 642 km above the Earth.

FIGURE 2.3 – Illustration of the satellites LAGEOS, LAGEOS 2, and GRACE orbits that was used to measure the Lense-Thirring effect. The long red arrow is the combination of the nodal longitudes of the LAGEOS satellites. Source: (CIUFOLINI; PAVLIS, 2004)

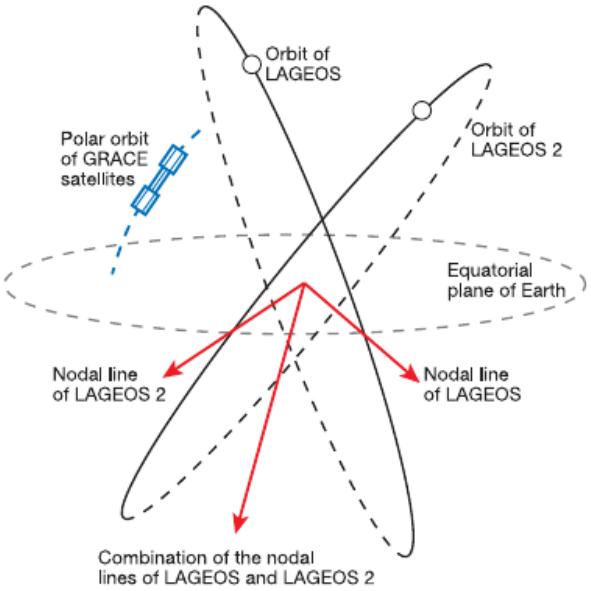

- At the start of the experiment, align both the telescope and the spin axis of each gyroscope with a distant reference point a guide star.
- Keeping the telescope aligned with the guide star for a year, as the spacecraft makes over 5.000 orbits around the Earth, and measure the change in the spin-axis alignment of each gyro over this period in both the plane of the orbit (the geodetic precession) and orthogonally in the plane of the Earth's rotation (frame-dragging precession).

The GPB is NASA's second experiment to test General Relativity. The first was Gravity Probe A, which studied the effect of the gravitational field on the measurements of time using hydrogen clocks. This experiment is due to the gravitational redshift and it was the first test of gravitation proposed by Einstein and is known as one of three classic tests of General Relativity.

The existence of the gravitational redshift arises from the principle of equivalence so that a clock in one gravitational field is indistinguishable from another identical clock in an accelerated frame. The first measurement of gravitational redshift which had 1% of precision was performed by Robert Pound and Glen Rebka in 1960, using two atomic clocks in vertical movement in the tower of the University of Havard. The most accurate gravitational redshift test was performed by Vessot et. al. (VESSOT *et al.*, 1980).

The Gravity Probe A compared the elapsed time in two identical hydrogens, one on Earth and the other traveling for about two hours on a rocket. The Gravity Probe A

FIGURE 2.4 – Schematic representation of the LT (horizontal) and de-Sitter (vertical) precessions. In which the de-Sitter or Geodetic effect represents the precession due the space-time curvature caused by the Earth and the LT is caused by the way in which spacetime is dragged around by a rotating body. Source: (EVERITT *et al.*, 2011)

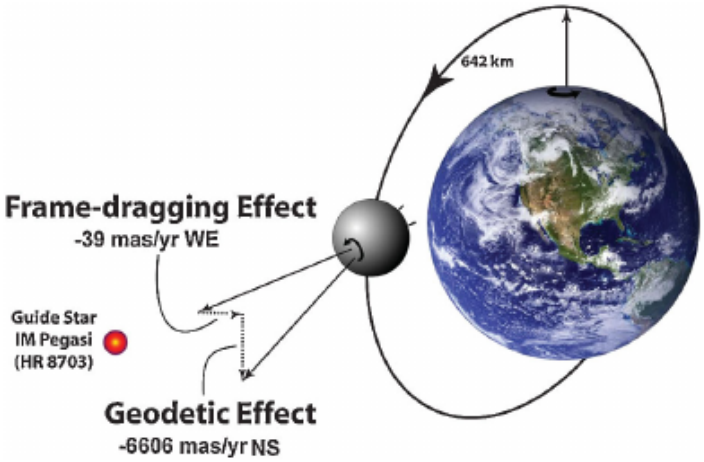

satellite was launched on June 18, 1976, at an altitude of 10.000 km in an approximately vertical trajectory. This experiment confirmed the prediction of gravitational redshift to an accuracy of 0.02%.

The main purpose of the GPB experiment is to detect the LT effect with high accuracy and about 1% error. After eighteen months of data analysis, the first results of the GPB experiment were presented, the de-Sitter effect[1] was clearly visible on the gyroscopes of the GPB, confirming Einstein's predictions to an accuracy of about 1.5% (EVERITT *et al.*, 2011), the GPB researchers explained that the deviations from the expected results arose from the torques produced on the gyroscopes (NASA, 2015). The results presented in September 2009 clearly show the existence of the LT effect, which was accurately measured at 14%. The signals from the four gyroscopes were analyzed independently and the results were combined and checked in several ways (EVERITT *et al.*, 2011).

TABLE 2.4 – Gravity Probe B test results. Source: (EVERITT *et al.*, 2011)

Source	de-Sitter effect (msa/year)	Lense-Thirring effect (msa/year)
Gyroscope 1	$-6.588,6 \pm 31.7$	-41.3 ± 24.6
Gyroscope 2	$-6.707,0 \pm 64.1$	-16.1 ± 29.7
Gyroscope 3	$-6.610,7 \pm 43.2$	-25.0 ± 12.1
Gyroscope 4	$-6.588,7 \pm 33.2$	-49.3 ± 11.4
Average	$\mathbf{-6.601,8 \pm 18.3}$	$\mathbf{-37.2 \pm 7.2}$
GR Prediction	$-6.606,1$	-39.2

The final results presented by the GPB are exposed in the Tab. 2.4, and as we can

[1]Some authors (CIUFOLINI, 1994) have interpreted the de Sitter effect as a kind of Lense-Thirring effect due to the orbital angular momentum of the central static mass.

see the results of Gravity Probe B were highly satisfactory and clearly show the existence of the LT effect, which was measured to an accuracy of approximately 14%. This was the first test of the drag effect of space, but the effect of distortion by mass distribution has already been verified in several astronomical observations.

Several experiments were proposed to measure frame-dragging or Lense-Thirring precession, and the gravitomagnetic field generated by the angular momentum of a body (CIUFOLINI *et al.*, 1997; CIUFOLINI; PAVLIS, 2004; CIUFOLINI *et al.*, 1996): from the observations of the LAGEOS (LAser GEOdynamics Satellite) and LAGEOS II satellites, that were launched in 1976 by NASA, and jointly in 1992 by ASI (Italian Space Agency) and NASA, respectively; to the Gravity Probe B space experiment launched by NASA in 2004. Frame-dragging was observed, by using LAGEOS and LAGEOS II, with approximately 10 % accuracy. In the figure 2.5, we present a timeline summarizing these main events and its respective accuracies.

In this chapter, we review the formalism of gravitomagnetism starting from the GR equations, we show that in the regime of weak field and slow-motion approximation the Einstein's field equations with an appropriated choice of potentials can be written in the same form as Maxwell's equations from the electromagnetism. We also have shown the *frame-dragging* or Lense-Thirring effect that is the effect caused by the movement of the mass. We also presented a timeline of the most important experiments made along with of almost 80 years that intent to test the Lense-Thirring effect.

FIGURE 2.5 – Timeline of the GR experiments

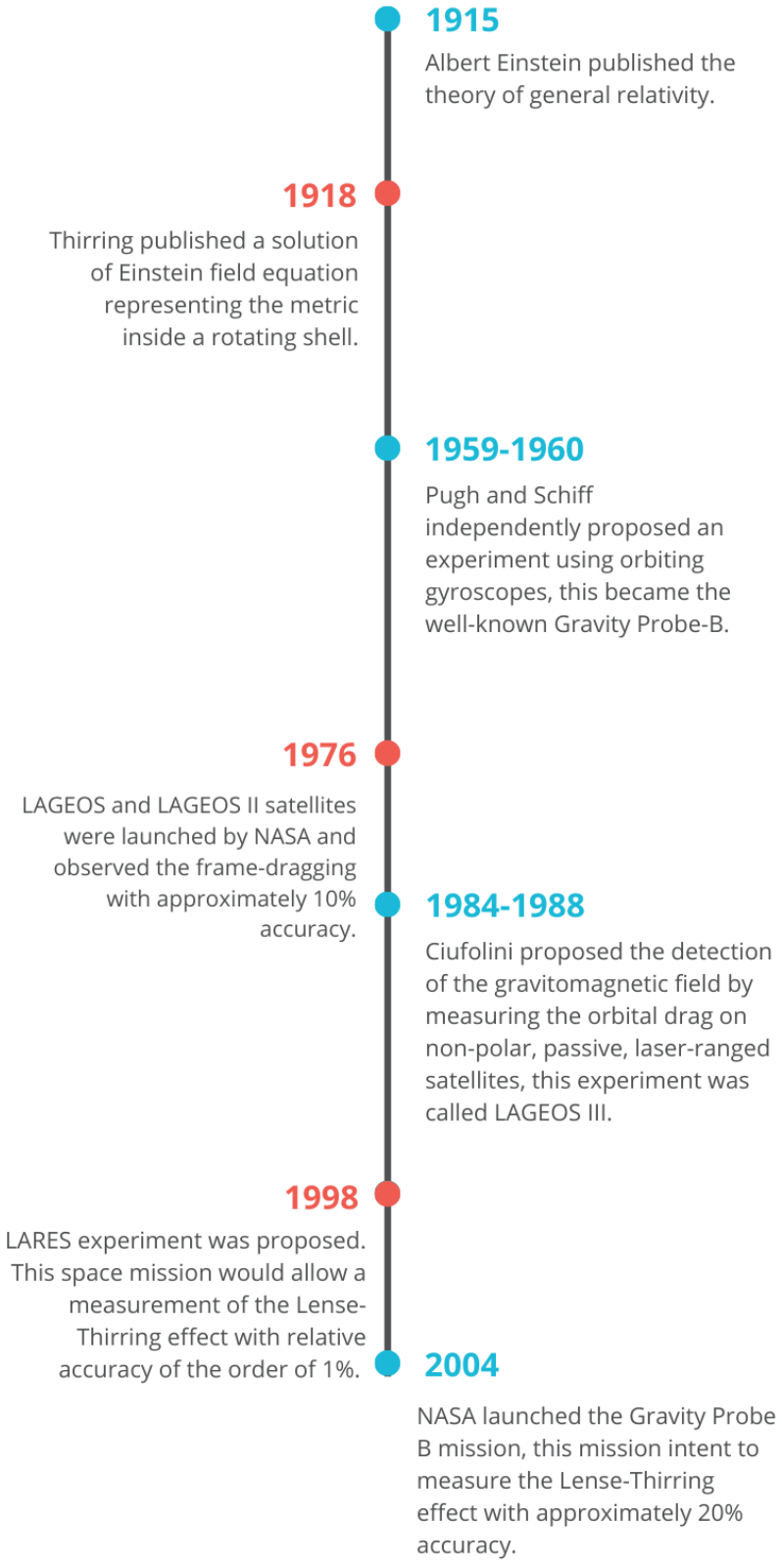

3 Beyond Gravitomagnetism Approximation

The expansion of both sides of Einstein's field equations in the weak-field approximation, up to terms of order $1/c^4$, is derived for the first time. This approach leads to an extended form of gravitomagnetism properly named Beyond Gravitomagnetism (BGEM). In this chapter will be presented the obtention of the formalism and the application to Mercury's perihelion advance and bending of light. We also compare our new approximation with other more known GR approximations, such as Newtonian, post-Newtonian and GEM in order to clarify the novelty of our BGEM formalism.

3.1 Expansion of Einstein's field equations

In order to solve the Einstein's field equations it is worth to work with the weak-field approximation, in this case, the metric tensor is assumed to be a perturbation of the Minkowski metric such that $g_{\mu\nu} = \eta_{\mu\nu} + h_{\mu\nu}$. Furthermore, defining the trace-reversed amplitude $\overline{h}_{\mu\nu} = h_{\mu\nu} - \frac{1}{2}\eta_{\mu\nu}h \quad \left(\overline{h} = -h\right)$, and introducing the gauge condition $\partial_\sigma \overline{h}^{\sigma\rho} = 0$, one obtains the linearized Einstein's field equations (WEYL, 1922; D'INVERNO, 1992; THORNE, 1986; MISNER *et al.*, 1973)

$$\Box^2 \bar{h}^{\mu\nu} = -\frac{16\pi G}{c^4} T^{\mu\nu}, \tag{3.1}$$

where $\Box^2$ is the D'Alembert operator, G is the gravitational constant, c is the speed of light and $T^{\mu\nu}$ is the energy-momentum tensor. However, due to the Bianchi identity, a direct mathematical consequence of the Einstein field equations is that the covariant divergence of the energy-momentum tensor of the matter is zero. Consequently, as stated by Landau & Lifshitz (LANDAU; LIFSHITZ, 1971), this equation does not generally express any conservation law. This is related to the fact that in a gravitational field the energy-momentum tensor of the matter alone is not conserved, rather it must be conserved together with the gravitational field.

Therefore, one possible way to explain the perihelion advance of planets in linearized theory is to include on the right-hand side of Einstein's field equations (3.1) an energy-momentum tensor term to account for matter-geometry coupling

$$\Box^2 \bar{h}^{\mu\nu} = -2\kappa(T^{\mu\nu} + t^{\mu\nu}). \tag{3.2}$$

where $\kappa = \frac{8\pi G}{c^4}$. The energy-momentum tensor $t_{\mu\nu}$ of the gravitational field itself, in other words, includes nonlinear terms. However, there is not a unique way to define $t_{\mu\nu}$ (FEYNMAN *et al.*, 2002; OHANIAN; RUFFINI, 2013). Our approach is to expand the metric $g_{\mu\nu}$ in small perturbations $h_{\mu\nu}$ around the Minkowski metric $\eta_{\mu\nu} = (1, -1, -1, -1)$ and expand $g_{\mu\nu}$ up to second order in $h_{\mu\nu}$ corresponding to $\mathcal{O}(1/c^4)$.

Following (WEINBERG, 2013), the metric can be expanded in powers of $\epsilon = v/c$ as

$$\begin{aligned} g_{00} &= \eta_{00} + \overset{2}{h}_{00} + \overset{4}{h}_{00} + \cdots \\ g_{0i} &= \overset{3}{h}_{0i} + \overset{5}{h}_{0i} + \cdots \\ g_{ij} &= \eta_{ij} + \overset{2}{h}_{ij} + \overset{4}{h}_{ij} + \cdots \end{aligned} \tag{3.3}$$

where the upper numbers indicate the order of expansion. The expansion can be justified from the following line element

$$ds^2 = g_{00}c^2dt^2 + 2g_{0i}cdtdx^i + g_{ij}dx^idx^j \tag{3.4}$$

or

$$\left(\frac{ds}{dt}\right)^2 = g_{00}c^2 + 2g_{0i}cv^i + g_{ij}v^iv^j \tag{3.5}$$

where a change $t \to -t$ implies $v^i \to -v^i$; thus g_{0i} must have odd powers in ϵ, and g_{00} and g_{ij} even powers. The inverse of the metric is obtained by taking $g^{\mu\alpha}g_{\alpha\nu} = \delta^\mu_{\ \nu}$, leading to

$$\begin{aligned} g^{0\alpha}g_{\alpha 0} &= g^{00}g_{00} + g^{0i}g_{i0} = 1 \\ g^{0\alpha}g_{\alpha j} &= g^{00}g_{0j} + g^{0i}g_{ij} = 0 \\ g^{i\alpha}g_{\alpha j} &= g^{i0}g_{0j} + g^{ik}g_{kj} = 0. \end{aligned} \tag{3.6}$$

also, the contravariant expansion of Eq.(3.3) is

$$\begin{aligned} g^{00} &= \eta^{00} + \overset{2}{h}^{00} + \overset{4}{h}^{00} + \cdots \\ g^{0i} &= \overset{3}{h}^{0i} + \overset{5}{h}^{0i} + \cdots \\ g^{ij} &= \eta^{ij} + \overset{2}{h}^{ij} + \overset{4}{h}^{ij} + \cdots. \end{aligned} \tag{3.7}$$

Therefore, by replacing the covariant and contravariant expanded metrics in the inverse metric, we obtain

$$\overset{2}{h}^{00} = -\overset{2}{h}_{00}, \qquad \overset{2}{h}^{ij} = -\overset{2}{h}_{ij}, \qquad \overset{3}{h}^{0i} = \overset{3}{h}_{0i}, \qquad \cdots . \tag{3.8}$$

In doing the calculations, every time derivative increases the order of the term by one. The results for the expansion of the Christoffel symbols are presented in Appendix A.1, and the Ricci tensor is obtained from the expanded Christoffel symbols as shown in eq. (2.8), can be expanded as

$$R_{00} = \overset{2}{R}_{00} + \overset{4}{R}_{00} + \cdots \tag{3.9}$$

$$R_{0j} = \overset{3}{R}_{0j} + \overset{5}{R}_{0j} + \cdots \tag{3.10}$$

$$R_{jk} = \overset{2}{R}_{jk} + \overset{4}{R}_{jk} + \cdots . \tag{3.11}$$

The components are

$$R_{00} = \Gamma^{\sigma}_{00,\sigma} - \Gamma^{\sigma}_{0\sigma,0} + \Gamma^{\rho}_{00}\Gamma^{\sigma}_{\rho\sigma} - \Gamma^{\rho}_{0\sigma}\Gamma^{\sigma}_{\rho 0}, \tag{3.12}$$

$$R_{0i} = \Gamma^{\sigma}_{0i,\sigma} - \Gamma^{\sigma}_{0\sigma,i} + \Gamma^{\rho}_{0i}\Gamma^{\sigma}_{\rho\sigma} - \Gamma^{\rho}_{0\sigma}\Gamma^{\sigma}_{\rho i}, \tag{3.13}$$

$$R_{ij} = \Gamma^{\sigma}_{ij,\sigma} - \Gamma^{\sigma}_{i\sigma,j} + \Gamma^{\rho}_{ij}\Gamma^{\sigma}_{\rho\sigma} - \Gamma^{\rho}_{i\sigma}\Gamma^{\sigma}_{\rho j}, \tag{3.14}$$

whose order by order gives

$$\overset{2}{R}_{00} = \overset{2}{\Gamma}^{i}_{00,i} \tag{3.15}$$

$$\overset{4}{R}_{00} = \overset{4}{\Gamma}^{i}_{00,i} - \overset{3}{\Gamma}^{i}_{0i,0} + \overset{2}{\Gamma}^{i}_{00}\overset{2}{\Gamma}^{j}_{ij} - \overset{2}{\Gamma}^{0}_{0i}\overset{2}{\Gamma}^{i}_{00} \tag{3.16}$$

$$\overset{3}{R}_{0i} = \overset{3}{\Gamma}^{j}_{0i,j} - \overset{2}{\Gamma}^{j}_{ij,0} \tag{3.17}$$

$$\overset{2}{R}_{ij} = \overset{2}{\Gamma}^{k}_{ij,k} - \overset{2}{\Gamma}^{0}_{i0,j} - \overset{2}{\Gamma}^{k}_{ik,j} \tag{3.18}$$

$$\overset{4}{R}_{ij} = \overset{4}{\Gamma}^{k}_{ij,k} - \overset{4}{\Gamma}^{0}_{i0,j} - \overset{4}{\Gamma}^{k}_{ik,j} + \overset{2}{\Gamma}^{k}_{ij}\overset{2}{\Gamma}^{0}_{k0} + \overset{2}{\Gamma}^{k}_{ij}\overset{2}{\Gamma}^{l}_{kl} - \overset{2}{\Gamma}^{0}_{i0}\overset{2}{\Gamma}^{0}_{0j} - \overset{2}{\Gamma}^{k}_{il}\overset{2}{\Gamma}^{l}_{kj} + \overset{3}{\Gamma}^{0}_{ij,0}. \tag{3.19}$$

In order to derive the metric up to fourth-order in $1/c$, we also have to expand Einstein's field equations. We write the field equations as

$$R_{\mu\nu} = \kappa\left(T_{\mu\nu} - \frac{1}{2}g_{\mu\nu}T\right) = T'_{\mu\nu} - \frac{1}{2}g_{\mu\nu}T' = S_{\mu\nu}, \tag{3.20}$$

where $T' = \kappa T$ and $T'_{\mu\nu} = \kappa T_{\mu\nu}$.

The components of the Ricci tensor are presented, up to $\mathcal{O}(\epsilon^4)$, in equations (A.30) to

(A.34) of the Appendix A.2. It is possible to make a great simplification in these equations by using the harmonic gauge condition[1],

$$g^{\mu\nu}\Gamma^{\alpha}_{\mu\nu} = 0, \tag{3.21}$$

whose terms of second, third, and fourth orders can be written, respectively, as

$$\frac{1}{2}\partial_i \overset{2}{h}_{00} + \partial_j \overset{2}{h}_{ij} - \frac{1}{2}\partial_i \overset{2}{h}_{jj} = 0, \tag{3.22}$$

$$\frac{1}{2}\partial_0 \overset{2}{h}_{00} - \partial_i \overset{3}{h}_{0i} + \frac{1}{2}\partial_0 \overset{2}{h}_{ii} = 0, \tag{3.23}$$

$$\begin{aligned} &-\frac{1}{2}\overset{2}{h}_{00}\partial_k \overset{2}{h}_{00} + \frac{1}{2}\partial_k \overset{4}{h}_{00} - \partial_0 \overset{3}{h}_{0k} + \frac{1}{2}\overset{2}{h}_{kl}\partial_l \overset{2}{h}_{00} \\ &-\frac{1}{2}\overset{2}{h}_{ij}\partial_k \overset{2}{h}_{ij} + \frac{1}{2}\overset{2}{h}_{ij}\partial_j \overset{2}{h}_{ki} + \frac{1}{2}\overset{2}{h}_{ij}\partial_i \overset{2}{h}_{jk} - \frac{1}{2}\partial_k \overset{4}{h}_{ii} \\ &+\partial_i \overset{4}{h}_{ki} - \frac{1}{2}\overset{2}{h}_{kl}\partial_l \overset{2}{h}_{ii} + \overset{2}{h}_{kl}\partial_i \overset{2}{h}_{li} = 0. \end{aligned} \tag{3.24}$$

Next, we take the derivative with respect to x^0 of (A.45) and (A.47). Also with respect to x^j of (A.47) and (A.51). Finally, with respect to x^k of (A.45). Working with equations (A.30) to (A.34), we obtain

$$\overset{2}{R}_{00} = \frac{1}{2}\nabla^2 \overset{2}{h}_{00}, \tag{3.25}$$

$$\overset{4}{R}_{00} = \frac{1}{2}\nabla^2 \overset{4}{h}_{00} - \frac{1}{2}\partial_0\partial_0 \overset{2}{h}_{00} + \frac{1}{2}\overset{2}{h}_{ij}\partial_i\partial_j \overset{2}{h}_{00} - \frac{1}{2}\left(\nabla \overset{2}{h}_{00}\right)^2, \tag{3.26}$$

$$\overset{3}{R}_{0i} = \frac{1}{2}\nabla^2 \overset{3}{h}_{0i}, \tag{3.27}$$

$$\overset{2}{R}_{ij} = \frac{1}{2}\nabla^2 \overset{2}{h}_{ij}, \tag{3.28}$$

$$\begin{aligned} \overset{4}{R}_{ij} = &\frac{1}{2}\nabla^2 \overset{4}{h}_{ij} + \frac{1}{2}\partial_i\partial_j \overset{4}{h}_{00} + \delta_{ij}\nabla^2\phi^2 - \delta_{ij}\partial_0\partial_0\phi \\ &- 2\partial_j\phi\partial_i\phi \end{aligned} \tag{3.29}$$

Now, we are able to work with the energy-momentum tensor. From (3.20) we can find

[1]The gauge calculations are described in Appendix A.3

the following expansions for the components of the tensor $T^{\mu\nu}$

$$
\begin{aligned}
T'^{00} =& \overset{2}{T}'^{00} + \overset{4}{T}'^{00} + \cdots = \frac{8\pi G}{c^4}\left(\overset{-2}{T}^{00} + \overset{0}{T}^{00} + \cdots\right), \\
T'^{0j} =& \overset{3}{T}'^{0j} + \cdots \frac{8\pi G}{c^4}\left(\overset{-1}{T}^{0j} + \ldots\right), \\
T'^{ij} =& \overset{4}{T}'^{ij} + \cdots = \frac{8\pi G}{c^4}\left(\overset{0}{T}^{ij} + \cdots\right),
\end{aligned}
$$

whose trace is

$$
T' = g_{00}T'^{00} + 2g_{0j}T'^{j0} + g_{ij}T'^{ji} = \overset{2}{T}' + \overset{3}{T}' + \overset{4}{T}' \tag{3.30}
$$

where

$$
\begin{aligned}
&\overset{2}{T}' = \overset{2}{T}'^{00}, \\
&\overset{3}{T}' = 0, \\
&\overset{4}{T}' = \overset{4}{T}'^{00} + \overset{2}{h}_{00}\overset{2}{T}'^{00} + \eta_{ij}\overset{4}{T}'^{ij}.
\end{aligned}
$$

It is important to note that when we explicitly introduce the constants, the order in $1/c$ of the terms changes. The covariant tensor $T'_{\mu\nu}$ is given by

$$
T'_{\mu\nu} = g_{\mu\alpha}g_{\nu\beta}T'^{\alpha\beta} = g_{\mu0}g_{\nu0}T'^{00} + g_{\mu0}g_{\nu j}T'^{0j} + g_{\mu i}g_{\nu0}T'^{i0} + g_{\mu i}g_{\nu j}T'^{ij} \tag{3.31}
$$

whose components are

$$
\begin{aligned}
&\overset{2}{T}'_{00} = \overset{2}{T}'^{00} \\
&\overset{4}{T}'_{00} = \overset{4}{T}'^{00} + 2\overset{2}{h}_{00}\overset{2}{T}'^{00} \\
&\overset{3}{T}'_{0i} = -\overset{3}{T}'^{0i} \\
&\overset{4}{T}'_{ij} = \overset{4}{T}'^{ij}.
\end{aligned}
$$

The expansion of the right-hand side of Einstein's field equation

$$
S_{00} = \overset{2}{S}_{00} + \overset{4}{S}_{00} + \cdots, \tag{3.32}
$$

$$
S_{0j} = \overset{3}{S}_{0j} + \cdots, \tag{3.33}
$$

$$
S_{ij} = \overset{2}{S}_{ij} + \cdots. \tag{3.34}
$$

Using 3.20, leads to

$$\overset{2}{S}_{00} = \frac{1}{2}\overset{2}{T'^{00}}, \tag{3.35}$$

$$\overset{3}{S}_{0j} = \overset{3}{T'_{0j}} = -\overset{3}{T'^{0j}} \tag{3.36}$$

$$\overset{4}{S}_{00} = \frac{1}{2}\left(\overset{4}{T'^{00}} + 2\overset{2}{h}_{00}\overset{2}{T'^{00}} + \overset{4}{T'^{ii}}\right), \tag{3.37}$$

$$\overset{2}{S}_{ij} = -\frac{1}{2}\eta_{ij}\overset{2}{T'^{00}}, \tag{3.38}$$

$$\overset{4}{S}_{ij} = \overset{4}{T'}_{ij} - \frac{1}{2}\left(\eta_{ij} + \overset{2}{h}_{ij}\right)\left(\overset{2}{T'^{00}} + \overset{4}{T'^{00}} + \overset{2}{h}_{00}\overset{2}{T'^{00}} + \eta_{kl}\overset{4}{T'^{kl}}\right). \tag{3.39}$$

Finally, the field equations become

$$\frac{1}{2}\nabla^2\overset{2}{h}_{00} = \frac{1}{2}\overset{2}{T'^{00}}, \tag{3.40}$$

$$\frac{1}{2}\nabla^2\overset{4}{h}_{00} - \frac{1}{2}\partial_0\partial_0\overset{2}{h}_{00} + \frac{1}{2}\overset{2}{h}_{ij}\partial_i\partial_j\overset{2}{h}_{00} - \frac{1}{2}\left(\nabla\overset{2}{h}_{00}\right)^2 = \frac{1}{2}\left(\overset{4}{T'^{00}} + 2\overset{2}{h}_{00}\overset{2}{T'^{00}} + \overset{4}{T'^{ii}}\right), \tag{3.41}$$

$$\frac{1}{2}\nabla^2\overset{3}{h}_{0j} = \overset{3}{T'}_{0j} = -\overset{3}{T'^{0j}}, \tag{3.42}$$

$$\frac{1}{2}\nabla^2\overset{2}{h}_{ij} = -\frac{1}{2}\eta_{ij}\overset{2}{T'^{00}}, \tag{3.43}$$

$$\frac{1}{2}\nabla^2\overset{4}{h}_{ij} + \frac{1}{2}\partial_i\partial_j\overset{4}{h}_{00} + \delta_{ij}\nabla^2\phi^2 - \delta_{ij}\partial_0\partial_0\phi - 2\partial_j\phi\partial_i\phi = \overset{4}{T'}_{ij} - \frac{1}{2}\eta_{ij}\overset{4}{T'^{00}} + \frac{1}{2}\eta_{ij}\overset{4}{T'^{kk}}. \tag{3.44}$$

The new variable $\overset{2}{h}_{00} = \frac{2\Phi}{c^2}$, can be substituted in (3.40), resulting in

$$\nabla^2\Phi = 4\pi\frac{G\overset{-2}{T^{00}}}{c^2} = 4\pi\rho, \tag{3.45}$$

where Φ is the Newtonian potential and $\rho = \frac{\overset{-2}{GT^{00}}}{c^2}$. This equation is analogous to the Gauss law in electrodynamics for the negative charge case, and the solution is straightforward:

$$\Phi(\vec{x}, t) = -\int \frac{\rho(\vec{x}, t)}{|\vec{x} - \vec{x}'|}d^3x'. \tag{3.46}$$

Furthermore, we can substitute in (3.42) the new variable $\overset{3}{h}_{0j} = -\frac{2A^j}{c^2} = \frac{2A_j}{c^2}$, resulting in

$$\nabla^2 A^j = \frac{4\pi}{c}\frac{2G\overset{-1}{T^{0j}}}{c} = \frac{4\pi}{c}J^j, \tag{3.47}$$

where $J^j = \frac{2G\overset{-1}{T^{0j}}}{c}$. This is analogous to the vector potential in electrodynamics due to the current of negative charges, whose solution is

$$\vec{A} = -\frac{1}{c}\int \frac{\vec{J}(\vec{x},t)}{|\vec{x}-\vec{x}'|}d^3x'. \tag{3.48}$$

The solution of (3.43) gives

$$\overset{2}{h}_{ij}(\vec{x},t) = -\delta_{ij}\frac{2G}{c^4}\int \frac{\overset{-2}{T^{00}}}{|\vec{x}-\vec{x}'|}d^3x' = \delta_{ij}\frac{2\Phi}{c^2}. \tag{3.49}$$

Using the above results in (3.41), and applying the identity $\nabla\Phi\cdot\nabla\Phi = \frac{1}{2}\nabla^2\Phi^2 - \Phi\nabla^2\Phi$, we obtain

$$\nabla^2\overset{4}{h}_{00} = \frac{2}{c^4}\frac{\partial^2\Phi}{\partial t^2} + \frac{2}{c^4}\nabla^2\Phi^2 + \frac{8\pi G}{c^4}\left(\overset{0}{T^{00}} + \overset{0}{T^{ii}}\right), \tag{3.50}$$

whose solution gives

$$\overset{4}{h}_{00} = \frac{2}{c^4}\Phi^2 + \frac{2\psi}{c^4}, \tag{3.51}$$

being ψ defined by

$$\psi = -\int \frac{d^3x'}{|\vec{x}-\vec{x}'|}\left[\frac{1}{4\pi}\frac{\partial^2\Phi}{\partial t^2} + G\left(\overset{0}{T^{00}} + \overset{0}{T^{ii}}\right)\right]. \tag{3.52}$$

Moreover, by solving (3.44) we can obtain the field equation for the $\overset{4}{h}_{ij}$ component

$$\begin{aligned}\nabla^2\overset{4}{h}_{ij} = &-\frac{\partial^2(2\phi^2+2\psi)}{\partial x^i\partial x^j c^4} - 2\delta_{ij}\nabla^2\frac{\phi^2}{c^4} + 2\delta_{ij}\frac{\partial_0\partial_0\phi}{c^2} \\ &+ 4\frac{\partial_j\phi\partial_i\phi}{c^4} + 2\overset{4}{T'}_{ij} - \eta_{ij}\overset{4}{T'^{00}} + \eta_{ij}\overset{4}{T'^{kk}}\end{aligned} \tag{3.53}$$

that leads to

$$\overset{4}{h}_{ij} = -2\frac{\phi^2}{c^4}\delta_{ij} + \frac{\chi_{ij}}{c^4} \tag{3.54}$$

where,

$$\chi_{ij} = -\frac{1}{4\pi}\int \frac{d^3x'}{|\vec{x}-\vec{x}'|}\left[-\frac{\partial^2(2\phi^2+2\psi)}{\partial x^i \partial x^j} + 2\delta_{ij}\frac{\partial^2\phi}{\partial t^2} \right.$$
$$\left. +4\partial_j\phi\partial_i\phi + 8\pi G\left(2\overset{4}{T}_{ij} - \eta_{ij}\overset{4}{T}^{00} + \eta_{ij}\overset{4}{T}^{kk}\right)\right] \tag{3.55}$$

Therefore, in this approximation the metric reads

$$g_{\mu\nu} = \begin{bmatrix} 1+\frac{2}{c^2}\Phi+\frac{2}{c^4}\Phi^2+\frac{2}{c^4}\psi & -2\frac{\vec{A}}{c^2} \\ -2\frac{\vec{A}}{c^2} & -\left(1-\frac{2\Phi}{c^2}+\frac{2\Phi^2}{c^4}\right)\delta_{ij}+\frac{\chi_{ij}}{c^4} \end{bmatrix}.$$

Also, the following line element corresponds to the spacetime metric of Beyond Gravitomagnetism:

$$ds^2 = \left(1+\frac{2}{c^2}\Phi+\frac{2}{c^4}\Phi^2+\frac{2}{c^4}\psi\right)c^2dt^2 + \frac{4}{c}(\vec{A}\cdot\vec{dx})\,dt$$
$$-\left[\left(1-\frac{2\Phi}{c^2}+\frac{2\Phi^2}{c^4}\right)\delta_{ij}-\frac{\chi_{ij}}{c^4}\right]dx^i dx^j, \tag{3.56}$$

where Φ is the gravitoelectric potential (or simply Newtonian potential) and $\vec{A}$ is the gravitomagnetic vector potential. The mass current concept remains known in conventional gravitomagnetism. Note that, in this metric, we have a quadratic term in the gravitoelectric potential. This term does not appear in conventional gravitomagnetism but is essential in achieving the exact value of Mercury's perihelion advance. Furthermore, we have the term χ, which also incorporates nonlinear terms.

In slow motion and weak-field approximation, General Relativity predicts that a rotating central body with mass, and angular momentum induces a gravitoelectric field that depends only on the mass of the body and also a smaller perturbation is known as gravitomagnetic field that depends on angular momentum and leads to the Lense-Thirring precession. The spacetime metric in the GEM formalism is given by eq. (2.48) (MASHHOON, 2003)

Moreover, the known *"post-Newtonian approximation"* proposed by Chandrasekhar in 1965, is the formalism of Newtonian theory plus post-Newtonian corrections (CHANDRASEKHAR, 1965). The corrections of post-Newtonian formalism (1PN) consist of the expansion of the metric tensor to find an approximate solution for Einstein's field equations. In this case, we have weak-field, slow-motion expansion, that gives: flat, empty spacetime in "zero-order", the Newtonian treatment of Solar System in the "first-order", and post-Newtonian corrections to the Newtonian treatment in "second order" (WILL, 2014; MISNER *et al.*, 1973).

TABLE 3.1 – The Minkowiski, Newtonian, Post-Newtonian, Gravitomagnetism and Beyond Gravitomagnetism expansions of the metric coefficients and its respective orders.

Level of approximation	g_{00}	g_{0i}	g_{ij}
Minkowiski	1	0	$-\delta_{ij}$
Newtonian	2Φ	0	0
post-Newtonian (CHANDRASEKHAR, 1965)	+ terms $\sim \epsilon^4$	+ terms $\sim \epsilon^3$	+ terms $\sim \epsilon^2$
post-post-Newtonian (CHANDRASEKHAR; ESPOSITO, 1970)	+ terms $\sim \epsilon^6$	+ terms $\sim \epsilon^5$	+ terms $\sim \epsilon^4$
Gravitomagnetism	+ terms $\sim \epsilon^2$	+ terms $\sim \epsilon^3$	+ terms $\sim \epsilon^2$
Beyond Gravitomagnetism	+ terms $\sim \epsilon^4$	+ terms $\sim \epsilon^3$	+ terms $\sim \epsilon^4$

In Tab. 3.1, we present the different types of approximations in the Einstein field equations compared with the one proposed in this work, i.e., the beyond Gravitomagnetism. In the Newtonian limit, the term of $1/c^2$ in the space metric function and terms of $1/c^3$ and higher are neglect. On the other hand, Gravitomagnetism includes terms of $1/c^2$ in the time and space metric functions and also terms of $1/c^3$ and introduces the vector potential. The post-Newtonian expansion takes into account terms of higher order of the Newtonian case. However, the beyond Gravitomagnetism presents terms of higher order than the Gravitomagnetic case.

3.2 Beyond Gravitomagnetism correction to Mercury's perihelion advance

3.2.1 Mercury's Perihelion Advance

In 1859, Le Verriere observed that the orbit of Mercury precessed by about 574.1 arcseconds per Earth-century and the Newtonian mechanics with the contribution of the perturbations caused by other planets predicts a precession of 531.6 arcseconds per Earth-century then the observed precession exceeds the calculated one by 43 arcseconds per Earth-century. It is also now known that corrections to the Newton-Kepler model are required to account for the perihelion advance of Venus, and also of Earth (DESHMUKH *et al.*, 2017).

Some years later, this discrepancy was solved by Einstein's general relativity theory which predicts the exact 43 arcseconds to the perihelion precession of Mercury (SHAPIRO *et al.*, 1972); this extra precession involves relativistic modifications of the gravitational

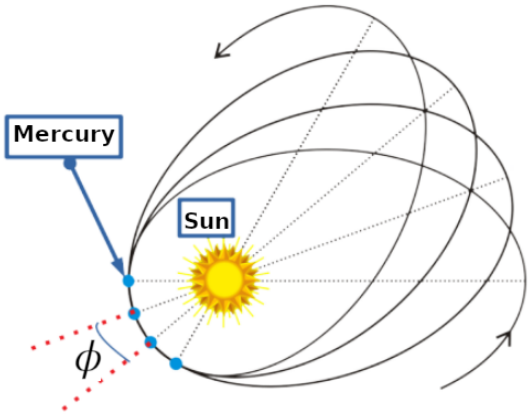

FIGURE 3.1 – The Mercury orbit around the Sun. The angle of precession at points closest to the Sun (perihelion) is identified by the angle ϕ. Source: (MIRANDA, 2019)

field and of the equation of motion and this was one of the classical tests of the general relativity. The perihelion advance is obtained by using the Schwarzschild solution to Einstein's field equation that considers a static Sun.

In Tab. 3.2, we present the astronomical data for the planet Mercury.

TABLE 3.2 – Mercury's astronomical data. Source:(NASA, 2019)

Lenght of the year	87.9691 Earth days
Mass m	$3.30104 \times 10^{23} kg$
Volume V	$6.0827208742 \times 10^{16} m^3$
Mean orbit velocity v_0	$4.7362 \times 10^4 m/s$
Orbit eccentricity e	0.20563593
Equatorial inclination	0 degrees

Therefore, in the following sections, we will discuss the problem of Mercury perihelion orbit and the deflection of light in the context of the beyond gravitomagnetism.

3.2.2 The Precession of Mercury's Perihelion with BGEM

Mercury's perihelion advance will be obtained by finding the orbit equation from ds^2 and solving the equation perturbatively – we follow (WEBER, 1961). To do so, we consider a static Sun, absence of source and boundary conditions for ϕ which implies $\vec{A} = \psi = \chi_{ij} = 0$, recovering the Newtonian case with additional terms of $\mathcal{O}(1/c^4)$. From the line element, we can find the Lagrangian for the system. Neglecting the mc term, we have

$$L = e^{\mu} c^2 \dot{t}^2 - e^{\nu}(\dot{r}^2 + r^2\dot{\theta}^2 + r^2 \sin\theta \dot{\phi}^2), \tag{3.57}$$

where $e^{\mu} = 1 + \frac{2\Phi}{c^2} + \frac{2\Phi^2}{c^4}$ and $e^{\nu} = 1 - \frac{2\Phi}{c^2} + \frac{2\Phi^2}{c^4}$. Furthermore, we can consider that for the perihelion advance the movement is restricted to a plane, thus working with fixed $\theta = \pi/2$ and $\dot{\theta} = 0$. Then, the Euler Lagrange equations for t and ϕ provide

$$\dot{t} = \frac{k}{e^{\mu}}, \qquad \dot{\phi} = \frac{l}{r^2 e^{\nu}}. \tag{3.58}$$

The constant k is related to the energy and the constant l is related to the angular momentum. Instead of using the Euler Lagrange equation for r we use the line element divided by ds^2

$$e^{\mu} c^2 \dot{t}^2 - e^{\nu}(\dot{r}^2 + r^2\dot{\theta}^2 + r^2 \sin\theta \dot{\phi}^2) = 1. \tag{3.59}$$

Employing Eq. (3.58) in Eq. (3.59) and defining $r = 1/u$, also considering $\frac{du}{ds} = \frac{du}{d\phi}\frac{d\phi}{ds}$, we obtain

$$\left(\frac{du}{d\phi}\right)^2 + u^2 + \frac{e^{\nu}}{l^2}\left(1 - \frac{k^2 c^2}{e^{\mu}}\right) = 0. \tag{3.60}$$

Taking the derivative of equation (3.60) with respect to ϕ, using the definitions of $e^{\mu}(u)$ and $e^{\nu}(u)$, expanding up to quadratic terms in u, and substituting

$$k^2 = \frac{2l^2 C}{c^2 R_S}, \tag{3.61}$$

where

$$C = \frac{GM_{\odot}m^2}{\ell^2} = \frac{1}{a(1-\epsilon^2)}, \tag{3.62}$$

we obtain a differential equation for the u variable. In (3.62), ℓ represents the angular momentum of the planet, a is the semi-major axis of the ellipse and ϵ is the eccentricity. The final result up to quadratic terms in u is

$$\begin{aligned} &\frac{d^2u}{d\phi^2}(1 - R_s u) - \frac{R_s}{2}\left(\frac{du}{d\phi}\right)^2 - \frac{3}{2}R_s u^2 \\ &+ u(1 - CR_s) - C = 0, \end{aligned} \tag{3.63}$$

where R_s is the Schwarzschild radius, i.e., $\frac{2GM}{c^2}$. For Mercury, $C = 1.8 \times 10^{-13}\,\mathrm{cm}^{-1}$. We know that u is periodic, so that this equation can be solved by expanding u in a Fourier series

$$u(\phi) = a_0 + a_1 \cos(\rho\phi), \tag{3.64}$$

assuming that at the perihelion $\phi = 0$, one obtains $a_0 + a_1 = C(1+\epsilon)$, that leads to

$$\rho = 1 - \frac{3CR_s}{2}, \tag{3.65}$$

and the perihelion – the point of the closest approach in the orbit – has the following advance

$$\Delta\phi = \frac{6\pi G M_\odot}{ac^2(1-\epsilon^2)}. \tag{3.66}$$

Equation (3.66) gives the same result obtained with Schwarzschild solution, which leads to a predicted advance of Mercury's perihelion of 42.95 arcsec/cy.

However, for the gravitomagnetic spacetime metric under the same conditions, i.e., considering static Sun ($\vec{A} = 0$), the time and space metric functions are, respectively, $e^\mu = 1 + \frac{2\Phi}{c^2}$ and $e^\nu = 1 - \frac{2\Phi}{c^2}$. Substituting then in the Lagrangian,

$$L = e^\mu c^2 \dot{t}^2 - e^\nu(\dot{r}^2 + r^2\dot{\theta}^2 + r^2 \sin\theta \dot{\phi}^2), \tag{3.67}$$

Doing the same calculations as before one finds, i.e., working with fixed $\theta = \pi/2$ and $\dot{\theta} = 0$, we find

$$\frac{k^2c^2}{(1-R_s u)} - \frac{l^2(\frac{du}{d\phi})^2}{(1+R_s u)} - \frac{u^2 l^2}{(1+R_s u)} = 1. \tag{3.68}$$

Expanding up to quadratic terms in u and substituting (3.61), one finds (see Appendix C)

$$\frac{d^2u}{d\phi^2}(1-R_s u) - \frac{R_s}{2}\left(\frac{du}{d\phi}\right)^2 - (\frac{3}{2}+C)R_s u^2 + (1-2C)\,R_s u - C = 0, \tag{3.69}$$

We can solve this equation by expanding u in a Fourier series as we did before in Eq.(3.64), but in this case of GEM with a static Sun the ρ is defined as

$$\rho = 1 - 2CR_s, \tag{3.70}$$

and since $\rho\phi = 2\pi$ that leads to following perihelion advance

$$\Delta\phi = \frac{8\pi G M_\odot}{ac^2(1-\epsilon^2)}. \tag{3.71}$$

This equation leads to a Mercury's perihelion advance of 57.2 arcsec/cy, which is 4/3 of the correct value. This difference can be attributed to the absence of the term $\frac{2\Phi^2}{c^4}$, which only appears when we use BGEM including higher-order corrections ($\frac{1}{c^4}$) in the space-time metric as we are going to explain in the next section.

3.2.3 Generalized Orbital Equation for the Problem of Mercury Perihelion Advance

In this subsection we intent to analyze the problem of mercury perihelion advance for this we will generalize the orbital equation. The Lagrangian of the system can be written as

$$L = e^{\mu}c^2\dot{t}^2 - e^{\nu}(\dot{r}^2 + r^2\dot{\theta}^2 + r^2\sin\theta\dot{\phi}^2), \tag{3.72}$$

where the time metric function e^{μ} and the space one e^{ν} are now written in a generalized form

$$\begin{aligned} e^{\mu} &= 1 + \frac{2A\Phi}{c^2} + \frac{2B\Phi^2}{c^4}, \\ e^{\nu} &= 1 - \frac{2D\Phi}{c^2} + \frac{2E\Phi^2}{c^4}, \end{aligned} \tag{3.73}$$

in which the constant C is given by Eq. (3.62) and A, B, D, and E are constants with values given in Table 3.3 that can reproduce the Newtonian, post-Newtonian (P1N), Gravitomagnetism (GEM), and BEGEM approximations in the case of a static Sun, which implies $\vec{A} = \psi = \chi_{ij} = 0$. Doing the same calculations as shown in section 3.2.2, we find a generalized orbital equation

$$\begin{aligned} &(1 + (D - 2A)R_s u)\frac{d^2u}{d\phi^2} - \frac{DR_s}{2}\left(\frac{du}{d\phi}\right)^2 \\ &- (AE + AD^2 - 2BD)CR_s^2u^2 + \left(\frac{D}{2} - 2A\right)R_s u^2 \\ &+ ((1 - (2AD - B)C)R_s u - AC = 0. \end{aligned} \tag{3.74}$$

Using the values of the Table 3.3 for the Newtonian case, the equation reads

$$(1 - 2R_s u)\frac{d^2u}{d\phi^2} - 2R_s u^2 + 1 - C = 0. \tag{3.75}$$

For the first post-Newtonian case, we find

$$(1 - R_s u)\frac{d^2u}{d\phi^2} - \frac{R_s}{2}\left(\frac{du}{d\phi}\right)^2 + CR_s^2u^2 - \frac{3}{2}R_s u^2 + (1 - C)R_s u - C = 0 \tag{3.76}$$

For the Gravitomagnetic case, we have

$$(1 - R_s u)\frac{d^2u}{d\phi^2} - \frac{R_s}{2}\left(\frac{du}{d\phi}\right)^2 - CR_s^2u^2 - \frac{3}{2}R_s u^2 + (1 - 2C)R_s u - C = 0. \tag{3.77}$$

Finally, for the beyond gravitomagnetic case, we found

$$(1 - R_s u)\frac{d^2u}{d\phi^2} - \frac{R_s}{2}\left(\frac{du}{d\phi}\right)^2 - \frac{3}{2}R_s u^2 + (1 - C)R_s u - C = 0. \tag{3.78}$$

From eq.(3.74), we can notice that the nonlinear term of the spacial part of the metric $\left(\frac{2E\Phi^2}{c^4}\right)$ is not relevant to the Mercury perihelion problem, since it yields only to negligible terms proportional to u^2 on the equation of motion, and does not appear in the linear term relevant for this problem, as you can see in (3.74). Moreover, we can also notice from eq.(3.74) that the nonlinear term of the temporal part of the metric $\left(\frac{2B\Phi^2}{c^4}\right)$ leads to a linear term $(BCR_s u)$ in the orbit equation which is essential to give the correct value for the Mercury's perihelion advance, and also explains why the gravitomagnetic approximation fails in explaining the perihelion problem while beyond gravitomagnetism and post-Newtonian approximations are successful.

TABLE 3.3 – Values of the constants A, B, D e E in the generalized form of the metric functions for Newtonian, post-Newtonian, Gravitomagnetism, and Beyond Gravitomagnetism approximations, where all cases consider static Sun which implies $\vec{A} = \psi = \chi_{ij} = 0$.

Approach	A	B	D	E
Newtonian	1	0	0	0
post-Newtonian	1	1	1	0
Gravitomagnetism	1	0	1	0
Beyond Gravitomagnetism	1	1	1	1

3.3 Deflection of Light According to Beyond Gravitomagnetism

3.3.1 Deflection of Light

The deflection of light is another classical test of general relativity. However, different from the Mercury's perihelion advance that was a problem already known, the deflection of light was proposed by Einstein as a test.

In response to Einstein's prediction of light deflection, Eddington and Dyson organized two expeditions to observe the eclipse of May 29, 1919, on Sobral (Brazil) and Principe (Gulf of Guinea). The experiment is done during the eclipse because observations of this effect are difficult to measure and stars near the Sun are only visible during a total eclipse of the Sun. In Figure 3.2, we have a scheme of the deflection of light, according to

Einstein's calculations. The angle of deflection of light is 1.75 arcsec or almost the double predicted with calculations of Newtonian mechanics.

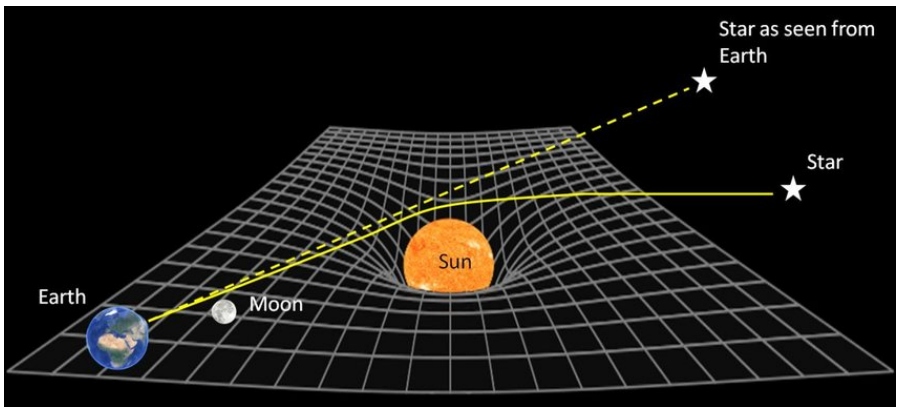

FIGURE 3.2 – Scheme of the deflection of light by the Sun. Source: (PAOLOZZI. *et al.*, 2015)

The experimental procedure consists of taking a photograph of the star field surrounding the eclipsed Sun and comparing this photograph with another one taken at night several months before or after when the Sun is not in the star field. One of the technical difficulties is that the eclipse photograph must be taken in the very short time interval. Two telescopes were used for the experiment, see Fig. 3.3. The main telescope had been withdrawn from the Greenwich Observatory. It had a very wide field of vision which in theory, would make it possible to photograph more stars around the Sun during the eclipse.

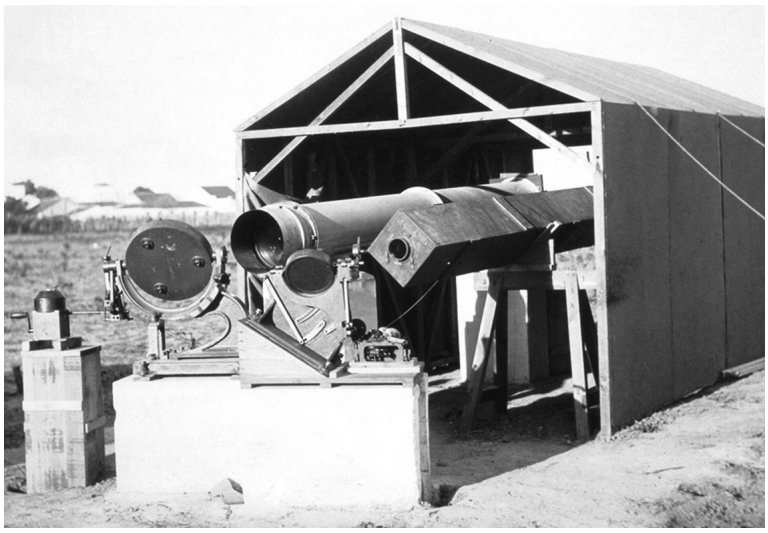

FIGURE 3.3 – Eclipse instruments at Sobral in Brazil. The two telescopes are mounted horizontally and mirrors (center left) are used to throw the Sun's image into them. Source:(OLIVEIRA *et al.*, 2019)

3.3.2 Deflection of Light with BGEM

In this section, we will approach the deflection in the context of the beyond gravitomagnetism from the lagrangian obtained in the section 3.1.

For the bending of light, we must again consider the metric Eq. (3.56) for a static Sun. The integrals Eq. (3.58) are still valid. However, to find how light propagates in a gravitational field we must take into account that light consists of photons. Instead of Eq. (3.59) we must consider a corresponding relation for null intervals. Setting the squared-line element equal to zero and dividing by ds^2:

$$e^{\mu}c^2\dot{t}^2 - e^{\nu}(\dot{r}^2 + r^2\dot{\theta}^2 + r^2\sin\theta\dot{\phi}^2) = 0. \tag{3.79}$$

Employing Eq. (3.58) in Eq. (3.79), and letting $r = 1/u$, leads to the equation

$$-e^{-\nu}l^2u_{\phi}^2 - e^{-\nu}l^2u^2 + e^{-\mu}k^2c^2 = 0. \tag{3.80}$$

Multiplying this equation by e^{μ} and deriving it with respect to ϕ and neglecting terms of order above u^2, we find

$$\frac{d^2u}{d\phi^2} + u = -R_s\left[\left(\frac{du}{d\phi}\right)^2 + u^2\right]. \tag{3.81}$$

This equation can be solved perturbatively, giving the first-order solution

$$u(\phi) = \frac{\cos\phi}{r_0} - \frac{R_s}{r_0^2} + \frac{R_s}{r_0^2}\cos\phi, \tag{3.82}$$

where r_0 is the impact parameter, i.e., if we consider the deviation of a photon by the Sun the minimum r_0 corresponds to the Sun's radius. In the limit $r \to \infty$, $u = 0$ and $\phi_{\infty} = \frac{\pi}{2} + \alpha_1$. Now, inserting ϕ_{∞} into Eq. (3.82), expanding $\cos\phi_{\infty}$ in Taylor series for small α_1 and solving for α_1 we obtain that

$$\alpha_1 = -\frac{2GM_{\odot}}{c^2r_0}. \tag{3.83}$$

The total deviation is then

$$\alpha = 2|\alpha_1| = \frac{4GM_{\odot}}{c^2r_0}. \tag{3.84}$$

The above outcome is equal to the GR result obtained by using the Schwarzschild metric. It is worth noticing that the deflection of light can be obtained even in the lowest order of approximation in our approach, i.e., in this problem the nonlinear terms can be neglected.

In this chapter, the expansion of both sides of Einstein's field equations in the weak-field approximation, up to terms of order $1/c^4$, were derived. This new approach leads to

an extended form of gravitomagnetism (GEM) properly named Beyond Gravitomagnetism (BGEM). The metric of BGEM includes a quadratic term in the gravitoelectric potential in the time and also space metric functions in contrast with first post-Newtonian 1PN approximation where the quadratic term appear only in the time metric function. This non-linear term does not appear in conventional GEM, but is essential in achieving the exact value of Mercury's perihelion advance as we have explicitly shown by generalizing the orbital equation. The new BGEM metric is also applied to the classical problem of light deflection by the Sun, but the contribution of the new non-linear terms produce higher order terms in this problem and can be neglected, giving the correct result obtained already in the Lense-Thirring (GEM) approximation.

4 Studies of Charged White dwarfs in the f(R,T) Gravity

As mentioned in the introduction, this work approach two subjects: the *gravitomagnetism effect* and the effect of $f(R, \mathcal{T})$ *gravity* in charged white dwarfs. Furthermore, in this part of the work, the equilibrium configuration of white dwarfs composed of a charged perfect fluid is investigated in the context of the $f(R, \mathcal{T})$ gravity. By considering the functional form $f(R, \mathcal{T}) = R + 2\chi\mathcal{T}$, where χ is the matter-geometry coupling constant, and for a Gaussian ansatz for the electric distribution, some physical properties of charged white dwarfs will be derived, namely: mass, radius, charge, electric field, effective pressure, and energy density; their dependence on the parameter χ will also be presented.

4.1 Motivation

The white dwarfs they are the final evolution state of main sequence stars with initial masses up to $8.5 - 10.6 M_{\odot}$. However, if the WD mass grows over 1.44 $M_{\odot}$ - known as Chandrasekhar mass limit (CHANDRASEKHAR, 1931) - as in binary systems, where the main star is receiving mass from a nearby star, a type Ia supernova (SNIa) explosion may occur. However, with the recently observed peculiar highly over-luminous SNeIa, such as, SN 2003fg, SN 2006gz, SN 2007if, SN 2009dc (HOWELL, 2006; SCALZO, 2010) it is possible to confirm the existence of a huge Ni-mass which leads to the possibility of massive super-Chandrasekhar white dwarfs with mass $2.1 - 2.8\ M_{\odot}$ as their most feasible progenitors.

To provide some physical mechanism where a super-Chandrasekhar white dwarf could support the gravitational collapse a lot of works have bubbled in the literature with different proposals. To cite some of them, we have: general relativistic (CARVALHO *et al.*, 2020c; BOSHKAYEV *et al.*, 2014), strong magnetic field (DAS; MUKHOPADHYAY, 2013; DAS; MUKHOPADHYAY, 2012; FRANZON; SCHRAMM, 2015; FRANZON; SCHRAMM, 2017; CHATTERJEE *et al.*, 2016; OTONIEL *et al.*, 2019; BERA; BHATTACHARYA, 2016), modified theories of gravity (PANAH; LIU, 2019; LIU; LÜ, 2019; CARVALHO *et al.*, 2017; DAS; MUKHOPADHYAY,

2015; BANERJEE *et al.*, 2017; KALITA; MUKHOPADHYAY, 2018), background gravity corrections (RAY *et al.*, 2019), rotation (BOSHKAYEV *et al.*, 2012; BOSHKAYEV *et al.*, 2011), noncommutativity (PAL; NANDI, 2019) and charge effects (LIU *et al.*, 2014; CARVALHO *et al.*, 2018).

Some works have also approached the coupling between charge and $f(R,\mathcal{T})$ gravity effects for stellar equilibrium (SHARIF; SIDDIQA, 2017; DEB *et al.*, 2019a; ABBAS; AHMED, 2019; SHARIF; WASEEM, 2018). Those works showed in particular, that charged objects have more stable configurations than non-charged ones. They also showed that the energy conditions are respected inside the compact objects.

Here, we are particularly interested to study the charge effects within the framework of the $f(R,\mathcal{T})$ gravity, for the hydrostatic equilibrium configurations of white dwarfs. A few works (JING; WEN, 2016; COSTA *et al.*, 2017; PANAH; LIU, 2019; DAS; MUKHOPADHYAY, 2015; KALITA; MUKHOPADHYAY, 2018; LIU; LÜ, 2019) have achieved stable stellar models to explain super-Chandrasekhar white dwarfs in the background of the different modified theories of gravity. Although few researchers (FREIRE *et al.*, 2012; JAIN *et al.*, 2016; BANERJEE *et al.*, 2017; SALTAS *et al.*, 2018) have studied WD properties via scalar-tensor or Horndeski theories they have only derived constraints on the parameters of the theories by comparing their results with WD observational data and not discussed the issue of super-Chandrasekhar white dwarfs lie in the range 2.1 - 2.8 $M_{\odot}$. Since, $f(R,\mathcal{T})$ gravity has remarkably explained both the late-time accelerated expanding phase of the Universe in the large scale and also passed the solar system test, it will also be very interesting to study compact stellar objects like WDs in the framework of $f(R,\mathcal{T})$ gravity theory. We shall going find that our investigation reveals that the present $f(R,\mathcal{T})$ gravity model can suitably explain the highly super-Chandrasekhar mass white dwarfs.

4.2 $f(R,\mathcal{T})$ gravity

The modified form of the Einstein-Hilbert action in the Einstein-Maxwell space-time is as follows (HARKO *et al.*, 2011):

$$S=\frac{1}{16\pi}\int d^4x f(R,\mathcal{T})\sqrt{-g}+\int d^4x\mathcal{L}_m\sqrt{-g}+\int d^4x\mathcal{L}_e\sqrt{-g}, \tag{4.1}$$

where $T_{\mu\nu}$ is the energy-momentum tensor of the matter distribution, $\mathcal{L}_m$ represents the Lagrangian for the matter distribution and $\mathcal{L}_e$ denotes the Lagrangian for the electromagnetic field.

Now, varying the action (4.1) with respect to the metric tensor component $g_{\mu\nu}$ we obtain the field equations of the model in $f(R,\mathcal{T})$ gravity theory as follows (HARKO *et al.*,

2011):

$$G_{\mu\nu} = \frac{1}{f_R(R,\mathcal{T})}\left[8\pi T_{\mu\nu} + \frac{1}{2}f(R,\mathcal{T})g_{\mu\nu} - \frac{1}{2}Rf_R(R,\mathcal{T})g_{\mu\nu} - (T_{\mu\nu}+\Theta_{\mu\nu})f_T(R,\mathcal{T}) + 8\pi E_{\mu\nu}\right], \quad (4.2)$$

where we define $f_R(R,\mathcal{T}) = \frac{\partial f(R,\mathcal{T})}{\partial R}$, $\Theta_{\mu\nu} = \frac{g^{\alpha\beta}\delta T_{\alpha\beta}}{\delta g^{\mu\nu}}$ and $f_{\mathcal{T}}(R,\mathcal{T}) = \frac{\partial f(R,\mathcal{T})}{\partial \mathcal{T}}$.

Here $\Box \equiv \partial_\mu(\sqrt{-g}g^{\mu\nu}\partial_\nu)/\sqrt{-g}$ is the D'Alambert operator, $R_{\mu\nu}$ is the Ricci tensor, ∇_μ represents the covariant derivative associated with the Levi-Civita connection of $g_{\mu\nu}$, $G_{\mu\nu}$ is the Einstein tensor and $E_{\mu\nu}$ is the electromagnetic energy-momentum tensor.

We define $T_{\mu\nu}$ and $E_{\mu\nu}$ as follows:

$$T_{\mu\nu} = (\rho + p)\, u_\mu u_\nu + p g_{\mu\nu}, \quad (4.3)$$

$$E_{\mu\nu} = \frac{1}{4\pi}\left(F^\gamma_\mu F_{\nu\gamma} - \frac{1}{4}g_{\mu\nu}F_{\gamma\beta}F^{\gamma\beta}\right), \quad (4.4)$$

where u_μ is the four velocity which satisfies the conditions $u_\mu u^\mu = 1$ and $u^\mu \nabla_\nu u_\mu = 0$, respectively, ρ and p represent matter density and pressure, respectively. In the present work, we consider $\mathcal{L}_m = -p$ and we obtain $\Theta_{\mu\nu} = -2T_{\mu\nu} - p g_{\mu\nu}$.

Now, the covariant divergence of Eq. (4.2) reads

$$\nabla^\mu T_{\mu\nu} = \frac{f_T(R,\mathcal{T})}{8\pi - f_T(R,\mathcal{T})}\left[(T_{\mu\nu}+\Theta_{\mu\nu})\nabla^\mu ln f_T(R,\mathcal{T}) + \nabla^\mu\Theta_{\mu\nu} - \frac{1}{2}g_{\mu\nu}\nabla^\mu T - \frac{8\pi}{f_T(R,\mathcal{T})}\nabla^\mu E_{\mu\nu}\right]. \quad (4.5)$$

Now, if we consider the simplest linear form of the function $f(R,\mathcal{T})$ as $f(R,\mathcal{T}) = R + 2\chi\mathcal{T}$, where χ is the matter-geometry coupling constant, the field equation for $f(R,\mathcal{T})$ gravity theory reads

$$G_{\mu\nu} = (8\pi + 2\chi)T_{\mu\nu} + 2\chi p g_{\mu\nu} + \chi\mathcal{T}g_{\mu\nu} + 8\pi E_{\mu\nu} = 8\pi\left(T^{eff}_{\mu\nu} + E_{\mu\nu}\right) = 8\pi T_{\mu\nu}, \quad (4.6)$$

where $T_{ab} = T^{eff}_{\mu\nu} + E_{\mu\nu}$ represents the energy-momentum tensor of the charged effective matter distribution and $T^{eff}_{\mu\nu}$ represents energy-momentum tensor of the effective fluid, i.e., "normal" matter and the new kind of fluid which originates due to the matter geometry coupling, given as

$$T^{eff}_{\mu\nu} = T_{\mu\nu}\left(1 + \frac{\chi}{4\pi}\right) + \frac{\chi}{8\pi}(\mathcal{T} + 2p)\, g_{\mu\nu}. \quad (4.7)$$

Substituting $f(R,\mathcal{T}) = R + 2\chi\mathcal{T}$ in Eq. (4.5), we obtain

$$(4\pi + \chi)\,\nabla^{\mu}T_{\mu\nu} = -\frac{1}{2}\chi\Big[g_{\mu\nu}\nabla^{\mu}\mathcal{T} + 2\nabla^{\mu}\,(pg_{\mu\nu}) + \frac{8\pi}{\chi}E_{\mu\nu}\Big]. \tag{4.8}$$

4.2.1 Stellar Equilibrium Equations

Let consider the interior space-time is described by the metric as follows (D'INVERNO, 1992):

$$ds^2 = e^{\nu(r)}dt^2 - e^{\lambda(r)}dr^2 - r^2(d\theta^2 + \sin^2\theta d\phi^2), \tag{4.9}$$

where the metric potentials ν and λ are the function of the radial coordinate r only.

Now substituting Eqs. (4.3) and (4.4) into Eq. (4.6) we find the explicit form of the Einstein field equation for the interior metric (4.9) as follows (MORAES *et al.*, 2016; CARVALHO *et al.*, 2017):

$$\begin{aligned} \mathrm{e}^{-\lambda}\left(\frac{\lambda'}{r} - \frac{1}{r^2}\right) + \frac{1}{r^2} &= (8\pi + 3\chi)\,\rho - \chi p + \frac{q^2}{r^4} \\ &= 8\pi\rho^{\mathit{eff}} + \frac{q^2}{r^4}, \end{aligned} \tag{4.10}$$

$$\begin{aligned} \mathrm{e}^{-\lambda}\left(\frac{\nu'}{r} + \frac{1}{r^2}\right) - \frac{1}{r^2} &= (8\pi + 3\chi)\,p - \chi\rho - \frac{q^2}{r^4} \\ &= 8\pi p^{\mathit{eff}} - \frac{q^2}{r^4}, \end{aligned} \tag{4.11}$$

where '$\prime$' denotes differentiation with respect to the radial coordinate r. Here ρ^{eff} and p^{eff} represent effective density and pressure of the effective matter distribution, respectively, and are given by

$$\rho^{\mathit{eff}} = \rho + \tfrac{\chi}{8\pi}\,(3\rho - p)\,, \tag{4.12}$$

$$p^{\mathit{eff}} = p - \tfrac{\chi}{8\pi}\,(\rho - 3p)\,, \tag{4.13}$$

where the terms depend on χ came from the trace of the energy-momentum tensor term included in the $f(R,\mathcal{T})$ theory.

The further essential stellar structure equations required to describe static and charged spherically symmetric sphere in $f(R,\mathcal{T})$ gravity theory are given as (TOLMAN, 1939;

OPPENHEIMER; VOLKOFF, 1939; DEB *et al.*, 2019a)

$$\frac{dm}{dr} = 4\pi\rho r^2 + \frac{q}{r}\frac{dq}{dr} + \frac{\chi}{2}(3\rho - p)\, r^2, \tag{4.14}$$

$$\frac{dq}{dr} = 4\pi\rho_e r^2 e^{\lambda/2}, \tag{4.15}$$

$$\begin{aligned}\frac{dp}{dr} = & \frac{1}{\left[1+\frac{\chi}{8\pi+2\chi}\left(1-\frac{d\rho}{dp}\right)\right]}\Bigg\{-(\rho+p)\left[\left\{4\pi\rho r + \frac{m}{r^2}\right.\right. \\ & - \left.\left.\frac{q^2}{r^3} - \frac{\chi}{2}(\rho - 3p)\, r\right\}\Big/\left(1 - \frac{2m}{r} + \frac{q^2}{r^2}\right)\right] \\ & + \frac{8\pi}{8\pi+2\chi}\frac{q}{4\pi r^4}\frac{dq}{dr}\Bigg\},\end{aligned} \tag{4.16}$$

where the metric potential e^{λ} have the usual Reisner-Nordström form

$$e^{-\lambda} = 1 - \frac{2m}{r} + \frac{q^2}{r^2}. \tag{4.17}$$

We describe the exterior space-time by the exterior Reissner-Nordström metric which is given as follows (D'INVERNO, 1992):

$$ds^2 = \left(1 - \frac{2M}{r} + \frac{Q^2}{r^2}\right)dt^2 - \frac{1}{\left(1 - \frac{2M}{r} + \frac{Q^2}{r^2}\right)}dr^2 - r^2(d\theta^2 + sin^2\theta d\phi^2). \tag{4.18}$$

In the present case, the modified Tolman-Oppenheimer-Volkoff (TOV) equation (TOLMAN, 1939; OPPENHEIMER; VOLKOFF, 1939; DEB *et al.*, 2019a) reads:

$$-\frac{\mathrm{d}p}{\mathrm{d}r} - \frac{1}{2}\nu'(\rho + p) + \frac{\chi}{8\pi+2\chi}(\rho' - p') + \frac{8\pi}{8\pi+2\chi}\frac{q}{4\pi r^4}\frac{\mathrm{d}q}{\mathrm{d}r} = 0. \tag{4.19}$$

4.3 Stellar properties

4.3.1 Equation of State

It is considered that the pressure and the energy density of the fluid contained in the spherical object are as follows (CHANDRASEKHAR, 1931; CHANDRASEKHAR, 1935)

$$p(k_F) = \frac{1}{3\pi^2\hbar^3}\int_0^{k_F}\frac{k^4}{\sqrt{k^2+m_e^2}}dk, \tag{4.20}$$

$$\rho(k_F) = \frac{1}{\pi^2\hbar^3}\int_0^{k_F}\sqrt{k^2+m_e^2}k^2dk + \frac{m_N\mu_e}{3\pi^2\hbar^3}k_F^3, \tag{4.21}$$

where m_e represents the electron mass, m_N the nucleon mass, $\hbar$ is the reduced Planck constant, μ_e is the ratio between the nucleon number and atomic number for ions and k_F represents the Fermi momentum of the electron. Equation (4.20) states the electric degeneracy pressure and (4.21) gives the total energy density as the sum of the relativistic electron energy density (first term of the right-hand side) and the energy density related to the rest mass of nucleons (second term of the right-hand side).

For numerical purposes we rewrite Eqs. (4.20) and (4.21) as (CARVALHO *et al.*, 2018; SHAPIRO; TEUKOLSKY, 1983)

$$p(x) = \epsilon_0 f(x), \tag{4.22}$$

$$\rho(x) = \epsilon_0 g(x), \tag{4.23}$$

where

$$f(x) = \frac{1}{24}\left[\left(2x^3 - 3x\right)\sqrt{x^2+1} + 3\,\mathrm{asinh}\,x\right], \tag{4.24}$$

$$g(x) = \frac{1}{8}\left[\left(2x^3 + x\right)\sqrt{x^2+1} - \mathrm{asinh}\,x\right] + 1215.26x^3, \tag{4.25}$$

with $\epsilon_0 = m_e/\pi^2\lambda_e^3$ and $x = k_F/m_e$ is the dimensionless Fermi momentum, λ_e represents the electron Compton wavelength. In the above equation we take $\mu_e = 2$.

4.3.2 Electric Charge Profile

We assume as in previous works that the star is mainly composed of degenerate material, so any charge present in the white dwarf would be concentrated close to the star's surface. Thus, following (CARVALHO *et al.*, 2018; NEGREIROS *et al.*, 2009) we model the electric charge distribution in terms of a Gaussian distribution

$$\rho_e = k\exp\left[-\frac{(r-R)^2}{b^2}\right], \tag{4.26}$$

where R is the radius of the star in the uncharged case, b is the width of the electric charge distribution. The parameter is considered to be $b = 10$ km since this is the order of magnitude of a WDs' atmosphere and represents less than 1% of the stars radius. We are considering in the WD a very small charge fluctuation from neutral case with a very tiny excess of electrons. Since electrons are lighter than ions they move near the star surface producing the small charge layer.

For comparable widths b of this layer, the WD structure does not change significantly, as we test it for values between $5-50$km and within this range mass and radius results have changed only $\sim 0.01\%$. The chosen charge profile mostly does not change the magnitude

of the total charge of the stars, as we will see later in Fig. 5, i.e., employing a different charge profile it yields the same order of the total charge for the charged stellar system ($Q \sim 10^{20}$C, see Refs. (NEGREIROS *et al.*, 2009; LIU *et al.*, 2014; ARBAÑIL; MALHEIRO, 2015; CARVALHO *et al.*, 2018; DEB *et al.*, 2018; DEB *et al.*, 2019a)). As one can check by comparing our previous work (CARVALHO *et al.*, 2018) with the work of Liu et al. (LIU *et al.*, 2014) that how the charge is distributed inside the star has no significant effect on its macroscopic features.

In our article, we have defined a quantity given by σ, as follows

$$\sigma = \int_0^\infty 4\pi r^2 \rho_e dr, \tag{4.27}$$

where σ would be the total charge of the star if we were working on a flat background space-time. So, in the framework of General Relativity (GR) within the finite limit of the stellar radius we can write $\frac{dQ}{dr} = e^{\frac{\lambda}{2}} \frac{d\sigma}{dr}$. In fact, since curvature effects are negligible in white dwarfs, σ is perfectly associated with the total charge (Q) of the star. So, σ represents the total charge and it is calculated from Eq. (4.27) we can certainly state that the chosen charge distribution leads to finite values of total charge and this choice of charge distribution has no infinite charge. We can estimate the proportionality constant k. Considering σ as a comparison parameter we can estimate k as

$$8\pi k = \sigma \left(\frac{\sqrt{\pi} b R^2}{2} + \frac{\sqrt{\pi} b^3}{4} \right)^{-1}. \tag{4.28}$$

The mass of the charged WDs as a function of their total radii is shown in Fig.4.1 for parametric values of χ and σ. It is worth to cite that $\chi = 0$ recovers GR results for charged and non-charged stars.

In order to observe the electric charge distribution in the star, the effective pressure inside the WD as a function of the radial coordinate is showed in Fig.4.2a, where few values of χ and $\rho_C = 10^{10}$g/cm^3 are considered. In the figure we can note that the pressure decays monotonically toward the baryonic surface, when it is attained, the pressure grows abruptly due to the beginning of the electrostatic layer. After this point the pressure decrease with the radial coordinate until it attains the surface of the stars, which results in an electric charge distribution as a spherical shell close to the surface of the WD. For Fig.4.2 we took into account $\rho_C = 10^{10}$g/cm^3 and different values of χ. Fig.4.2b shows the effective energy density as a function of the radial coordinate.

In the Fig. 4.2d the behavior of the electric field in the star is presented. We can note in the figure that the electric field exhibit a very abrupt increase from zero to 10^{16-17}V/m, this indicates that the baryonic surface ends and starts the electrostatic layer. The same behavior can be observed in Fig.4.2c - interface between baryonic and electrostatic layers

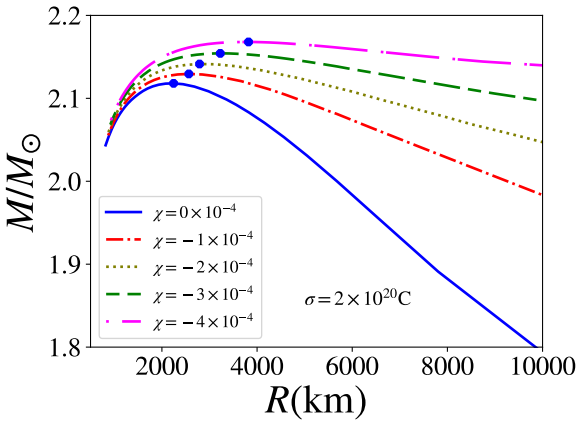

(a) Mass-radius relation of white dwarfs with varying χ and charge $\sigma = 2 \times 10^{20}$C fixed.

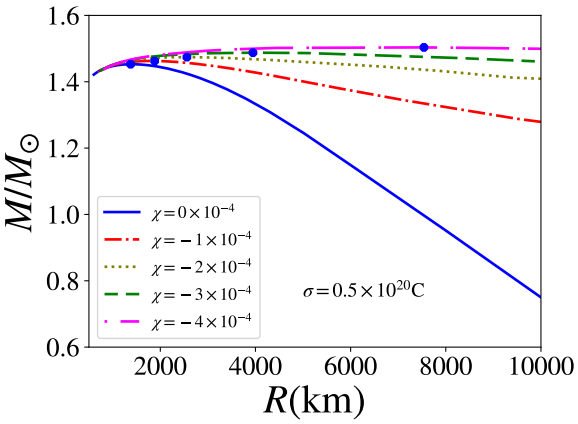

(b) Mass-radius relation of white dwarfs with varying χ and charge $\sigma = 0.5 \times 10^{20}$C fixed.

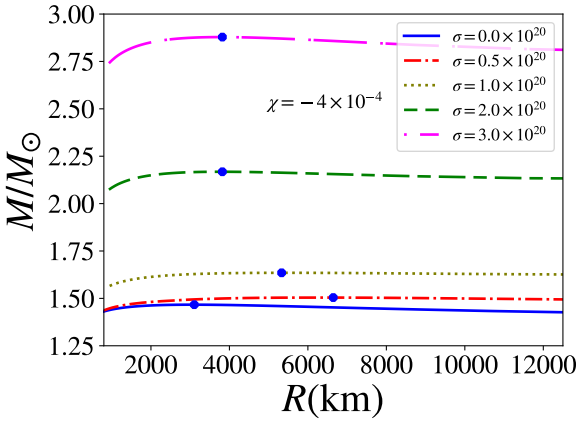

(c) Mass-radius relation of white dwarfs with varying σ and $\chi = -4 \times 10^{-4}$.

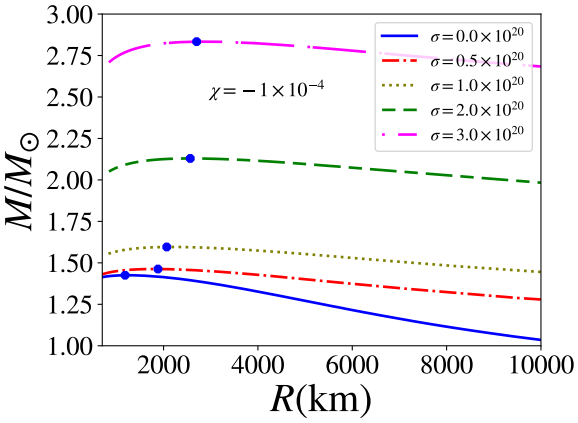

(d) Mass-radius relation of white dwarfs with varying σ and $\chi = -1 \times 10^{-4}$.

FIGURE 4.1 – (color online) Mass-radius relation of white dwarfs for the parametric chosen values of χ and σ.

- where we present the charge profile.

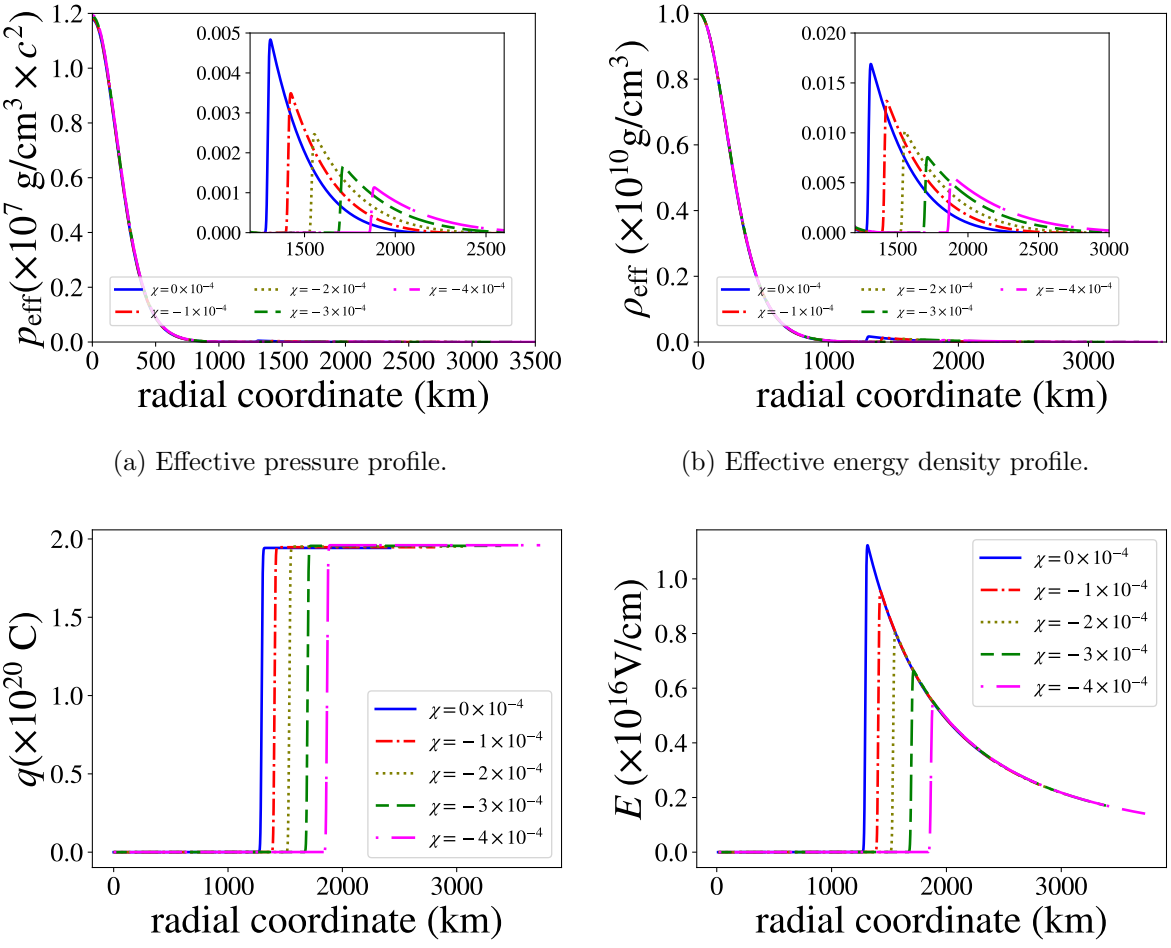

(a) Effective pressure profile.

(b) Effective energy density profile.

(c) Charge profile.

(d) Electric field profile.

FIGURE 4.2 – (color online) Profiles for several values of χ, $\sigma = 2 \times 10^{20}$C and central density of $\rho_C = 10^{10}$g/cm^3 .

As we can see in Fig. 4.1 the mass of the stars grows as the total radius decreases until it attains a maximum mass point. It is important to remark that the maximum mass grows with the decrement of χ. The total radius increases when fixed star masses are considered, which implies that the effects of the $f(R, \mathcal{T})$ gravity are very important in the determination of the stellar radius. In addition, curves in Fig. 4.1 present a similar behavior in comparison with the mass-radius relations of the white dwarfs as reported by Carvalho and collaborators in Ref. (CARVALHO *et al.*, 2017).

Here in this work, we consider values of $\sigma = 2 \times 10^{20}$C and $\sigma = 0.5 \times 10^{20}$C. The value of total charge 10^{20}C has shown to saturate the electric field limit at the surface of the star, i.e., the Schwinger limit ($\sim 1.3 \times 10^{18}$ V/m) for a mass of 2.199 $M_\odot$ (CARVALHO *et al.*, 2018). We also can see in Fig. 4.1 that the mass-radius curves tend to a plateau when χ is $\approx -4 \times 10^{-4}$. This result is corroborated by the one obtained in Ref. (CARVALHO *et*

al., 2017).

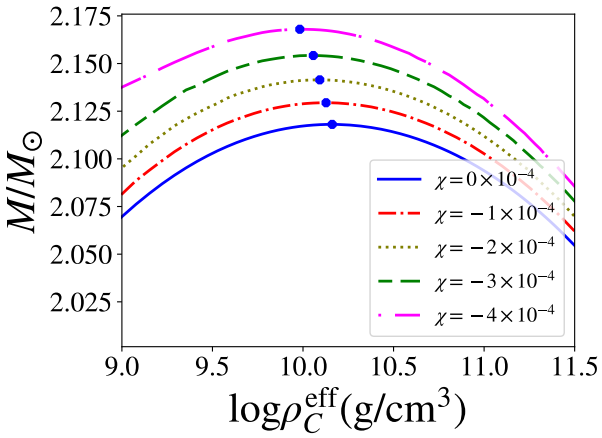

FIGURE 4.3 – Mass-central density relation of white dwarfs for several values of χ and $\sigma = 2 \times 10^{20}$C.

In Fig. 4.3 we present the mass-central density relation of static, charged and non-charged WDs for five different values of χ and $\sigma = 2 \times 10^{20}$C. As in previous works (NEGREIROS *et al.*, 2009; LIU *et al.*, 2014; ARBAÑIL; MALHEIRO, 2015; CARVALHO *et al.*, 2018; DEB *et al.*, 2018; DEB *et al.*, 2019a) we can see that the charge produces a force, repulsive in nature, which helps the one generated by the radial pressure to support more mass against the gravitational collapse, so the masses in the charged case can be larger than in the non-charged one. We present also the radius-central density relation in Fig.4.4. To construct figures 4.3 and 4.4, we used effective central energy density, defined as in Eq. (4.12).

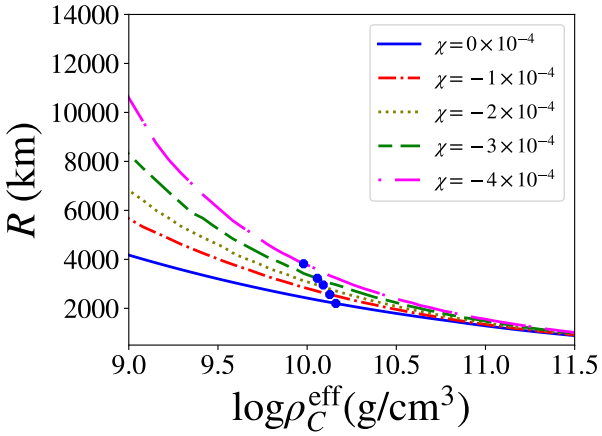

FIGURE 4.4 – Central energy density versus total radius of white dwarfs for several values of χ and $\sigma = 2 \times 10^{20}$C.

In Fig.4.5 is showed the total charge of the star as a function of the central effective energy density for the chosen parametric values of χ and $\sigma = 2 \times 10^{20}$C. One can see that

the total charge slightly varies with the increasing effective central density. The values of total charge may seem to be huge as it is 39-40 orders of magnitude larger than the elementary one. However, if we calculate the total number of electrons inside the neutral core of the WDs we obtain $N \sim 10^{56}$ electrons, and considering the total charge of the stars to be 10^{20}C, the exceeding number of electrons are of order $N \sim 10^{39}$, which means deviations from charge neutrality is actually negligible and the apparent high total charge is feasible.

Instead of such high surface charge of the order $\sim 10^{20}$C the charged stellar system should be more stable due to the balance of the forces, viz., the inward and attractive gravitational force would be counterbalanced by the combined effect of the exterior and repulsive hydrodynamic force, electric force and the force originates due to coupling between the matter and geometric terms.

Hence, the present system is stable and capable of sustaining the apparently large amount of charge. Importantly, the study of similar kind of charged astrophysical systems are also found in several recent articles, such as (NEGREIROS *et al.*, 2009; LIU *et al.*, 2014; ARBAÑIL; MALHEIRO, 2015; CARVALHO *et al.*, 2018; DEB *et al.*, 2018; DEB *et al.*, 2019a). On the other hand, to explain the super-Chandrasekhar white dwarf in this work we have considered strongly charged white dwarf (WD) model in the background of $f(R, \mathcal{T})$ gravity theory. Although, till this date, no charged WD has been observed, still, the present study is important in the theoretical aspect in explaining the super-Chandrasekhar white dwarfs which are hardly explained in the framework of General Relativity (GR).

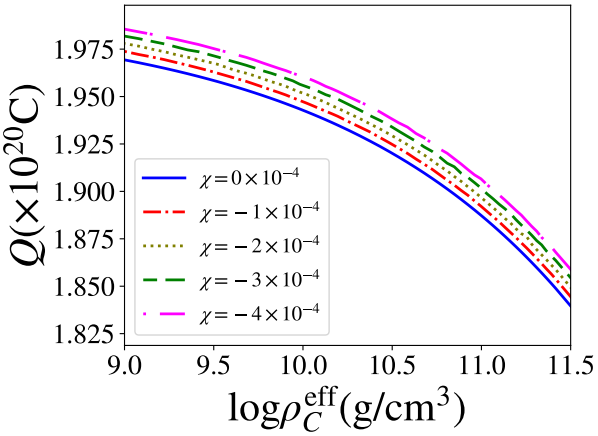

FIGURE 4.5 – Total charge versus central energy density of white dwarfs for several values of χ and $\sigma = 2 \times 10^{20}$C.

In Table 4.1 we present the maximum masses (M_{max}) for the charged WD in $f(R, \mathcal{T})$ gravity with their total radii (R) and effective central energy densities (ρ_C^{eff}) for each value of χ used in this work. It is possible to note that more massive and large charged WDs are found with the decrement of χ. We also note an important effect caused by the $f(R, \mathcal{T})$

TABLE 4.1 – The values for the constant χ and the maximum masses of the charged white dwarfs in $f(R,\mathcal{T})$ gravity with their respective radii, effective central densities, charges and electric fields at the surface of the stars for the value of $\sigma = 2 \times 10^{20}$C.

χ	$M_{\max}/M_{\odot}$	R (km)	ρ_C^{eff}(g/cm^3)	Q(C)	E(V/m)
-0×10^{-4}	2.11	2201	1.45×10^{10}	1.94×10^{20}	3.59×10^{17}
-1×10^{-4}	2.13	2565	1.34×10^{10}	1.94×10^{20}	2.65×10^{17}
-2×10^{-4}	2.14	2954	1.23×10^{10}	1.95×10^{20}	2.01×10^{17}
-3×10^{-4}	2.15	3227	1.14×10^{10}	1.95×10^{20}	1.69×10^{17}
-4×10^{-4}	2.17	3820	9.60×10^{9}	1.96×10^{20}	1.21×10^{17}

gravity theory that is the increase of the radii, which contributes to the stability of the star, since it reduces the surface electric field. From table 4.1 one can realize that as the values of χ decrease the stellar system become more massive and larger in size turning itself into a less dense compact stellar object as predicted by Carvalho et al. in their study (CARVALHO *et al.*, 2018).

We have also predicted in Table 4.2 different physical parameters of the compact stellar system due to the variation of σ for a chosen parametric value of $\chi = -4 \times 10^{-4}$. Table 4.2 features that with the increasing values of σ as usually the mass of the white dwarfs increase along with their surface charge and electric field, whereas the stellar system becomes gradually denser as it's central density increase gradually with the increasing values of σ.

Note that $f(R,\mathcal{T})$ should affect all the stars from low mass WDs to the super-Chandrasekhar limit of the mass for WDs and our study can suitably explain all the WDs. In table II, we have predicted *the maximum mass points* for $\chi = -4 \times 10^{-4}$ and parametric chosen values of σ which also can be seen from Fig. 4.1c. Readers should carefully notice that for $\chi = -4 \times 10^{-4}$ and $\sigma = 0$ the M-R curve is not predicting the WDs have far low mass compared to the maximum mass point 1.47 $M_{\odot}$. However, this happened only because with the appropriate choice of χ and σ as we wanted to show WDs in the super-Chandrasekhar mass interval. We find for σ in the range $2 \times 10^{20} - 3 \times 10^{20}$ C the present $f(R,\mathcal{T})$ model is suitable to predict different physical parameters of the highly super-Chandrasekhar white dwarfs having mass $2.17 - 2.88$ $M_{\odot}$.

It is worth mentioning that the maximum electric field obtained in this work do not surpass the Schwinger limit of 1.3×10^{18}V/m for charge screening by pair production (CARVALHO *et al.*, 2018; MADSEN, 2008) (see Tables 4.1 and 4.2), which means that the $f(R,\mathcal{T})$ gravity enhances stability of the charged stars. However, it is possible to show WDs even in the low mass limit with the appropriate choice of χ and σ as shown in Figs. 4.1b-4.1d.

In this chapter, the equilibrium configuration of white dwarfs composed of a charged

TABLE 4.2 – The values for the constant σ and the maximum masses of the charged white dwarfs in $f(R,\mathcal{T})$ gravity with their respective radii, effective central densities, charges and electric fields at the surface of the stars for $\chi = -4 \times 10^{-4}$.

σ (C)	$M_{\max}/M_{\odot}$	R (km)	ρ_C^{eff}(g/cm^3)	Q(C)	E(V/m)
0.0×10^{20}	1.47	2940	3.37×10^{9}	-	-
0.5×10^{20}	1.50	6647	2.60×10^{9}	4.94×10^{19}	1.00×10^{16}
1.0×10^{20}	1.63	5330	4.29×10^{9}	9.86×10^{19}	3.12×10^{16}
2.0×10^{20}	2.17	3820	9.60×10^{9}	1.96×10^{20}	1.21×10^{17}
3.0×10^{20}	2.88	3770	9.94×10^{9}	2.94×10^{20}	1.86×10^{17}

perfect fluid was investigated in the context of the $f(R,\mathcal{T})$ gravity, for which R and $\mathcal{T}$ stand for the Ricci scalar and the trace of the energy-momentum tensor, respectively. By considering the functional form $f(R,\mathcal{T}) = R + 2\chi\mathcal{T}$, where χ is the matter-geometry coupling constant, and for a Gaussian ansatz for the electric distribution, some physical properties of charged white dwarfs were derived, namely: mass, radius, charge, electric field, effective pressure, and energy density; their dependence on the parameter χ was also derived. In particular, the χ value important for the equilibrium configurations of charged white dwarfs has the same scale of 10^{-4} as that for non-charged stars, and the order of the charge was 10^{20}C, which is scales with the value of one solar mass, i.e., $\sqrt{G}M_{\odot} \sim 10^{20}$C.

We have also shown that charged white dwarf stars in the context of the $f(R,\mathcal{T})$ have surface electric fields below the Schwinger limit of 1.3×10^{18}V/m. In particular, a striking feature of the coupling between the effects of charge and $f(R,\mathcal{T})$ gravity theory is that the modifications in the background gravity increase the stellar radius, which in turn diminishes the surface electric field, thus enhancing stellar stability of charged stars in comparison with GR theory. Most importantly, our study revealed that the present $f(R,T)$ gravity model can suitably explain the super-Chandrasekhar limiting mass white dwarfs, which are supposed to be the reason behind the over-luminous SNeIa and remain mostly unexplained in the background of GR.

5 Conclusions

5.0.1 Beyond Gravitomagnetism

In slow motion and weak-field approximation, General Relativity predicts that a rotating central body with mass and angular momentum induces a gravitoelectric field that depends only on the mass of the body and also a smaller perturbation known as gravitomagnetic field that depends on angular momentum and leads to the Lense-Thirring precession.

Moreover, the known *"post-Newtonian approximation"* is the formalism of Newtonian theory plus post-Newtonian corrections (CHANDRASEKHAR, 1965). The corrections of post-Newtonian formalism consists of the expansion of the metric tensor to find an approximate solution for Einstein's field equations. In this case, we have weak-field, slow motion expansion, that gives: flat, empty spacetime in "zero order", the Newtonian treatment of Solar System in the "first order", and post-Newtonian corrections to the Newtonian treatment in "second order" (MISNER *et al.*, 1973).

In the present Thesis, we developed for the first time a generalized metric obtained from the expansion of both sides of Einstein's field equation up to $1/c^4$ in the weak-field regime. The proposed metric corresponds to a form of *Beyond Gravitomagnetism*. The metric has gravitoelectric and gravitomagnetic potentials already present in conventional GEM, but includes quadratic terms in the gravitational potential Φ and further terms up to fourth order in $1/c^4$.

It is important to note that the spacetime metric in the conventional GEM form showed in equation (2.48) only has linear terms in Φ and when applied to Mercury's perihelion advance it gives 57.2 arcsec/cy, which corresponds to 4/3 of the correct value, while the metric of beyond gravitomagnetic approach showed in (3.56), which takes into account terms up to $1/c^4$, presents quadratic term in Φ leading to the observed Mercury's perihelion advance of 42.95 arcsec/cy. Thus, in BGEM formalism we can easily prove that the solution for Mercury's perihelion advance comes from the nonlinear terms, which means that it cannot be solved with the linear theory.

Therefore, the beyond gravitomagnetic metric tested for Mercury's perihelion advance

and for the deflection of light gives in both cases the same results as GR, showing that the higher order terms recover GR results. Although Mercury's perihelion advance is a nonlinear problem, which depends on the nonlinearity of the field equations, the deflection of light emerges from a linear approximation, by simply neglecting the nonlinear terms in the BGEM metric. This is so because only terms in $1/c^2$ are needed to describe the light deflection effect. The problem is then solved with the reduced metric of conventional gravitomagnetism.

The BGEM approximation developed here, together with the two tests of GR we performed, was published in (ROCHA *et al.*, 2021), and the article is include in the end of this Thesis. Furthermore, other publications in conference proceedings preceded this article (ROCHA *et al.*, 2015; ROCHA *et al.*, 2016; ROCHA *et al.*, 2017).

Note that the problems tested here did not make use of the full metric, but only of the static terms. The *Beyond Gravitomagnetism* approach opens the possibility of studying problems such as the flat rotation curve of galaxies, possibly explaining the observations without the introduction of dark matter.

5.0.2 Charged White Dwarfs in the f$(R, \mathcal{T})$

In this part of the Thesis we investigate the effects of a specific modified theory of gravity, namely, the $f(R, \mathcal{T})$ gravity, in the structure of charged white dwarfs. Previous works regarding charge effects in neutron and quark stars described in f$(R, \mathcal{T})$ gravity were done in our group (CARVALHO *et al.*, 2020a; CARVALHO *et al.*, 2020c), and they motivated us to performed the same investigation in white darfs. Furthermore, white dwarfs described in f$(R, \mathcal{T})$ gravity was done also in our group, that allow a good description for massive WDs with larger radii observed in nature (CARVALHO *et al.*, 2017). However, in this modified gravity theory we could not obtain a large increase in the maximum mass for white dwarfs. The possibility to overpass the Chandrasekhar mass limit in f$(R, \mathcal{T})$ gravity considering charge effects motivated us to do this work. The procedure started from the derivation of the hydrostatic equilibrium equation for such a theory, with the addition of the charged effects. We suppose a Gaussian ansatz for the net charge distribution.

The main goal was to check the imprints of the extra material terms that comes from the energy-momentum trace $\mathcal{T}$-dependence of the theory on charged WD properties.

The equilibrium configurations of charged white dwarfs were analyzed for $f(R, \mathcal{T}) = R + 2\chi\mathcal{T}$ with different values of χ and central densities. We observed that the charged white dwarfs can be affected by the extended theory of gravity in the maximum mass and radius depending on the value of χ.

We found that for $\chi = -4 \times 10^{-4}$ and $\sigma = 3 \times 10^{20}$ C, the maximum mass of the

charged WD is 2.88 $M_{\odot}$, and the radii have considerable increasing. This larger radius yields a smaller surface electric field, thus enhancing the stellar stability of charged stars.

The possibility of explaining the highly super-Chandrasekhar limiting mass white dwarfs as a progenitors of the peculiar over-luminous super-SNeIa in the framework of $f(R, \mathcal{T})$ gravity theory was also raised by Deb and collaborators in their work (DEB *et al.*, 2019a). In the present work we have successfully explained the highly super-Chandrasekhar limiting mass white dwarfs having mass $2.17 - 2.88\ M_{\odot}$ which remained hardly explained in the framework of GR. These results were published recently in (ROCHA *et al.*, 2020), and the corresponding article is included in the end of this Thesis.

Furthermore, when explaining super-Chandrasekhar white dwarfs with modified theories of gravity one may wonder super-luminous supernovae would be more common since modified gravity would affect all stars. However, our present study reveals that one can easily explain WDs having sub and super-Chandrasekhar masses by employing suitable choices of parametric values for σ and χ.

Since gravitational fields are smaller for WDs than for neutron stars (NS) or strange stars (SS), the scale parameter χ used for WDs is small when compared to the values used for NSs and, and also the values of χ used for NSs are smaller than the ones used for SSs (MORAES *et al.*, 2016). Solar system constraints also indicate χ must be of order $\sim 10^{-13}$ (ORDINES; CARLSON, 2019).

This indicates that the more compact the system more deviations from GR theory are needed and the parameter χ may mimic a kind of chameleon mechanism, where the parameter scale depends on the density (or compactness/field regime) of the system (MORAES *et al.*, 2018; CARVALHO *et al.*, 2018; BRAX *et al.*, 2008). As a final comment, the present work not only pushing the maximum mass limit for white dwarfs beyond the standard value of the Chandrasekhar mass-limit, but also plausibly explaining the requirement of the application of $f(R, \mathcal{T})$ gravity theory in studying astrophysical observations.

Bibliography

ABBAS, G.; AHMED, R. Charged perfect fluid gravitational collapse in f(R, T) gravity. **Mod. Phys. Lett. A**, World Scientific Publishing Co., v. 34, n. 20, p. 1950153, Apr 2019. ISSN 0217-7323.

ARBAÑIL, J. D. V.; MALHEIRO, M. Stability of charged strange quark stars. **AIP Conf. Proc.**, American Institute of Physics, v. 1693, n. 1, p. 030007, Dec 2015. ISSN 0094-243X.

AZAM, M.; MARDAN, S. A.; NOUREEN, I.; REHMAN, M. A. Charged cylindrical polytropes with generalized polytropic equation of state. **Eur. Phys. J. C**, Springer Berlin Heidelberg, v. 76, n. 9, p. 510–9, Sep 2016. ISSN 1434-6052.

BANERJEE, S.; SHANKAR, S.; SINGH, T. P. Constraints on modified gravity models from white dwarfs. **J. Cosmol. Astropart. Phys.**, IOP Publishing, v. 2017, n. 10, p. 004, Oct 2017. ISSN 1475-7516.

BELOBORODOV, A. M. Gravitational bending of light near compact objects. **The Astrophysical Journal Letters**, IOP Publishing, v. 566, n. 2, p. L85, 2002.

BERA, P.; BHATTACHARYA, D. Mass–radius relation of strongly magnetized white dwarfs: dependence on field geometry, GR effects and electrostatic corrections to the EOS. **Mon. Not. R. Astron. Soc.**, Oxford Academic, v. 456, n. 3, p. 3375–3385, Mar 2016. ISSN 0035-8711.

BERTOLAMI, O.; BÖHMER, C. G.; HARKO, T.; LOBO, F. S. N. Extra force in $f(R)$ modified theories of gravity. **Phys. Rev. D**, American Physical Society, v. 75, n. 10, p. 104016, May 2007. ISSN 2470-0029.

BIEMOND, J. Which gravitomagnetic precession rate will be measured by Gravity Probe B? **ArXiv Physics e-prints**, 2004.

BOSHKAYEV, K.; RUEDA, J.; RUFFINI, R. ON THE MAXIMUM MASS OF GENERAL RELATIVISTIC UNIFORMLY ROTATING WHITE DWARFS. **Int. J. Mod. Phys. E**, World Scientific Publishing Co., v. 20, n. supp01, p. 136–140, Dec 2011. ISSN 0218-3013.

BOSHKAYEV, K.; RUEDA, J. A.; RUFFINI, R.; SIUTSOU, I. ON GENERAL RELATIVISTIC UNIFORMLY ROTATING WHITE DWARFS. **Astrophys. J.**, IOP Publishing, v. 762, n. 2, p. 117, Dec 2012. ISSN 0004-637X.

BOSHKAYEV, K.; RUEDA, J. A.; RUFFINI, R.; SIUTSOU, I. General relativistic white dwarfs and their astrophysical implications. **Journal of the Korean Physical Society**, The Korean Physical Society, v. 65, n. 6, p. 855–860, Sep 2014. ISSN 1976-8524.

BRAX, P.; BRUCK, C. van de; DAVIS, A.-C.; SHAW, D. J. $f(R)$ gravity and chameleon theories. **Phys. Rev. D**, American Physical Society, v. 78, n. 10, p. 104021, Nov 2008. ISSN 2470-0029.

BUCHMAN, S.; LIPA, J. A.; KEISER, G. M.; MUHLFELDER, B.; TURNEAURE, J. P. The Gravity Probe B gyroscope. **Class. Quantum Grav.**, IOP Publishing, v. 32, n. 22, p. 224004, Nov 2015.

CAPOZZIELLO, S. CURVATURE QUINTESSENCE. **Int. J. Mod. Phys. D**, World Scientific Publishing Co., v. 11, n. 04, p. 483–491, Apr 2002. ISSN 0218-2718.

CAPOZZIELLO, S.; LAURENTIS, M. D.; FARINELLI, R.; ODINTSOV, S. D. Mass-radius relation for neutron stars in f(R) gravity. **Phys.Rev.D**, v. 93, n. 2, Sep 2015.

CARROLL, S. M.; DUVVURI, V.; TRODDEN, M.; TURNER, M. S. Is cosmic speed-up due to new gravitational physics? **Phys. Rev. D**, American Physical Society, v. 70, n. 4, p. 043528, Aug 2004. ISSN 2470-0029.

CARVALHO, G. A.; ARBAÑIL, J. D. V.; MARINHO, R. M.; MALHEIRO, M. White dwarfs with a surface electrical charge distribution: equilibrium and stability. **Eur. Phys. J. C**, Springer Berlin Heidelberg, v. 78, n. 5, p. 411–7, May 2018. ISSN 1434-6052.

CARVALHO, G. A.; LOBATO, R. V.; MORAES, P. H. R. S.; ARBANIL, J. D. V.; OTONIEL, E.; R. JR., M. M.; MALHEIRO, M. Stellar equilibrium configurations of white dwarfs in the f (R, T) gravity. **EUROPEAN PHYSICAL JOURNAL C**, FAPESP, v. 77, n. 12, 2017. ISSN 1434-6044. Disponível em: <https://bv.fapesp.br/en-/publicacao/148328/stellar-equilibrium-configurations-of-white-dwarfs-in-the-f>.

CARVALHO, G. A.; MORAES, P. H. R. S.; SANTOS, S. I. dos; GONÇALVES, B. S.; MALHEIRO, M. Hydrostatic equilibrium configurations of neutron stars in a non-minimal geometry-matter coupling theory of gravity. **Eur. Phys. J. C**, Springer Berlin Heidelberg, v. 80, n. 5, p. 483–7, May 2020. ISSN 1434-6052.

CARVALHO, G. A.; SANTOS, S. I. D.; MORAES, P. H. R. S.; MALHEIRO, M. Strange stars in energy–momentum-conserved f(R,T) gravity. **Int. J. Mod. Phys. D**, World Scientific Publishing Co., v. 29, n. 10, p. 2050075, Jun 2020. ISSN 0218-2718.

CARVALHO, G. A.; SANTOS, S. I. D.; MORAES, P. H. R. S.; MALHEIRO, M. Strange stars in energy–momentum-conserved f(R,T) gravity. **Int. J. Mod. Phys. D**, World Scientific Publishing Co., v. 29, n. 10, p. 2050075, Jun 2020. ISSN 0218-2718.

CHANDRASEKHAR, S. The Maximum Mass of Ideal White Dwarfs. **Astrophys. J.**, v. 74, p. 81, Jul 1931. ISSN 0004-637X.

CHANDRASEKHAR, S. The Highly Collapsed Configurations of a Stellar Mass. (Second Paper.). **Mon. Not. R. Astron. Soc.**, Oxford Academic, v. 95, n. 3, p. 207–225, Jan 1935. ISSN 0035-8711.

CHANDRASEKHAR, S. The Post-Newtonian Equations of Hydrodynamics in General Relativity. **Astrophys. J**, v. 142, p. 1488–1512, Nov 1965.

CHANDRASEKHAR, S.; ESPOSITO, F. P. The $2\frac{1}{2}$-POST-NEWTONIAN Equations of Hydrodynamics and Radiation Reaction in General Relativity. **Astrophys. J**, v. 160, p. 153, Apr 1970.

CHASHCHINA, O. I.; IORIO, L.; SILAGADZE, Z. K. Elementary derivation of the Lense-Thirring precession. **Acta Phys. Polon. B**, v. 40, p. 2363–2378, Aug 2008.

CHATTERJEE, D.; FANTINA, A. F.; CHAMEL, N.; NOVAK, J.; OERTEL, M. On the maximum mass of magnetized white dwarfs. **Mon.Not.Roy.Astron.Soc**, v. 469, n. 1, p. 95–109, Oct 2016.

CIUFOLINI, I. Measurement of the Lense–Thirring drag on high-altitude, laser-ranged artificial satellites. **Phys. Rev. Lett.**, American Physical Society, v. 56, n. 4, p. 278–281, Jan 1986.

CIUFOLINI, I. Test of the gravitomagnetic field via laser-ranged satellites. **Found. Phys.**, Kluwer Academic Publishers-Plenum Publishers, v. 16, n. 3, p. 259–265, Mar 1986.

CIUFOLINI, I. A comprehensive introduction to the LAGEOS gravitomagnetic experiment: From the importance of the gravitomagnetic field in physics to preliminary error analysis and error budget. **Int. J. Mod. Phys. A**, World Scientific Publishing Co., v. 04, n. 13, p. 3083–3145, Aug 1989.

CIUFOLINI, I. Gravitomagnetism and status of the lageos iii experiment. **Classical and Quantum Gravity**, IOP Publishing, v. 11, n. 6A, p. A73, 1994.

CIUFOLINI, I. On a new method to measure the gravitomagnetic field using two orbiting satellites. **Nuov. Cim. A**, Società Italiana di Fisica, v. 109, n. 12, p. 1709–1720, Dec 1996.

CIUFOLINI, I. Frame-dragging, gravitomagnetism and Lunar Laser Ranging. **New Astronomy**, Elsevier B.V., v. 15, n. 3, p. 332–337, 2010. ISSN 13841076.

CIUFOLINI, I.; DOBROWOLNY, M.; IESS, L. Effect of particle drag on the LAGEOS node and measurement of the gravitomagnetic field. **Nuov. Cim. B**, Societ à Italiana di Fisica, v. 105, n. 5, p. 573–588, May 1990.

CIUFOLINI, I.; LUCCHESI, D.; VESPE, F.; MANDIELLO, A. Measurement of dragging of inertial frames and gravitomagnetic field using laser-ranged satellites. **Nuov. Cim. A**, Società Italiana di Fisica, v. 109, n. 5, p. 575–590, May 1996.

CIUFOLINI, I.; LUCCHESI, D.; VESPE, F.; CHIEPPA, F. Measurement of gravitomagnetism. **Europhys. Lett.**, IOP Publishing, v. 39, n. 4, p. 359–364, aug 1997.

CIUFOLINI, I.; PAOLOZZI, A.; PARIS, C. Overview of the LARES Mission: orbit, error analysis and technological aspects. **J. Phys. Conf. Ser.**, v. 354, n. 1, p. 012002, 2012.

CIUFOLINI, I.; PAVLIS, E. C. A confirmation of the general relativistic prediction of the Lense–Thirring effect. **Nature**, Nature Publishing Group, v. 431, n. 7011, p. 958–960, Oct 2004.

CIUFOLINI, I.; PAVLIS, E. C.; RIES, J.; KOENIG, R.; SINDONI, G.; PAOLOZZI, A.; NEWMAYER, H. **Gravitomagnetism and its measurement with laser ranging to the LAGEOS satellites and GRACE Earth gravity models**. [S.l.]: Springer, 2010. 371-434 p.

CIUFOLINI, I.; WHEELER, J. A. **Gravitation and inertia**. [S.l.]: Princeton university press, 1995.

CIUFOLINI I., P. A. *et al.* A test of General Relativity using the LARES and LAGEOS satellites and a GRACE Earth gravity model. **âEur. Phys. J. C**, Springer, v. 76, n. 3, p. 120, 2016.

CIUFOLINI I., P. A.; PAVLIS, E. *et al.* The LARES Space Experiment: LARES Orbit, Error Analysis and Satellite Structure. **SpringerLink**, Springer, Dordrecht, p. 467–492, 2010.

CLARK, S.; TUCKER, R. Gauge symmetry and gravito-electromagnetism. **Classical and Quantum Gravity**, v. 17, p. 4125–4157, 2000.

COSTA, J. E. S.; HADJIMICHEF, D.; MACHADO, M. V. T.; KÖPP, F.; VOLKMER, G. L.; RAZEIRA, M.; VASCONCELLOS, C. A. Z. Equilibrium configurations of white dwarfs in the pseudo-complex general relativity. **Astron. Nachr.**, John Wiley & Sons, Ltd, v. 338, n. 9-10, p. 1085–1089, Dec 2017. ISSN 0004-6337.

DAS, U.; MUKHOPADHYAY, B. Strongly magnetized cold degenerate electron gas: Mass-radius relation of the magnetized white dwarf. **Phys. Rev. D**, American Physical Society, v. 86, n. 4, p. 042001, Aug 2012. ISSN 2470-0029.

DAS, U.; MUKHOPADHYAY, B. New Mass Limit for White Dwarfs: Super-Chandrasekhar Type Ia Supernova as a New Standard Candle. **Phys. Rev. Lett.**, American Physical Society, v. 110, n. 7, p. 071102, Feb 2013. ISSN 1079-7114.

DAS, U.; MUKHOPADHYAY, B. Modified Einstein's gravity as a possible missing link between sub- and super-Chandrasekhar type Ia supernovae. **J. Cosmol. Astropart. Phys.**, IOP Publishing, v. 2015, n. 05, p. 045, May 2015. ISSN 1475-7516.

DEB, D.; KETOV, S. V.; KHLOPOV, M.; RAY, S. Study on charged strange stars in f(R, T) gravity. **J. Cosmol. Astropart. Phys.**, IOP Publishing, v. 2019, n. 10, p. 070, Oct 2019. ISSN 1475-7516.

DEB, D.; KETOV, S. V.; MAURYA, S. K.; KHLOPOV, M.; MORAES, P. H. R. S.; RAY, S. Exploring physical features of anisotropic strange stars beyond standard maximum mass limit in f(R,T) gravity. **Mon. Not. R. Astron. Soc.**, v. 485, n. 4, p. 5652–5665, Jun 2019. ISSN 0035-8711.

DEB, D.; KHLOPOV, M.; RAHAMAN, F.; RAY, S.; GUHA, B. K. Anisotropic strange stars in the Einstein–Maxwell spacetime. **Eur. Phys. J. C**, Springer Berlin Heidelberg, v. 78, n. 6, p. 465–13, Jun 2018. ISSN 1434-6052.

DENG, X.-M.; XIE, Y. Improved upper bounds on Kaluza–Klein gravity with current Solar System experiments and observations. **Eur. Phys. J. C**, Springer Berlin Heidelberg, v. 75, n. 11, p. 539–8, Nov 2015. ISSN 1434-6052.

DESHMUKH, P.; PILLAY, K. J.; RAJU, T. S.; DUTTA, S.; BANERJEE, T. Gtr component of planetary precession. **Resonance**, Springer, v. 22, n. 6, p. 577–596, 2017.

D'INVERNO, R. **Introducing Einstein's Relativity**. [S.l.]: Clarendon Press, 1992.

EINSTEIN, A. **Die Grundlage der allgemeinen Relativitätstheorie**. [S.l.]: Springer, 1923. 81-124 p.

EVERITT, C. W. F.; DEBRA, D. B. *et al.* Gravity Probe B: Final Results of a Space Experiment to Test General Relativity. **Phys. Rev. Lett.**, American Physical Society, v. 106, n. 22, p. 221101, may 2011.

FEYNMAN, R.; MORINIGO, F.; WAGNER, W.; HATFIELD, B.; PINES, D. **Feynman Lectures On Gravitation**. [S.l.]: Westview Press, 2002. ISBN 978-081334038-8.

FRANZON, B.; SCHRAMM, S. Effects of strong magnetic fields and rotation on white dwarf structure. **Phys. Rev. D**, American Physical Society, v. 92, n. 8, p. 083006, Oct 2015. ISSN 2470-0029.

FRANZON, B.; SCHRAMM, S. AR Scorpii and possible gravitational wave radiation from pulsar white dwarfs. **Mon. Not. R. Astron. Soc.**, Oxford Academic, v. 467, n. 4, p. 4484–4490, Jun 2017. ISSN 0035-8711.

FREIRE, P. C. C.; WEX, N.; ESPOSITO-FARÈSE, G.; VERBIEST, J. P. W.; BAILES, M.; JACOBY, B. A.; KRAMER, M.; STAIRS, I. H.; ANTONIADIS, J.; JANSSEN, G. H. The relativistic pulsar–white dwarf binary PSR J1738+0333 – II. The most stringent test of scalar–tensor gravity. **Mon. Not. R. Astron. Soc.**, Oxford Academic, v. 423, n. 4, p. 3328–3343, Jul 2012. ISSN 0035-8711.

HABIB, S.; HOLZ, D. E.; KHEYFETS, A.; MATZNER, R. A.; MILLER, W. A.; TOLMAN, B. W. Spin dynamics of the LAGEOS satellite in support of a measurement of the Earth's gravitomagnetism. **Phys. Rev. D**, APS, v. 50, n. 10, p. 6068, 1994.

HARKO, T.; LOBO, F. S. N.; NOJIRI, S.; ODINTSOV, S. D. $f(R,T)$ gravity. **Phys. Rev. D**, American Physical Society, v. 84, n. 2, p. 024020, Jul 2011. ISSN 2470-0029.

HEAVISIDE, O. **A gravitational and electromagnetic analogy**. [S.l.]: The Electrician, 1893.

HOWELL, D. A. e. a. The type Ia supernova SNLS-03D3bb from a super-Chandrasekhar-mass white dwarf star. **Nature**, See full text options at Nature Publishing Group, v. 443, n. 7109, p. 308–311, Sep 2006. ISSN 1476-4687.

IORIO, L. A gravitomagnetic effect on the orbit of a test body due to the Earth's variable angular momentum. **Int. J. Mod. Phys. D**, World Scientific Publishing Co., v. 11, n. 05, p. 781–787, May 2002.

IORIO, L. On the reliability of the so-far performed tests for measuring the Lense–Thirring effect with the LAGEOS satellites. **New Astron.**, North-Holland, v. 10, n. 8, p. 603–615, Aug 2005.

IORIO, L. A Critical Analysis of a Recent Test of the Lense–Thirring Effect with the LAGEOS Satellites. **J. Geod.**, Springer-Verlag, v. 80, n. 3, p. 128–136, Jun 2006. ISSN 1432-1394.

IORIO, L. A comment on the paper "On the orbit of the LARES satellite", by I. Ciufolini. **Planet. Space Sci.**, Pergamon, v. 55, n. 10, p. 1198–1200, Jul 2007. ISSN 0032-0633.

IORIO, L. An assessment of the measurement of the Lense–Thirring effect in the Earth gravity field, in reply to: "On the measurement of the Lense–Thirring effect using the nodes of the LAGEOS satellites, in reply to "On the reliability of the so far performed tests for measuring the Lense–Thirring effect with the LAGEOS satellites" by L. Iorio," by I. Ciufolini and E. Pavlis. **Planet. Space Sci.**, Pergamon, v. 55, n. 4, p. 503–511, Mar 2007. ISSN 0032-0633.

IORIO, L. An Assessment of the Systematic Uncertainty in Present and Future Tests of the Lense-Thirring Effect with Satellite Laser Ranging. **Space Sci. Rev.**, Springer Netherlands, v. 148, n. 1, p. 363–381, Dec 2009. ISSN 1572-9672.

IORIO, L. Mars and frame-dragging: study for a dedicated mission. **Gen. Relativ. Gravitation**, Springer US, v. 41, n. 6, p. 1273–1284, Jun 2009. ISSN 1572-9532.

IORIO, L. Towards a 1% measurement of the Lense-Thirring effect with LARES? **Adv. Space Res.**, Pergamon, v. 43, n. 7, p. 1148–1157, Apr 2009. ISSN 0273-1177.

IORIO, L. Will the recently approved LARES mission be able to measure the Lense–Thirring effect at 1%? **Gen. Relativ. Gravitation**, Springer US, v. 41, n. 8, p. 1717–1724, Aug 2009. ISSN 1572-9532.

IORIO, L. On the impact of the atmospheric drag on the LARES mission. **Acta Phys.Polon.B**, v. 41, p. 753–765, 2010.

IORIO, L. Gravitomagnetism and the Earth?Mercury range. **Advances in Space Research**, v. 48, n. 8, p. 1403–1410, 2011. ISSN 0273-1177.

IORIO, L. Some considerations on the present-day results for the detection of frame-dragging after the final outcome of GP-B. **EPL**, IOP Publishing, v. 96, n. 3, p. 30001, Oct 2011. ISSN 0295-5075.

IORIO, L. The impact of the orbital decay of the LAGEOS satellites on the frame-dragging tests. **Adv. Space Res.**, Pergamon, v. 57, n. 1, p. 493–498, Jan 2016. ISSN 0273-1177.

IORIO, L. A comment on "A test of general relativity using the LARES and LAGEOS satellites and a GRACE Earth gravity model", by I. Ciufolini et al. **Eur. Phys. J. C**, Springer Berlin Heidelberg, v. 77, n. 2, p. 73–8, Feb 2017. ISSN 1434-6052.

IORIO, L. On Testing Frame-Dragging with LAGEOS and a Recently Announced Geodetic Satellite. **Universe**, Multidisciplinary Digital Publishing Institute, v. 4, n. 11, p. 113, Oct 2018. ISSN 2218-1997.

IORIO, L. A HERO for General Relativity. **Universe**, Multidisciplinary Digital Publishing Institute, v. 5, n. 7, p. 165, Jul 2019. ISSN 2218-1997.

IORIO, L. A comment on 'Lense–Thirring frame dragging induced by a fast-rotating white dwarf in a binary pulsar system' by V. Venkatraman Krishnan et al. **Mon. Not. R. Astron. Soc.**, Oxford Academic, v. 495, n. 3, p. 2777–2785, Jul 2020. ISSN 0035-8711.

IORIO, L. The Short-period S-stars S4711, S62, S4714 and the Lense–Thirring Effect due to the Spin of Sgr A∗. **Astrophys. J.**, American Astronomical Society, v. 904, n. 2, p. 186, Dec 2020. ISSN 1538-4357.

IORIO, L.; CORDA, C. Gravitomagnetism and Gravitational Waves. **Open Astron.**, v. 4, n. 1, Aug 2011.

IORIO, L.; LICHTENEGGER, H. I. M.; RUGGIERO, M. L.; CORDA, C. Phenomenology of the Lense-Thirring effect in the solar system. **Astrophysics and Space Science**, Springer, v. 331, n. 2, p. 351–395, 2011.

IORIO, L.; LUCCHESI, D. M.; CIUFOLINI, I. The LARES mission revisited: an alternative scenario. **Class. Quantum Grav.**, IOP Publishing, v. 19, n. 16, p. 4311–4325, Aug 2002.

IORIO, L.; RUGGIERO, M. L.; CORDA, C. Novel considerations about the error budget of the LAGEOS-based tests of frame-dragging with GRACE geopotential models. **Acta Astronaut.**, Pergamon, v. 91, p. 141–148, Oct 2013. ISSN 0094-5765.

JACKSON, J. D. **Classical electrodynamics**. 3rd ed.. ed. New York, {NY}: Wiley, 1999. ISBN 9780471309321.

JAIN, R. K.; KOUVARIS, C.; NIELSEN, N. G. White Dwarf Critical Tests for Modified Gravity. **Phys. Rev. Lett.**, American Physical Society, v. 116, n. 15, p. 151103, Apr 2016. ISSN 1079-7114.

JING, Z.-Z.; WEN, D.-H. A New Solution in Understanding Massive White Dwarfs. **Chin. Phys. Lett.**, v. 33, n. 05, p. 50401–050401, May 2016. ISSN 0256-307X.

KALITA, S.; MUKHOPADHYAY, B. Modified Einstein's gravity to probe the sub- and super-Chandrasekhar limiting mass white dwarfs: a new perspective to unify under- and over-luminous type Ia supernovae. **J. Cosmol. Astropart. Phys.**, IOP Publishing, v. 2018, n. 09, p. 007, Sep 2018. ISSN 1475-7516.

KARLSSON, A. **A gravitomagnetic thought experiment for undergraduates**. [S.l.], 2006. 7 p. (Technical Report LUTEDX/(TEAT-7150)/1-7/(2006), TEAT-7150).

KRISHNAN, V. V. *et al.* Lense–Thirring frame dragging induced by a fast-rotating white dwarf in a binary pulsar system. **Science**, American Association for the Advancement of Science, v. 367, n. 6477, p. 577–580, Jan 2020.

LÄMMERZAHL, C.; NEUGEBAUER, G. The Lense–Thirring Effect: From the Basic Notions to the Observed Effects. **SpringerLink**, Springer, Berlin, Heidelberg, p. 31–51, 2001.

LANDAU, L. D.; LIFSHITZ, E. M. **The Classical Theory of Fields, 3rd Revised Edition**. [S.l.]: Pwegamon Presss, 1971.

LIU, H.; ZHANG, X.; WEN, D. One possible solution of peculiar type Ia supernovae explosions caused by a charged white dwarf. **Phys. Rev. D**, American Physical Society, v. 89, n. 10, p. 104043, May 2014. ISSN 2470-0029.

LIU, H. L.; LÜ, G. L. Properties of white dwarfs in Einstein-Λ gravity. **J. Cosmol. Astropart. Phys.**, IOP Publishing, v. 2019, n. 02, p. 040, Feb 2019. ISSN 1475-7516.

LOBATO, R. V.; MALHEIRO, M.; COELHO, J. G. Magnetars and white dwarf pulsars. **Int. J. Mod. Phys. D**, World Scientific Publishing Co., v. 25, n. 09, p. 1641025, Jul 2016. ISSN 0218-2718.

LUCCHESI, D.; VISCO, M.; PERON, R.; BASSAN, M.; PUCACCO, G.; PARDINI, C.; ANSELMO, L.; MAGNAFICO, C. A 1% Measurement of the Gravitomagnetic Field of the Earth with Laser-Tracked Satellites. **Universe**, Multidisciplinary Digital Publishing Institute, v. 6, n. 9, p. 139, Aug 2020. ISSN 2218-1997.

LUCCHESI, D. M. The Lense–Thirring effect measurement and LAGEOS satellites orbit analysis with the new gravity field model from the CHAMP mission. **Adv. Space Res.**, Pergamon, v. 39, n. 2, p. 324–332, Jan 2007.

LUCCHESI, D. M.; ANSELMO, L.; BASSAN, M.; MAGNAFICO, C.; PARDINI, C.; PERON, R.; PUCACCO, G.; VISCO, M. General Relativity Measurements in the Field of Earth with Laser-Ranged Satellites: State of the Art and Perspectives. **Universe**, Multidisciplinary Digital Publishing Institute, v. 5, n. 6, p. 141, Jun 2019. ISSN 2218-1997.

MADSEN, J. Universal Charge-Radius Relation for Subatomic and Astrophysical Compact Objects. **Phys. Rev. Lett.**, American Physical Society, v. 100, n. 15, p. 151102, Apr 2008. ISSN 1079-7114.

MASHHOON, B. Gravitoelectromagnetism: A Brief Review. **arXiv**, Nov 2003.

MASHHOON, B. Time-varying gravitomagnetism. **Classical Quantum Gravity**, IOP Publishing, v. 25, n. 8, p. 085014, Apr 2008.

MASHHOON, B.; GRONWALD, F.; LICHTENEGGER, H. I. M. Gravitomagnetism and the Clock Effect. In: **Gyros, Clocks, Interferometers...: Testing Relativistic Graviy in Space**. Berlin, Germany: Springer, 2001. p. 83–108. ISBN 978-3-540-41236-6.

MASHHOON, B.; GRONWALD, F.; THEISS, D. On measuring gravitomagnetism via spaceborne clocks: a gravitomagnetic clock effect. **Ann. Phys. (Berl.)**, v. 511, p. 135–152, 1999.

MASHHOON, B.; HEHL, F. W.; THEISS, D. S. On the gravitational effects of rotating masses: the Lense–Thirring papers. **Gen. Rel. Grav.**, v. 16, n. 8, p. 711–750, Aug 1984.

MASHHOON, B.; HEHL, F. W.; THEISS, D. S. On the gravitational effects of rotating masses: The Thirring-Lense papers. **General Relativity and Gravitation**, v. 16, n. 8, p. 711–750, 1984. ISSN 00017701.

MERLONI, A.; VIETRI, M.; STELLA, L.; BINI, D. On gravitomagnetic precession around black holes. **Mon. Not. R. Astron. Soc.**, Oxford Academic, v. 304, n. 1, p. 155–159, Mar 1999.

MIRANDA, O. D. Avanço do Periélio de Mercúrio – O Primeiro Sucesso da Teoria da Relatividade Geral de Einstein. **Conexões - Ciência e Tecnologia**, v. 13, n. 2, p. 7–20, 2019.

MISNER, C.; MISNER, U.; THORNE, K.; WHEELER, J.; THORNE, U. **Gravitation**. [S.l.]: W. H. Freeman, 1973. (Gravitation, pt. 3). ISBN 9780716703440.

MOORE, T. A. **A General Relativity Workbook**. [S.l.]: Blurb, Incorporated, 2015. ISBN 9781320894395.

MORAES, P. H. R. S.; Arbañil, J. D. V.; Malheiro, M. Stellar equilibrium configurations of compact stars in f(R,T) theory of gravity. **J. Cosmol. Astropart. Phys.**, v. 2016, n. 6, p. 005, jun. 2016.

MORAES, P. H. R. S.; ARBAÑIL, J. D. V.; CARVALHO, G. A.; LOBATO, R. V.; OTONIEL, E.; MARINHO, R. M.; MALHEIRO, M. **Compact Astrophysical Objects in $f(R,T)$ gravity**. Jun 2018. [Online; accessed 5. Aug. 2021]. Disponível em: <https://inspirehep.net/literature/1677332>.

MORAES, P. H. R. S.; ARBAÑIL, J. D. V.; MALHEIRO, M. Stellar equilibrium configurations of compact stars in f(R,T) theory of gravity. **J. Cosmol. Astropart. Phys.**, IOP Publishing, v. 2016, n. 06, p. 005, Jun 2016. ISSN 1475-7516.

MURPHY, T. W. Lunar Ranging, Gravitomagnetism, and APOLLO. **Space Science Reviews**, v. 148, n. 1, p. 217–223, 2009. ISSN 1572-9672.

MURPHY, T. W.; NORDTVEDT, K.; TURYSHEV, S. G. Gravitomagnetic Influence on Gyroscopes and on the Lunar Orbit. **Phys. Rev. Lett.**, American Physical Society, v. 98, n. 7, p. 071102, Feb 2007.

NASA. Gravity Probe B: Testing Einstein's Universe. 2015. Disponível em: <http://einstein.stanford.edu/MISSION/mission1.html>.

NASA. Aug 2019. [Online; accessed 12. Aug. 2019]. Disponível em: <https://solarsystem.nasa.gov/planets/mercury/overview>.

NEGREIROS, R. P.; WEBER, F.; MALHEIRO, M.; USOV, V. Electrically charged strange quark stars. **Phys. Rev. D**, American Physical Society, v. 80, n. 8, p. 083006, Oct 2009. ISSN 2470-0029.

NOJIRI, S.; ODINTSOV, S. D. Modified gravity with negative and positive powers of curvature: Unification of inflation and cosmic acceleration. **Phys. Rev. D**, American Physical Society, v. 68, n. 12, p. 123512, Dec 2003. ISSN 2470-0029.

OHANIAN, H. C.; RUFFINI, R. **Gravitation and Spacetime**. [S.l.]: Cambridge University Press, 2013.

OLAUSEN, S. A.; KASPI, V. M. THE McGILL MAGNETAR CATALOG∗. **Astrophys. J. Suppl. Ser.**, American Astronomical Society, v. 212, n. 1, p. 6, Apr 2014. ISSN 0067-0049.

OLIVEIRA, L. N. d.; KENNEFICK, D.; NETO, A. D.; VANZELLA, D. A. T.; CARVALHO, R. R. d.; MATSAS, G.; ALMEIDA, E. F. d.; VEIGA, C.; TEIXEIRA, R. Quando a luz se curvou.[depoimento a marcos pivetta e rodrigo de oliveira andrade]. **Pesquisa FAPESP**, n. 278, p. 19–23, 2019.

OPPENHEIMER, J. R.; VOLKOFF, G. M. On Massive Neutron Cores. **Phys. Rev.**, American Physical Society, v. 55, n. 4, p. 374–381, Feb 1939. ISSN 1536-6065.

ORDINES, T. M.; CARLSON, E. D. Limits on f (R ,T) gravity from Earth's atmosphere. **Phys. Rev. D**, v. 99, n. 10, p. 104052, May 2019. ISSN 1550-7998.

OTONIEL, E.; FRANZON, B.; CARVALHO, G. A.; MALHEIRO, M.; SCHRAMM, S.; WEBER, F. Strongly Magnetized White Dwarfs and Their Instability Due to Nuclear Processes. **Astrophys. J.**, v. 879, n. 1, p. 46, Jul 2019. ISSN 0004-637X.

PAL, S. K.; NANDI, P. Effect of dynamical noncommutativity on the limiting mass of white dwarfs. **Phys. Lett. B**, North-Holland, v. 797, p. 134859, Oct 2019. ISSN 0370-2693.

PANAH, B. E.; LIU, H. L. White dwarfs in de Rham-Gabadadze-Tolley like massive gravity. **Phys. Rev. D**, American Physical Society, v. 99, n. 10, p. 104074, May 2019. ISSN 2470-0029.

PAOLOZZI., A.; PARIS., C.; SINDONI., G.; TARTAGLIA., A. The lares mission: An opportunity to teach general relativity - frame dragging and lense-thirring effect. In: INSTICC. **Proceedings of the 7th International Conference on Computer Supported Education - CSEDU,**. [S.l.]: SciTePress, 2015. p. 343–348. ISBN 978-989-758-108-3. ISSN 2184-5026.

PARK R. S., F. W. M. *et al.* Precession of Mercury's Perihelion from Ranging to the MESSENGER Spacecraft. **Astron. J.**, IOP Publishing, v. 153, n. 3, p. 121, 2017.

PEEBLES, P. J. E.; RATRA, B. The cosmological constant and dark energy. **Rev. Mod. Phys.**, American Physical Society, v. 75, p. 559–606, Apr 2003.

PFISTER, H. On the history of the so-called Lense-Thirring effect. **Gen. Rel. Grav.**, Springer US, v. 39, n. 11, p. 1735–1748, Nov 2007.

PFISTER, H. **Gravitomagnetism: From Einstein's 1912 Paper to the Satellites LAGEOS and Gravity Probe B**. [S.l.]: Springer Link, 2014. 191–197 p.

RAY, A.; MAITY, P.; MAJUMDAR, P. Background gravity correction to the limiting mass of white dwarfs. **Eur. Phys. J. C**, Springer Berlin Heidelberg, v. 79, n. 2, p. 97–7, Jan 2019. ISSN 1434-6052.

RAY, S.; ESPÍNDOLA, A. L.; MALHEIRO, M.; LEMOS, J. P. S.; ZANCHIN, V. T. Electrically charged compact stars and formation of charged black holes. **Phys. Rev. D**, American Physical Society, v. 68, n. 8, p. 084004, Oct 2003. ISSN 2470-0029.

RENZETTI, G. Are higher degree even zonals really harmful for the LARES/LAGEOS frame-dragging experiment? **Can. J. Phys.**, v. 90, n. 9, p. 883–888, Aug 2012. ISSN 0008-4204.

RENZETTI, G. First results from LARES: An analysis. **New Astron.**, North-Holland, v. 23-24, p. 63–66, Oct 2013. ISSN 1384-1076.

RENZETTI, G. History of the attempts to measure orbital frame-dragging with artificial satellites. **Open Physics**, Versita, v. 11, n. 5, p. 531–544, May 2013.

RENZETTI, G. Some reflections on the Lageos frame-dragging experiment in view of recent data analyses. **New Astron.**, North-Holland, v. 29, p. 25–27, May 2014. ISSN 1384-1076.

RENZETTI, G. On Monte Carlo simulations of the LAser RElativity Satellite experiment. **Acta Astronaut.**, v. 113, p. 164–168, May 2015. ISSN 0094-5765.

ROCHA, F.; CARVALHO, G. A.; DEB, D.; MALHEIRO, M. Study of the charged super-Chandrasekhar limiting mass white dwarfs in the $f(R, \mathcal{T})$ gravity. **Phys. Rev. D**, American Physical Society, v. 101, n. 10, p. 104008, May 2020. ISSN 2470-0029.

ROCHA, F.; MALHEIRO, M.; JR., R. M. On some Aspects of Gravitomagnetism and Correction for Perihelion Advance. **J. Phys. Conf. Ser.**, v. 706, p. 052014, 2016.

ROCHA, F.; MALHEIRO, M.; JR., R. M. The gravitomagnetism in the solar system. **Int. J. Mod. Phys. Conf. Ser.**, v. 45, p. 1760052, 2017.

ROCHA, F.; MALHEIRO, M.; MARINHO, R. Gravitomagnetic correction for perihelion advance. **AIP Conference Proceedings**, American Institute of Physics, v. 1693, n. 1, p. 050010, Dec 2015.

ROCHA, F.; MARINHO, R.; MALHEIRO, M.; CARVALHO, G. A.; LUDWIG, G. O. Beyond gravitomagnetism with applications to Mercury's perihelion advance and the bending of light. **Int. J. Mod. Phys. D**, World Scientific Publishing Co., p. 2150073, Jun 2021. ISSN 0218-2718.

SALTAS, I. D.; SAWICKI, I.; LOPES, I. White dwarfs and revelations. **J. Cosmol. Astropart. Phys.**, IOP Publishing, v. 2018, n. 05, p. 028, May 2018. ISSN 1475-7516.

SCALZO, R. A. e. a. NEARBY SUPERNOVA FACTORY OBSERVATIONS OF SN 2007if: FIRST TOTAL MASS MEASUREMENT OF A SUPER-CHANDRASEKHAR-MASS PROGENITOR. **Astrophys. J.**, IOP Publishing, v. 713, n. 2, p. 1073–1094, Mar 2010. ISSN 0004-637X.

SCHMID, C. Mach's principle: Exact frame-dragging via gravitomagnetism in perturbed Friedmann-Robertson-Walker universes with $K = (\pm 1, 0)$. **Phys. Rev. D**, American Physical Society, v. 79, n. 6, p. 064007, Mar 2009.

SHABANI, H.; FARHOUDI, M. Cosmological and solar system consequences of $f(R, T)$ gravity models. **Phys. Rev. D**, American Physical Society, v. 90, n. 4, p. 044031, Aug 2014. ISSN 2470-0029.

SHAPIRO, I. I.; PETTENGILL, G. H.; ASH, M. E.; INGALLS, R. P.; CAMPBELL, D. B.; DYCE, R. B. Mercury's Perihelion Advance: Determination by Radar. **Phys. Rev. Lett.**, American Physical Society, v. 28, n. 24, p. 1594–1597, jun 1972.

SHAPIRO, S. L.; TEUKOLSKY, S. A. **Black Holes, White Dwarfs, and Neutron Stars**. [S.l.: s.n.], 1983. ISBN 978-047187316-7.

SHARIF, M.; SIDDIQA, A. Study of charged stellar structures in f(R, T) gravity. **Eur. Phys. J. Plus**, Springer Berlin Heidelberg, v. 132, n. 12, p. 529–10, Dec 2017. ISSN 2190-5444.

SHARIF, M.; WASEEM, A. Charged compact objects in f(R,T) gravity. **Int. J. Mod. Phys. D**, World Scientific Publishing Co., v. 28, n. 02, p. 1950033, Sep 2018. ISSN 0218-2718.

TAJMAR, M.; MATOS, C. D. Gravitomagnetic fields in rotating superconductors to solve tate's Cooper pair mass anomaly. **AIP Conference Proceedings**, v. 813, p. 1415–1420, 2006. ISSN 0094243X.

THORNE, K. S. **Black Holes: The Membrane Paradigm (The Silliman Memorial Lectures Series)**. [S.l.]: Yale University Press, 1986.

TOLMAN, R. C. Static Solutions of Einstein's Field Equations for Spheres of Fluid. **Phys. Rev.**, American Physical Society, v. 55, n. 4, p. 364–373, Feb 1939. ISSN 1536-6065.

VESPE, F. The perturbations of Earth penumbra on LAGEOS II perigee and the measurement of Lense-Thirring gravitomagnetic effect. **Adv. Space Res.**, Pergamon, v. 23, n. 4, p. 699–703, Jan 1999.

VESSOT, R. F. C.; LEVINE, M. W.; MATTISON, E. M.; BLOMBERG, E. L.; HOFFMAN, T. E.; NYSTROM, G. U.; FARREL, B. F.; DECHER, R.; EBY, P. B.; BAUGHER, C. R.; WATTS, J. W.; TEUBER, D. L.; WILLS, F. D. Test of Relativistic Gravitation with a Space-Borne Hydrogen Maser. **Phys. Rev. Lett.**, American Physical Society, v. 45, n. 26, p. 2081–2084, 1980.

VETŐ, B. Gravity Probe B experiment and gravitomagnetism. **Eur. J. Phys.**, IOP Publishing, v. 31, n. 5, p. 1123–1130, Jul 2010.

WEBER, J. **General Relativity And Gravitational Waves**. [S.l.]: Interscience Publishers Inc., 1961.

WEINBERG, S. Cosmology. **Annals of Physics**, v. 54, p. 612, 2008.

WEINBERG, S. **Gravitation and Cosmology: Principles and Applications of the General Theory of Relativity**. [S.l.]: Wiley, 2013.

WEYL, H. **Space–time–matter**. [S.l.]: Dutton, 1922.

WILL, C. M. The Confrontation between General Relativity and Experiment. **Living Rev. Relativ.**, Springer International Publishing, v. 17, n. 1, p. 1–117, Dec 2014. ISSN 1433-8351.

Appendix A - Some derivations

A.1 Expanded Christoffel symbols

In this part of the appendix we will present the expanded Christoffel symbols up to $\mathcal{O}(\epsilon^4)$ that were used for the obtention of the Beyond Gravitomagnetism formalism in the section 3.1 of this work. Therefore, the expansion of the Christoffel symbols is given by

$$\Gamma^{\mu}_{\alpha\beta} = \frac{1}{2}g^{\alpha\sigma}\left(-g_{\alpha\beta,\sigma} + g_{\sigma\alpha,\beta} + g_{\beta\sigma,\alpha}\right) = \frac{1}{2}g^{\alpha\sigma}\left(-h_{\alpha\beta,\sigma} + h_{\sigma\alpha,\beta} + h_{\beta\sigma,\alpha}\right) \tag{A.1}$$

up to $\mathcal{O}(\epsilon^4)$ is

$$\overset{3}{\Gamma}{}^{0}_{00} = \frac{1}{2}\overset{2}{h}_{00,0} \tag{A.2}$$

$$\overset{2}{\Gamma}{}^{0}_{0j} = \frac{1}{2}\left(-\overset{3}{h}_{0j,0} + \overset{2}{h}_{00,j} + \overset{3}{h}_{j0,0}\right) = \frac{1}{2}\overset{2}{h}_{00,j} \tag{A.3}$$

$$\overset{4}{\Gamma}{}^{0}_{0j} = \frac{1}{2}h^{0\sigma}\left(-\overset{2}{h}_{0j,\sigma} + h_{\sigma 0,j} + h_{j\sigma,0}\right) = \frac{1}{2}\overset{2}{h}{}^{00}\overset{2}{h}_{00,j} = -\frac{1}{2}\overset{2}{h}_{00}\overset{2}{h}_{00,j} \tag{A.4}$$

$$\overset{3}{\Gamma}{}^{0}_{ij} = \frac{1}{2}\left(-\overset{2}{h}_{ij,0} + \overset{3}{h}_{0i,j} + \overset{3}{h}_{j0,i}\right) \tag{A.5}$$

$$\overset{2}{\Gamma}{}^{i}_{00} = \frac{1}{2}\eta^{i\sigma}\left(-\overset{2}{h}_{00,\sigma} + h_{\sigma 0,0} + h_{0\sigma,0}\right) = \frac{1}{2}\overset{2}{h}_{00,i} \tag{A.6}$$

$$\overset{4}{\Gamma}{}^{i}_{00} = \frac{1}{2}(\eta^{i\sigma} + h^{i\sigma})\left(-\overset{2}{h}_{00,\sigma} - \overset{4}{h}_{00,\sigma} + h_{\sigma 0,0} + h_{0\sigma,0}\right) = \frac{1}{2}\left(\overset{4}{h}_{00,i} - 2\overset{3}{h}_{0i,0} - \overset{2}{h}{}^{ik}\overset{2}{h}_{00,k}\right) \tag{A.7}$$

$$\overset{3}{\Gamma}{}^{i}_{0j} = \frac{1}{2}\eta^{i\sigma}\left(-\overset{2}{h}_{0j,\sigma} + h_{\sigma 0,j} + h_{j\sigma,0}\right) = \frac{1}{2}\left(\overset{3}{h}_{0j,i} - \overset{3}{h}_{i0,j} - \overset{2}{h}_{ij,0}\right) \tag{A.8}$$

$$\overset{2}{\Gamma}{}^{i}_{jk} = \frac{1}{2}\eta^{i\sigma}\left(-\overset{2}{h}_{jk,\sigma} + h_{\sigma j,k} + h_{k\sigma,j}\right) = \frac{1}{2}\left(\overset{2}{h}_{jk,i} - \overset{2}{h}_{ij,k} - \overset{2}{h}_{ki,j}\right) \tag{A.9}$$

$$\overset{4}{\Gamma}{}^{i}_{jk} = \frac{1}{2}\left(\overset{4}{h}_{jk,i} - \overset{4}{h}_{ij,k} - \overset{4}{h}_{ki,j}\right) + \frac{1}{2}\left(\overset{2}{h}_{il}\overset{2}{h}_{jk,l} - \overset{2}{h}_{il}\overset{2}{h}_{lj,k} - \overset{2}{h}_{il}\overset{2}{h}_{kl,j}\right) \tag{A.10}$$

$$\overset{4}{\Gamma}{}^{k}_{ij} = \frac{1}{2}\left(\overset{4}{h}_{ij,k} - \overset{4}{h}_{ki,j} - \overset{4}{h}_{jk,i}\right) + \frac{1}{2}\left(\overset{2}{h}_{kl}\overset{2}{h}_{ij,l} - \overset{2}{h}_{kl}\overset{2}{h}_{li,j} - \overset{2}{h}_{kl}\overset{2}{h}_{jl,i}\right) \tag{A.11}$$

$$\overset{4}{\Gamma}{}^{k}_{ik} = -\frac{1}{2}\overset{4}{h}_{kk,i} - \frac{1}{2}\overset{2}{h}_{kl}\overset{2}{h}_{lk,i} \tag{A.12}$$

$$\overset{4}{\Gamma}{}^{0}_{i0} = -\frac{1}{2}\overset{2}{h}_{00}\overset{2}{h}_{00,i} \tag{A.13}$$

$$\overset{2}{\Gamma}{}^{k}_{ij} = \frac{1}{2}\left(\overset{2}{h}_{ij,k} - \overset{2}{h}_{ki,j} - \overset{2}{h}_{jk,i}\right) \tag{A.14}$$

$$\overset{2}{\Gamma}{}^{l}_{kj} = \frac{1}{2}\left(\overset{2}{h}_{kj,l} - \overset{2}{h}_{lk,j} - \overset{2}{h}_{jl,k}\right) \tag{A.15}$$

$$\overset{2}{\Gamma}{}^{k}_{il} = \frac{1}{2}\left(\overset{2}{h}_{il,k} - \overset{2}{h}_{ki,l} - \overset{2}{h}_{lk,i}\right) \tag{A.16}$$

$$\overset{2}{\Gamma}{}^{l}_{kl} = -\frac{1}{2}\overset{2}{h}_{ll,k} \tag{A.17}$$

A.2 Ricci tensor

Now, we will find the Ricci tensor expanded up to $\mathcal{O}(\epsilon^4)$ from the expansion of Christoffel symbols that we already obtained in A.1. So, the Ricci tensor:

$$R_{\mu\nu} = R^{\sigma}{}_{\mu\sigma\nu} = \Gamma^{\sigma}_{\mu\nu,\sigma} - \Gamma^{\sigma}_{\mu\sigma,\nu} + \Gamma^{\rho}_{\mu\nu}\Gamma^{\sigma}_{\rho\sigma} - \Gamma^{\rho}_{\mu\sigma}\Gamma^{\sigma}_{\rho\nu}, \tag{A.18}$$

can be expanded as

$$R_{00} = \overset{2}{R}_{00} + \overset{4}{R}_{00} + \cdots, \tag{A.19}$$

$$R_{0j} = \overset{3}{R}_{0j} + \overset{5}{R}_{0j} + \cdots, \tag{A.20}$$

$$R_{jk} = \overset{2}{R}_{jk} + \overset{4}{R}_{jk} + \cdots. \tag{A.21}$$

The components are

$$R_{00} = \Gamma^{\sigma}_{00,\sigma} - \Gamma^{\sigma}_{0\sigma,0} + \Gamma^{\rho}_{00}\Gamma^{\sigma}_{\rho\sigma} - \Gamma^{\rho}_{0\sigma}\Gamma^{\sigma}_{\rho 0}, \tag{A.22}$$

$$R_{0i} = \Gamma^{\sigma}_{0i,\sigma} - \Gamma^{\sigma}_{0\sigma,i} + \Gamma^{\rho}_{0i}\Gamma^{\sigma}_{\rho\sigma} - \Gamma^{\rho}_{0\sigma}\Gamma^{\sigma}_{\rho i}, \tag{A.23}$$

$$R_{ij} = \Gamma^{\sigma}_{ij,\sigma} - \Gamma^{\sigma}_{i\sigma,j} + \Gamma^{\rho}_{ij}\Gamma^{\sigma}_{\rho\sigma} - \Gamma^{\rho}_{i\sigma}\Gamma^{\sigma}_{\rho j}, \tag{A.24}$$

whose order by order gives

$$\overset{2}{R}_{00} = \overset{2}{\Gamma}{}^{i}_{00,i} \tag{A.25}$$

$$\overset{4}{R}_{00} = \overset{4}{\Gamma}{}^{i}_{00,i} - \overset{3}{\Gamma}{}^{i}_{0i,0} + \overset{2}{\Gamma}{}^{i}_{00}\overset{2}{\Gamma}{}^{j}_{ij} - \overset{2}{\Gamma}{}^{0}_{0i}\overset{2}{\Gamma}{}^{i}_{00} \tag{A.26}$$

$$\overset{3}{R}_{0i} = \overset{3}{\Gamma}{}^{j}_{0i,j} - \overset{2}{\Gamma}{}^{j}_{ij,0} \tag{A.27}$$

$$\overset{2}{R}_{ij} = \overset{2}{\Gamma}{}^{k}_{ij,k} - \overset{2}{\Gamma}{}^{0}_{i0,j} - \overset{2}{\Gamma}{}^{k}_{ik,j} \tag{A.28}$$

$$\overset{4}{R}_{ij} = \overset{4}{\Gamma}{}^{k}_{ij,k} - \overset{4}{\Gamma}{}^{0}_{i0,j} - \overset{4}{\Gamma}{}^{k}_{ik,j} + \overset{2}{\Gamma}{}^{k}_{ij}\overset{2}{\Gamma}{}^{0}_{k0} + \overset{2}{\Gamma}{}^{k}_{ij}\overset{2}{\Gamma}{}^{l}_{kl} - \overset{2}{\Gamma}{}^{0}_{i0}\overset{2}{\Gamma}{}^{0}_{0j} - \overset{2}{\Gamma}{}^{k}_{il}\overset{2}{\Gamma}{}^{l}_{kj} + \overset{3}{\Gamma}{}^{0}_{ij,0}. \tag{A.29}$$

The Ricci components up to $\mathcal{O}(\epsilon^4)$ become

$$\overset{2}{R}_{00} = \frac{1}{2}\nabla^2 \overset{2}{h}_{00}, \tag{A.30}$$

$$\begin{aligned}\overset{4}{R}_{00} =& \frac{1}{2}\nabla^2 \overset{4}{h}_{00} + \frac{1}{2}\partial_0\partial_0 \overset{2}{h}_{ii} - \partial_0\partial_i \overset{3}{h}_{0i} + \frac{1}{2}\partial_j \overset{2}{h}_{ij}\partial_i \overset{2}{h}_{00}, \\ &+ \frac{1}{2}\overset{2}{h}_{ij}\partial_i\partial_j \overset{2}{h}_{00} - \frac{1}{4}\partial_i \overset{2}{h}_{00}\partial_i \overset{2}{h}_{00} - \frac{1}{4}\partial_i \overset{2}{h}_{00}\partial_i \overset{2}{h}_{jj},\end{aligned} \tag{A.31}$$

$$\overset{3}{R}_{0i} = \frac{1}{2}\nabla^2 \overset{3}{h}_{0i} - \frac{1}{2}\left(\partial_i\partial_0 \overset{2}{h}_{jj} - \partial_i\partial_j \overset{2}{h}_{0j} - \partial_j\partial_0 \overset{2}{h}_{ij}\right), \tag{A.32}$$

$$\begin{aligned}\overset{2}{R}_{ij} =& \frac{1}{2}\nabla^2 \overset{2}{h}_{ij} + \frac{1}{2}\Big(-\partial_i\partial_j \overset{2}{h}_{00} + \partial_i\partial_j \overset{2}{h}_{kk} - \partial_k\partial_j \overset{2}{h}_{ik} \\ &- \partial_k\partial_i \overset{2}{h}_{kj}\Big),\end{aligned} \tag{A.33}$$

$$\begin{aligned}\overset{4}{R}_{ij} =& \frac{1}{2}\nabla^2 \overset{4}{h}_{ij} - \partial_j\partial_k \overset{4}{h}_{ki} + \frac{1}{2}\partial_k \overset{2}{h}_{kl}\partial_l \overset{2}{h}_{ij} + \frac{1}{2}\overset{2}{h}_{kl}\partial_l\partial_k \overset{2}{h}_{ij} \\ &- \partial_k \overset{2}{h}_{kl}\partial_j \overset{2}{h}_{li} - \overset{2}{h}_{kl}\partial_j\partial_k \overset{2}{h}_{li} + \frac{1}{4}\partial_j \overset{2}{h}_{00}\partial_i \overset{2}{h}_{00} \\ &+ \frac{1}{2}\overset{2}{h}_{00}\partial_i\partial_j \overset{2}{h}_{00} + \frac{1}{2}\partial_i\partial_j \overset{4}{h}_{kk} + \frac{1}{4}\partial_j \overset{2}{h}_{kl}\partial_i \overset{2}{h}_{kl} \\ &+ \frac{1}{2}\overset{2}{h}_{kl}\partial_i\partial_j \overset{2}{h}_{kl} + \frac{1}{4}\partial_k \overset{2}{h}_{ij}\partial_k \overset{2}{h}_{00} - \frac{1}{2}\partial_j \overset{2}{h}_{ki}\partial_k \overset{2}{h}_{00} \\ &- \frac{1}{4}\partial_k \overset{2}{h}_{ij}\partial_k \overset{2}{h}_{ll} + \frac{1}{2}\partial_j \overset{2}{h}_{ki}\partial_k \overset{2}{h}_{ll} - \frac{1}{2}\partial_k \overset{2}{h}_{il}\partial_l \overset{2}{h}_{kj} \\ &+ \frac{1}{2}\partial_k \overset{2}{h}_{il}\partial_k \overset{2}{h}_{jl} - \frac{1}{2}\partial_0\partial_0 \overset{2}{h}_{ij} + \partial_j\partial_0 \overset{3}{h}_{0i}.\end{aligned} \tag{A.34}$$

A.3 Harmonic Gauge

In this section we will introduce the calculation of the harmonic gauge, as we show in 3.1, it is possible to make a great simplification with this gauge. Then, working with the gauge,

$$g^{\mu\nu}\Gamma^{\alpha}_{\mu\nu} = 0, \tag{A.35}$$

$$g^{0\nu}\Gamma^{\alpha}_{0\nu} + g^{i\nu}\Gamma^{\alpha}_{i\nu} = 0 \tag{A.36}$$

$$g^{00}\Gamma^{\alpha}_{00} + g^{0i}\Gamma^{\alpha}_{0i} + g^{i0}\Gamma^{\alpha}_{i0} + g^{ij}\Gamma^{\alpha}_{ij} = 0 \tag{A.37}$$

$$g^{00}\Gamma^{\alpha}_{00} + 2g^{0i}\Gamma^{\alpha}_{0i} + g^{ij}\Gamma^{\alpha}_{ij} = 0. \tag{A.38}$$

With $\alpha = 0$, we have

$$g^{00}\Gamma^{0}_{00} + 2g^{0i}\Gamma^{0}_{0i} + g^{ij}\Gamma^{0}_{ij} = 0, \tag{A.39}$$

and with $\alpha = k$,

$$g^{00}\Gamma^{k}_{00} + 2g^{0i}\Gamma^{k}_{0i} + g^{ij}\Gamma^{k}_{ij} = 0. \tag{A.40}$$

Up to second order, we have

$$\eta^{00}\overset{2}{\Gamma}{}^{k}_{00} + \eta^{ij}\overset{2}{\Gamma}{}^{k}_{ij} = 0 \tag{A.41}$$

$$\frac{1}{2}\overset{2}{h}_{00,k} + \frac{1}{2}\left(-\overset{2}{h}_{ki,j} - \overset{2}{h}_{jk,i} + \overset{2}{h}_{ij,k}\right)\eta^{ij} = 0 \tag{A.42}$$

$$\frac{1}{2}\overset{2}{h}_{00,k} - \frac{1}{2}\overset{2}{h}_{ii,k} + \frac{1}{2}\overset{2}{h}_{ki,i} + \frac{1}{2}\overset{2}{h}_{ik,i} = 0, \tag{A.43}$$

that leads to

$$\frac{1}{2}\overset{2}{h}_{00,k} + \overset{2}{h}_{ki,i} - \frac{1}{2}\overset{2}{h}_{ii,k} = 0 \tag{A.44}$$

or

$$\frac{1}{2}\overset{2}{h}_{00,i} + \overset{2}{h}_{ij,j} - \frac{1}{2}\overset{2}{h}_{jj,i} = 0. \tag{A.45}$$

Up to third order, we have

$$\eta^{00}\overset{3}{\Gamma}{}^{0}_{00} + \eta^{ij}\overset{3}{\Gamma}{}^{0}_{ij} = 0 \tag{A.46}$$

$$\frac{1}{2}\overset{2}{h}_{00,0} + \frac{1}{2}\left(-\overset{2}{h}_{ij,0} + \overset{3}{h}_{0i,j} + \overset{3}{h}_{j0,i}\right)\eta^{ij} = 0$$

$$\frac{1}{2}\overset{2}{h}_{00,0} - \overset{3}{h}_{0i,i} + \frac{1}{2}\overset{2}{h}_{ii,0} = 0. \tag{A.47}$$

Up to fourth order, we have

$$\overset{2}{h}^{00}\overset{2}{\Gamma}^{k}_{00} + \eta^{00}\overset{4}{\Gamma}^{k}_{00} + \overset{2}{h}^{ij}\overset{2}{\Gamma}^{k}_{ij} + \eta^{ij}\overset{4}{\Gamma}^{k}_{ij} = 0 \tag{A.48}$$

$$\begin{aligned}=&\frac{1}{2}\overset{2}{h}^{00}\overset{2}{h}_{00,k} + \frac{1}{2}\overset{4}{h}_{00,k} - \overset{3}{h}_{0k,0} - \frac{1}{2}\overset{2}{h}^{kl}\overset{2}{h}_{00,l} + \frac{1}{2}\overset{2}{h}^{ij}\overset{2}{h}_{ij,k} - \frac{1}{2}\overset{2}{h}^{ij}\overset{2}{h}_{ki,j} - \frac{1}{2}\overset{2}{h}^{ij}\overset{2}{h}_{jk,i}\\ &\frac{1}{2}\left(\overset{4}{h}_{ij,k} - \overset{4}{h}_{ki,j} - \overset{4}{h}_{jk,i}\right)\eta^{ij} + \frac{1}{2}\left(\overset{2}{h}_{kl}\overset{2}{h}_{ij,l} - \overset{2}{h}_{kl}\overset{2}{h}_{li,j} - \overset{2}{h}_{kl}\overset{2}{h}_{jl,i}\right)\eta^{ij} = 0\end{aligned} \tag{A.49}$$

$$\begin{aligned}=&-\frac{1}{2}\overset{2}{h}_{00}\overset{2}{h}_{00,k} + \frac{1}{2}\overset{4}{h}_{00,k} - \overset{3}{h}_{0k,0} + \frac{1}{2}\overset{2}{h}_{kl}\overset{2}{h}_{00,l} - \frac{1}{2}\overset{2}{h}_{ij}\overset{2}{h}_{ij,k} + \frac{1}{2}\overset{2}{h}_{ij}\overset{2}{h}_{ki,j} + \frac{1}{2}\overset{2}{h}_{ij}\overset{2}{h}_{jk,i}\\ &-\frac{1}{2}\overset{4}{h}_{ii,k} + \frac{1}{2}\overset{4}{h}_{ki,i} + \frac{1}{2}\overset{4}{h}_{ik,i} - \frac{1}{2}\overset{2}{h}_{kl}\overset{2}{h}_{ii,l} + \frac{1}{2}\overset{2}{h}_{kl}\overset{2}{h}_{li,i} + \frac{1}{2}\overset{2}{h}_{kl}\overset{2}{h}_{il,i} = 0\end{aligned} \tag{A.50}$$

$$\begin{aligned}=&-\frac{1}{2}\overset{2}{h}_{00}\overset{2}{h}_{00,k} + \frac{1}{2}\overset{4}{h}_{00,k} - \overset{3}{h}_{0k,0} + \frac{1}{2}\overset{2}{h}_{kl}\overset{2}{h}_{00,l} - \frac{1}{2}\overset{2}{h}_{ij}\overset{2}{h}_{ij,k} + \frac{1}{2}\overset{2}{h}_{ij}\overset{2}{h}_{ki,j} + \frac{1}{2}\overset{2}{h}_{ij}\overset{2}{h}_{jk,i}\\ &-\frac{1}{2}\overset{4}{h}_{ii,k} + \overset{4}{h}_{ki,i} - \frac{1}{2}\overset{2}{h}_{kl}\overset{2}{h}_{ii,l} + \overset{2}{h}_{kl}\overset{2}{h}_{li,i} = 0\end{aligned} \tag{A.51}$$

Derivative of Eq.(A.45) with respect to x^0 gives

$$\frac{1}{2}\overset{2}{h}_{00,i0} + \overset{2}{h}_{ij,j0} - \frac{1}{2}\overset{2}{h}_{jj,i0} = 0, \tag{A.52}$$

Eq.(A.47) with respect to x^0 gives

$$\frac{1}{2}\overset{2}{h}_{00,00} - \overset{3}{h}_{0i,i0} + \frac{1}{2}\overset{2}{h}_{ii,00} = 0, \tag{A.53}$$

Eq.(A.47) with respect to x^j gives

$$\frac{1}{2}\overset{2}{h}_{00,0j} - \overset{3}{h}_{0i,ij} + \frac{1}{2}\overset{2}{h}_{ii,0j} = 0. \tag{A.54}$$

After renaming the indices of Eqs.(A.52), (A.54) $-$ (A.52) gives

$$\overset{2}{h}_{ii,0j} - \overset{3}{h}_{0i,ij} - \overset{2}{h}_{ij,i0} = 0 \tag{A.55}$$

and finally we derive Eq.(A.45) with respect to x^k and symmetrize, resulting in

$$\overset{2}{h}_{00,ik} + \overset{2}{h}_{ij,jk} - \overset{2}{h}_{jj,ik} + \overset{2}{h}_{kj,ji} = 0. \tag{A.56}$$

Derivative of Eq.(A.51) with respect to x^j and renaming the indices, leads to

$$-\frac{1}{2}\overset{2}{h}_{00,j}\overset{2}{h}_{00,i}-\frac{1}{2}\overset{2}{h}_{00}\overset{2}{h}_{00,ij}+\frac{1}{2}\overset{4}{h}_{00,ij}-\overset{3}{h}_{0i,0j}+\frac{1}{2}\overset{2}{h}_{il,j}\overset{2}{h}_{00,l}+\frac{1}{2}\overset{2}{h}_{il}\overset{2}{h}_{00,lj}-\frac{1}{2}\overset{2}{h}_{kl,j}\overset{2}{h}_{kl,i}-\frac{1}{2}\overset{2}{h}_{kl}\overset{2}{h}_{kl,ij}$$
$$+\frac{1}{2}\overset{2}{h}_{kl,j}\overset{2}{h}_{ik,l}+\frac{1}{2}\overset{2}{h}_{kl}\overset{2}{h}_{ik,lj}+\frac{1}{2}\overset{2}{h}_{kl,j}\overset{2}{h}_{li,k}+\frac{1}{2}\overset{2}{h}_{kl}\overset{2}{h}_{li,kj}-\frac{1}{2}\overset{4}{h}_{kk,ij}+\overset{4}{h}_{ik,kj}-\frac{1}{2}\overset{2}{h}_{il,j}\overset{2}{h}_{kk,l}-\frac{1}{2}\overset{2}{h}_{il}\overset{2}{h}_{kk,lj}$$
$$+\overset{2}{h}_{il,j}\overset{2}{h}_{lk,k}+\overset{2}{h}_{il}\overset{2}{h}_{lk,kj}=0 \tag{A.57}$$

Now using Eqs.(A.53, A.55, A.56, A.57) in Eqs. (A.30,A.31,A.32,A.33,A.51) results

$$\overset{2}{R}_{00}=\frac{1}{2}\nabla^2\overset{2}{h}_{00} \tag{A.58}$$
$$\overset{4}{R}_{00}=\frac{1}{2}\nabla^2\overset{4}{h}_{00}-\frac{1}{2}\overset{2}{h}_{00,00}+\frac{1}{2}\overset{2}{h}_{ij}\overset{2}{h}_{00,ij}-\frac{1}{2}\left(\nabla\overset{2}{h}_{00}\right)^2 \tag{A.59}$$
$$\overset{3}{R}_{0i}=\frac{1}{2}\nabla^2\overset{3}{h}_{0i} \tag{A.60}$$
$$\overset{2}{R}_{ij}=\frac{1}{2}\nabla^2\overset{2}{h}_{ij} \tag{A.61}$$
$$\overset{4}{R}_{ij}=\frac{1}{2}\nabla^2\overset{4}{h}_{ij}+\frac{1}{2}\overset{4}{h}_{00,ij}+\delta_{ij}\nabla^2\phi^2-\delta_{ij}\phi_{,00}-2\phi_{,j}\phi_{,i}. \tag{A.62}$$

A.4 Mercury's Perihelion Advance with GR

The Mercury's perihelion advance can be derived from the Schwarzschild's[1] line element

$$ds^2=\left(1-\frac{2m}{r}\right)dt^2-\frac{1}{1-\frac{2m}{r}}dr^2-r^2(d\theta^2+\sin^2\theta d\phi^2), \tag{A.63}$$

where m is the mass of the Sun in relativistic units.

From the Schwarzschild line element it is possible to deduce the motion of a test mass or in our case a planet (D'INVERNO, 1992). Since the test particle moves along a timelike geodesic, the Lagrangian is identical to the kinetic energy, and $g_{\alpha\beta}\dot{x}^\alpha\dot{x}^\beta=1$. Then, the Lagrangian L is as follows:

$$L=\frac{m}{2}g_{\alpha\beta}\frac{dx^\alpha}{d\tau}\frac{dx^\beta}{d\tau} \tag{A.64}$$

$$L=\frac{m}{2}g_{\alpha\beta}\dot{x}^\alpha\dot{x}^\beta \tag{A.65}$$

where, τ is the proper time.

Therefore, from (A.63), the Lagrangian for Mercury's force-free motion is given by the

[1]In the Schwarzschild solution, it is considered an object static and spherically symmetric.

following equation:

$$L = \frac{m}{2}\left[\left(1 - \frac{2m}{r}\right)\dot{t}^2 - \frac{1}{1-\frac{2m}{r}}\dot{r}^2 - r^2\dot{\theta}^2 - r^2\sin^2\theta\dot{\phi}^2\right] = \frac{m}{2}. \tag{A.66}$$

Now, we can apply Euler-Lagrange equation to (A.65), then we have

$$\frac{d}{d\tau}[(1 - \frac{2m}{r}\dot{t}] = 0, \tag{A.67}$$

$$\frac{d}{d\tau}(r^2\dot{\phi}) - r^2\sin\theta\cos\theta\dot{\phi}^2 = 0, \tag{A.68}$$

$$\frac{d}{d\tau}(r^2\sin^2\theta\dot{\phi}) = 0. \tag{A.69}$$

Since, Mercury's motion involves four equations: $t = t(\tau)$, $r = r(\tau)$, $\theta = \theta(\tau)$ and $\phi = \phi(\tau)$, the equations (A.66), (A.67), (A.68) and (A.69) provide sufficient information. Let's consider motion in the equatorial plane, for this we assume that $\theta = \pi/2$ and $\dot{\theta} = 0$. Integrating (A.69) and (A.67) gives respectively,

$$r^2\dot{\phi} = l, \tag{A.70}$$

$$\left(1 - \frac{2m}{r}\right)\dot{t} = k, \tag{A.71}$$

where, l and k are constants and l represents the angular momentum. Now, substitute (A.71) and $\theta = \pi/2$ into (A.66), gives

$$\frac{k^2}{1-\frac{2m}{r}} - \frac{\dot{r}^2}{1-\frac{2m}{r}} - r^2\dot{\phi}^2 = 1. \tag{A.72}$$

Let $u = 1/r$, then

$$\dot{r} = \frac{dr}{d\tau} = \frac{d}{d\tau}(\frac{1}{u}) = -\frac{1}{u^2}(\frac{du}{d\phi})(\frac{d\phi}{d\tau}) = -\frac{1}{u^2}(\frac{du}{d\phi})lu^2, \tag{A.73}$$

$$\dot{r} = -l(\frac{du}{d\phi}). \tag{A.74}$$

Let us substitute (A.70) and (A.74) into (A.72), then we get

$$\frac{k^2}{1-2mu} - \frac{l^2\frac{du}{d\phi}}{1-2mu} - l^2u^2 = 1. \tag{A.75}$$

Multiplying it by $\frac{1-2mu}{l^2}$

$$\frac{k^2}{l^2} - (\frac{du}{d\phi})^2 - u^2(1-2mu) = \frac{1-2mu}{l^2} \tag{A.76}$$

leads to

$$(\frac{du}{d\phi})^2 + u^2 = \frac{k^2-1}{l^2} + \frac{2m}{l^2}u + 2mu^3. \tag{A.77}$$

That differentiating this equation and dividing by 2, we get a second order differential equation for Mercury's motion:

$$\frac{d^2u}{d\phi^2} + u = \frac{m}{l^2} + 3mu^2. \tag{A.78}$$

We can solve this equation using a perturbation method. Introducing a parameter $\epsilon = \frac{3m^2}{l^2}$, this equation can be rewriten as

$$u'' + u = \frac{m}{l^2} + \epsilon(\frac{l^2u^2}{m}). \tag{A.79}$$

Assuming the solution in the form $u = u_0 + \epsilon u_1 + \mathcal{O}(\epsilon^2)$, we have

$$u_0'' + u_0 - \frac{m}{l^2} + \epsilon(u_1'' + u_1 - \frac{l^2u_0^2}{m} + \mathcal{O}(\epsilon^2)) = 0. \tag{A.80}$$

For the first approximation of a solution, we will equate the coefficients of ϵ, ϵ^2, $\cdots$ to zero. Then, $u_0 = \frac{m}{l^2}(1 - e\cos\phi)$ is the zeroth order solution to (A.80)[2]. Now, we can examine the coefficient of ϵ in (A.80)

$$u_1'' + u_1 = \frac{l^2u_0^2}{m}, \tag{A.81}$$

$$u_1'' + u_1 = \frac{m}{l^2}(1 + e\cos\phi)^2, \tag{A.82}$$

$$u_1'' + u_1 = \frac{m}{l^2}(1 + 2e\cos\phi + e^2\cos^2\phi), \tag{A.83}$$

$$u_1'' + u_1 = \frac{m}{l^2}(1 + \frac{1}{2}e^2) + \frac{2me}{l^2}\cos\phi + \frac{me^2}{2l^2}\cos 2\phi.. \tag{A.84}$$

Now, we will use a general solution $u_1 = A + B\phi\sin\phi + C\cos 2\phi$ and solve for this coefficients

$$u_1' = B\sin\phi + B\phi\cos\phi - 2C\sin 2\phi, \tag{A.85}$$

[2]The full solution is $u_0 = \frac{m}{l^2}(1 - e\cos(\phi - \phi_0)$, but we can set ϕ_0 to zero for simplicity.

$$u_1'' = 2B\cos 2\phi - B\phi\sin\phi - 4C\cos 2\phi, \tag{A.86}$$

then,

$$u_1'' + u_1 = (A) + (2B)\cos\phi + (-3C)\cos 2\phi. \tag{A.87}$$

Comparing (A.87) to (A.84), we find

$$A = \frac{m}{l^2}(1 + \frac{1}{2}e^2), \tag{A.88}$$

$$B = \frac{me}{l^2}, \tag{A.89}$$

$$C = -\frac{me^2}{6l^2}. \tag{A.90}$$

Hence,

$$u_1 = \frac{m}{l^2}(1 + \frac{1}{2}e^2) + \frac{me}{l^2}\phi\sin\phi - \frac{me^2}{6l^2}\cos 2\phi, \tag{A.91}$$

and, the general solution to first order is $u \approx u_0 + \epsilon u_1$,

$$u \approx u_0 + \frac{\epsilon m}{l^2}[1 + e\phi\sin\phi + e^2(\frac{1}{2} - \frac{1}{6}\cos 2\phi)]. \tag{A.92}$$

We note that the $e\phi\sin\phi$ term increases after each revolution, and hence becomes dominant. Then, substituting our solution for u_0, neglecting the other terms in the correction, we obtain a simplified version of (A.92)

$$u \approx \frac{m}{l^2}(1 + e\cos\phi + \epsilon e\phi\sin\phi), \tag{A.93}$$

$$u \approx \frac{m}{l^2}[1 + e\cos[\phi(1-\epsilon)]]. \tag{A.94}$$

This equation satisfies (A.80) to first order by differentiating and substituting. From (A.94) it is possible to see that Mercury's orbit is no longer an ellipse. It is still periodic, but the period (P) is now given by the following equation

$$\mathrm{P} = \frac{2\pi}{1-\epsilon} \approx 2\pi(1+\epsilon), \tag{A.95}$$

and Mercury's perihelion precession per orbit ($\Delta\phi$), is given by subtracting 2π from its period

$$\Delta\phi \approx 2\pi\epsilon = \frac{6\pi m_r^2}{l_r^2}, \tag{A.96}$$

where, ϵ is dimensionless, m_r is the mass of the Sun in relativistic units and l_r is Mercury's

angular momentum in relativistic units. Converting m_r and l_r into non-relativistic units gives the more useful form of the perihelion shift

$$\Delta\phi \approx \frac{6\pi G^2 M_\odot}{c^2 l^2}, \tag{A.97}$$

where G is the Gravitational constant, $M_\odot$ is the Sun's mass, c is the speed of light and l is Mercury's angular momentum per unit mass.

Now, using Kepler's second and third laws to rewrite an approximation of Mercury's perihelion precession. Then, from Kepler's second law

$$\frac{dA}{dt} = \frac{L}{2\mu}, \tag{A.98}$$

where, A is the area swept out by the orbit, L is the angular momentum and μ is the reduced mass. Integrating this equation over one elliptical orbit,

$$\pi ab = \frac{L}{2\mu}T \tag{A.99}$$

$$\pi ab \approx \frac{hT}{2}. \tag{A.100}$$

For an ellipse, $b^2 = a^2(1-e^2)$, so

$$T^2 = \frac{4\pi^2(1-e^2)a^4}{h^2}. \tag{A.101}$$

From Kepler's third law,

$$T^2 = \frac{4\pi^2 a^3}{G(m+m_m)}, \tag{A.102}$$

where, m_m is Mercury's mass. Since, m_m is very small compared to m, it can be neglected

$$T^2 \approx \frac{4\pi^2 a^3}{Gm}. \tag{A.103}$$

And from this equation we can solve for G^2m^2:

$$G^2m^2 = \frac{16\pi^4 a^6}{T^2}(\frac{1}{T^2}). \tag{A.104}$$

Replacing (A.101) into (A.104), we have

$$G^2m^2 = \frac{4\pi^2 a^2 h^2}{T^2(1-e^2)}. \tag{A.105}$$

Combining (A.101) and (A.97) gives an equation for Mercury's relativistic perihelion precession per orbit

$$\Delta\phi = \frac{24\pi^3 a^2}{cT^2(1-e^2)} \tag{A.106}$$

where, a is the semimajor axis of Mercury's orbit, c is the speed of light, T is the period of Mercury's orbit and e is the eccentricity of Mercury's orbit. Using the data for Mercury, this equation gives a perihelion shift of 42.9 arcsec per century.

FOLHA DE REGISTRO DO DOCUMENTO

1. CLASSIFICAÇÃO/TIPO	2. DATA	3. REGISTRO N°	4. N° DE PÁGINAS
TD	22 de setembro de 2021	DCTA/ITA/TD-022/2021	93

5. TÍTULO E SUBTÍTULO:

Beyond-gravitomagnetism approximation of general relativity applied to solar system and compact objects in modified theories of gravity.

6. AUTOR(ES):

Flavia Pereira da Rocha

7. INSTITUIÇÃO(ÕES)/ÓRGÃO(S) INTERNO(S)/DIVISÃO(ÕES):

Instituto Tecnológico de Aeronáutica – ITA

8. PALAVRAS-CHAVE SUGERIDAS PELO AUTOR:

General Relativity, Gravitomagnetism, Extended theories of gravity.

9.PALAVRAS-CHAVE RESULTANTES DE INDEXAÇÃO:

Campos gravitacionais; Eletromagnetismo; Gravidade; Teoria da relatividade; Astrofísica; Física.

10. APRESENTAÇÃO: **(X) Nacional ( ) Internacional**

ITA, São José dos Campos. Curso de Doutorado. Programa de Pós-Graduação em Física. Área de Física Nuclear. Orientador: Manuel Máximo Bastos Malheiro de Oliveira; coorientador: Gerson Otto Ludwig. Defesa em 27/08/2021. Publicada em 2021.

11. RESUMO:

In this work, the expansion of both sides of Einstein's field equations in the weak-field approximation, up to terms of order $1/c^4$, is derived. This approach leads to an extended form of gravitomagnetism properly named Beyond Gravitomagnetism (BGEM). The metric of BGEM includes a quadratic term in the gravitoelectric potential. This term does not appear in conventional gravitomagnetism, but is essential in achieving the exact value of Mercury's perihelion advance. The new metric is also applied to the classical problem of light deflection by the Sun, giving the correct result and showing the feasibility of this approach. Another subject approached in this work concerns to the equilibrium configuration of white dwarfs composed of a charged perfect fluid are investigated in the context of the $f(R,\mathcal{T})$ gravity, for which R and $\mathcal{T}$ stand for the Ricci scalar and the trace of the energy-momentum tensor, respectively. By considering the functional form $f(R, \mathcal{T})=R+2\chi \mathcal{T}$, where χ is the matter-geometry coupling constant, and for a Gaussian ansatz for the electric distribution, some physical properties of charged white dwarfs were derived, namely: mass, radius, charge, electric field, effective pressure and energy density; their dependence on the parameter χ was also derived. We have showed that charged white dwarf stars in the context of the $f(R,\mathcal{T})$ have surface electric fields below the Schwinger limit of 1.3×10^{18}V/m. In particular, a striking feature of the coupling between the effects of charge and $f(R,\mathcal{T})$ gravity theory is that the modifications in the background gravity increase the stellar radius, which in turn diminishes the surface electric field, thus enhancing stellar stability of charged stars in comparison with General Relativity (GR). Most importantly, our study reveals that the present $f(R,\mathcal{T})$ gravity model can suitably explain the super-Chandrasekhar limiting mass white dwarfs, which are suppose to be the reason behind the over-luminous SNeIa and remain mostly unexplained in the background of GR theory.

12. GRAU DE SIGILO:

(X) OSTENSIVO ( ) RESERVADO ( ) SECRETO